SoftGlove

Finger Force Feedback

L.I.A. Gelling &
J. van der Knaap

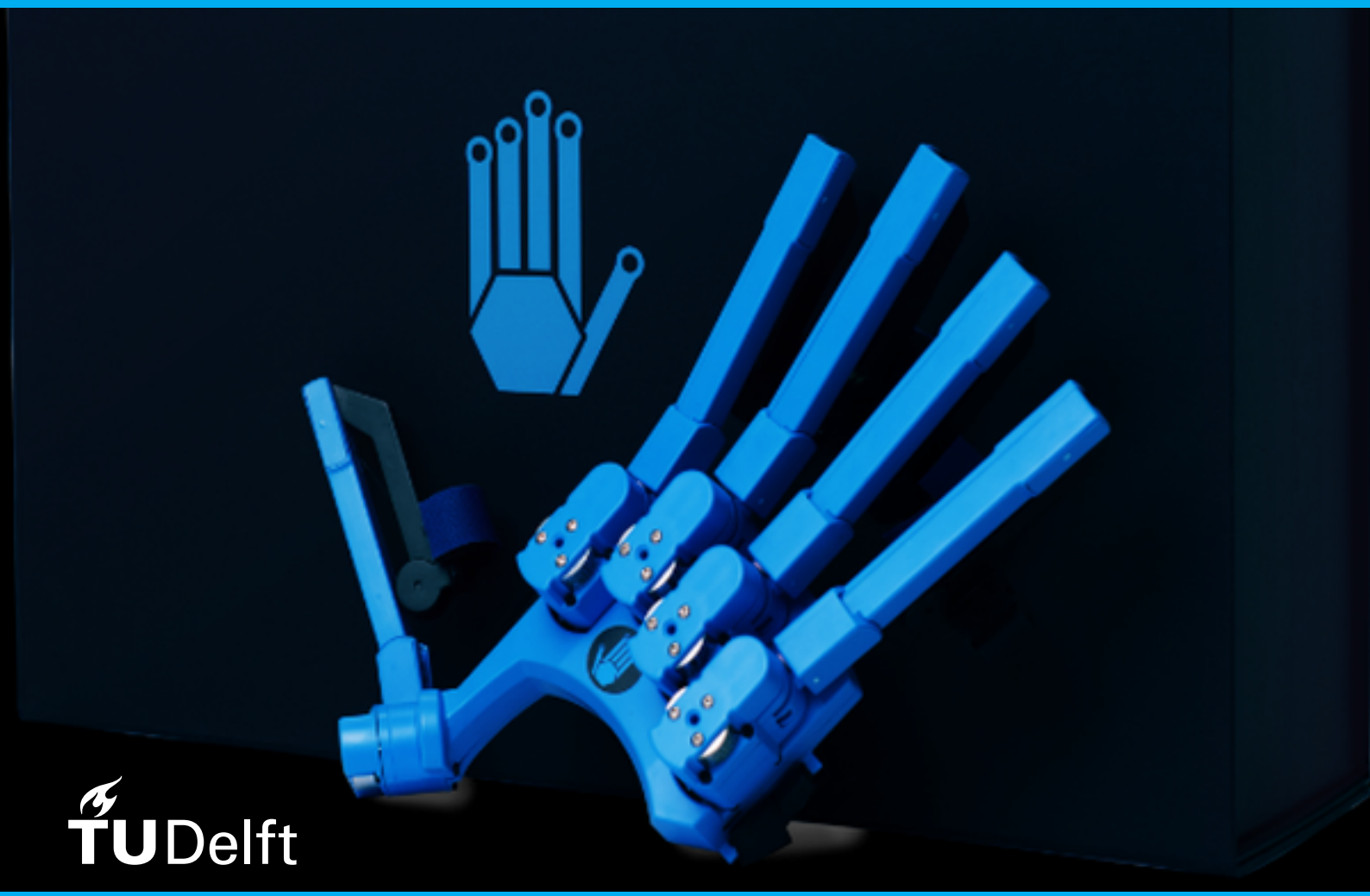

TU Delft

SoftGlove

Finger Force Feedback

by

L.I.A. Gelling &
J. van der Knaap

To obtain the degree of Bachelor of Science Electrical Engineering
at the Delft University of Technology,
to be defended on June 28, 2019

Authors:	L.I.A. Gelling	J. van der Knaap
Project duration:	April 23, 2019 – July 5, 2019	
Thesis committee:	Dr. M. Spirito	TU Delft, chair
	Dr. ir. C.J.M. Verhoeven	TU Delft, supervisor
	Dr. J. Dong	TU Delft
	Ing. C. Lam	SenseGlove

This thesis is confidential and cannot be made public until May 1, 2025.

TU Delft

Abstract

The company SenseGlove is specialized in making gloves that integrate with virtual reality. This glove is currently an exoskeleton that is able to track hand movements and give feedback from the virtual world to the user. This thesis evaluates the finger force feedback design that is made for an improvement of the current exoskeleton to a soft version in cooperation with SenseGlove. This improvement includes the step up to a wireless glove powered on a battery instead of USB. The finger force feedback actuators are the biggest power consumers within the complete system and therefore the power conversions are also part of the finger force feedback design. Beside the already named subsystems, the glove consists of Finger Vibrotactile feedback, Palm Vibrotactile Feedback, a battery protection system, a battery charging system and a microcontroller. The subsystems Finger Vibrotactile feedback and Palm Vibrotactile Feedback will be discussed in Th. [1] and Th. [2] respectively. In this thesis the control of the finger force feedback actuators and the design and testing of the power conversions which consists of a boost and a buck conversion are discussed. The sensitivity to instability in power converters and the importance of proper PCB layout design are outlined. This instability is shown and ways to avoid this instability are discussed. A first PCB design is made where functionality was tested. Afterwards, an improved design is made which is representative for a final prototype and is able to fit in the soft version of the glove, the SoftGlove.

Preface

This thesis was commissioned by Delft University of Technology and is part of the Bachelor graduation project for the study Electrical Engineering. This thesis is written about finger force feedback design in virtual reality gloves. In cooperation with SenseGlove a new electronics design for virtual reality gloves is made. The interaction between the real world and virtual reality is becoming more and more popular and is developing very rapidly towards consumer friendly virtual reality gloves and even virtual reality suits. There is growing demand for interaction between the virtual and real world, especially when it comes to easily wearable and cheap devices. Beside these consumers, also companies are interested in virtual environments for training simulations, which is safer and cheaper than reality training situations. Research in this field is therefore not only interesting for the technology industry, but also business wise. For Electrical Engineering students, being part of this development and research is a perfect graduation opportunity.

Acknowledgements

This work would not have been possible without the support of many people. We are grateful to all of those with whom we have had the pleasure to work during this and other related projects. We would especially like to thank Dr. ir. C.J.M. Verhoeven, the supervisor of our project, and SenseGlove, the company that gave the opportunity for this graduation project. The ones from SenseGlove that took the time to help us: Dan Shor, Chun Lam, Michelle Corten and Max Lammers. Without out them this project would have never been successful. We also want to thank Dr. T. Batista Soeiro for his expertise in power conversion, Dr. M. Spirito for being chair at our defence and Dr. J. Dong for being part of the thesis committee.

Secondly we want to thank our families, especially our parents who gave the opportunity to study and achieve the Bachelor of Science in Electrical Engineering. Last but not least Delft University of Technology, the university that provides the Bachelor Electrical Engineering.

Contents

1 Introduction

Since the late 90's research on force feedback and haptic feedback has been done. Haptic feedback is defined as the use of sense of touch to communicate with users [3]. Force feedback is the most obvious and iconic part of feedback in virtual reality, allowing people to "grab" or "squeeze" items in a virtual environment, by applying force to the fingers that stops them from moving through a virtual object. The implementation of this force feedback has to take into account the differences of human perception [4] as well as the differences in body size [5]. Existing force feedback systems are based on different mechanisms, such as changing pressure using pumps [6], this is called pneumatic feedback. Also the twisted string mechanism [7] connected to a DC motor is used in designs. Various possibilities of controlling the DC motor exist for such force feedback systems. For example, a PWM control signal [8] is used to change the torque of the DC motor [9]. Throughout time, research on force feedback is done for different applications, such as rehabilitation for people who had an accident which caused hand injury [10], tele-operations using a full force feedback arm [11] and prevention of muscle fatigue and injury [12]. Recent research is done on possible use of deep learning for position estimation and control of a glove [13] and possibilities to increase the degree of immersion by using tactile feedback in a soft glove [14]. All these different feedback methods are currently combined in so called virtual reality gloves. These gloves give the user the ability to feel an object that only "exists" in virtual reality. By making use of virtual reality glasses, the object and hand movements can also be visually experienced. It is clear that the applications of a accurate force feedback system are infinite. Research and development in this area is therefore necessary and can be seen as a major step towards a society with more and more interaction between humans and machines.

Thesis Objective

The company SenseGlove makes gloves that can interact with virtual reality by making use of haptic and force feedback. The current version of the product uses an exoskeleton. This design limits the capability and the scale of implementation for augmented reality applications. Therefore a soft version of the glove is required, the SoftGlove. In this thesis the finger force feedback of this SoftGlove is discussed and in detail elaborated. The actuators for the force feedback have a relatively high power consumption, therefore the power conversions from the input voltage to the required voltages is part of the finger force feedback subsystem. The input voltage has to be boosted to the required actuator voltage, which can be achieved with a boost converter design [15]. The efficiency of this boost converter is important because of the high power consumption. The design [16] and the possible use of multiple boost converters [17] has effect on this efficiency and has to be taken in account. Previous research towards the electric design [18] and the haptic feedback [19] for the SoftGlove is used for the development of the final prototype.

Thesis Outline

This thesis consist of a general part and a part focused on the detailed design, implementation and testing of the finger force feedback subsystem. The general part contains the requirements and the design choices that are applicable for all subsystems and will therefore be included in all theses. The

requirements will be discussed in the second chapter and the general design choices in the third chapter. Next, the design of the finger force feedback subsystem is discussed in chapter four. In chapter four is elaborated on the implementation of the design and the results of the prototype. After showing the results, discussion follows in chapter six and conclusions are given in chapter seven.

2 Requirements

This chapter discusses the general requirements that are the result of the assignment from the company SenseGlove. After detailed research, the original assignment is changed to the final assignment. The assignments and requirements are a result of collaboration with SenseGlove about the time and practical limitations of the project. The final assignment and requirements splits the complete system in three subsystems. Finally the requirements that are specific for the finger force feedback subsystem are discussed.

2.1. Assignment

The current version of the product uses an exoskeleton. This design limits the capability and the scale of implementation for augmented reality applications. Therefore a soft/fabric version of the old design is an important development. This soft version should have at least similar capabilities as the current exoskeleton glove, with the exception of finger tracking and added vibrotactile feedback in the palm of the hand. The first assignment made by SenseGlove is discussed in Sec. 2.1.1. After discussions with the company about the project and research on the subject, the constraints did not completely fit the assignment. Therefore the assignment was modified in collaboration with SenseGlove, this assignment is discussed in Sec. 2.1.2.

2.1.1. Original Assignment

The original assignment was to design and realize a semi-flex PCB for the SoftGlove, which integrates per finger force feedback, linear resonant actuators in the fingertips and a Lofelt haptic actuator on the palm of the hand, including firmware, where communication to the PC through USB according to the SenseGlove protocol is possible. As an optional assignment, the glove can be outfitted with a wireless communication link. This assignment can be found in Appendix A.3.2.

2.1.2. Final Assignment

After detailed research it was apparent that some changes needed to be made to the assignment. The semi-flex PCB material is rated to bend a maximum amount of five times to make inserting the PCB in a housing easier [20]. It is not made to bend continuously back and forth and is therefore not suited for bending with the movement of the wrist. Another option would be to use a fully flexible PCB. However the design of a fully flexible PCB adds significant complexity to the design process, as described in [21]. Because of this, the use of a rigid PCB is chosen, which can be mounted on the wrist in the form of several modules.

Secondly there were some concerns about the assignments challenge level as the finger force feedback is already optimized for the current SenseGlove. Therefore it was decided to make the system work with a battery so the product could become entirely wireless. When making the SoftGlove wireless, power supply by a battery is needed which makes the power conversions for the finger force feedback more complicated. However, the SoftGlove must have the ability to be powered via USB at 5 V with a maximum of 4 A. This results in a maximum available power of 20 W.

2.2. General Requirements

Based on the final assignment that is discussed in Sec. 2.1.2, requirements are set that are applicable for the whole system that should be made for the SoftGlove. The requirements can be divided in mandatory requirements, cost factors and stretch goals. All of these are listed below.

Mandatory

1. The glove must have per finger force feedback.
2. The glove must have per finger vibrotactile feedback.
3. The glove must have a larger vibrotactile feedback core in the palm of the hand.
4. The glove must support USB-based firmware updates.
5. The glove may not have a power consumption over 20 W.
6. The average latency of the PCB may be no more than 40 ms. How this latency is defined is discussed in Sec. 3.2.
7. The PCB must have over current protection.
8. The PCB must have over voltage protection.
9. The PCB must have reverse current protection.
10. The glove must stay under 40°C

Cost Factors

1. The latency of the glove should be as low as possible.
2. Extensions of the glove should take up minimal space on the wrist or other parts of the body.
3. The glove must have a minimal power consumption.
4. The feedback placement on the glove should be optimized where the sensitivity of the human skin is highest.
5. The glove should be as durable as possible.
6. The glove should fit a wide audience as comfortably as possible. This means the product should fit both men and women with a range of different sizes of wrists and hands.

Stretch Goals

1. The glove would benefit from being compatible with SenseGlove Communication Protocol [22].
2. The glove would benefit from having a wireless communication link.
3. The glove would benefit from using a mobile power source

2.3. Subsystems

It is clear the glove has three major feedback methods, finger force feedback, finger vibrotactile feedback and palm vibrotactile feedback. The finger force feedback can hold the fingers back when they are grasping an object in virtual reality, creating the illusion of a solid object. The other two feedback methods are comprised of vibrations of actuators on the hand, creating the feeling of a buzz when touching something in the virtual environment. The finger vibrotactile feedback is comprised of a smaller actuator on each finger, whereas the palm vibrotactile feedback is a larger actuator in the hand palm. Because there are three types of feedback, the complete system is split up in these three subsystems. Based on the complexity of each subsystem, some secondary tasks are divided to the subsystems. An overview of the placement of all feedback subsystems is shown in Fig. 2.1.

2.3.1. Finger Force Feedback

The iconic form of feedback from the virtual environment to the client is the Finger Force Feedback, allowing people to ”grab” or ”squeeze” items in a virtual environment, by applying force to the fingers that stops them from moving through a virtual object. This will be done using the actuators provided by SenseGlove. The actuators provide feedback on the top of all fingers, marked in blue in Fig. 2.1.

This subsystem will use the most power and the highest voltage, and will therefore be accountable for designing the power converters.

2.3.2. Finger Vibrotactile Feedback

The more subtle, but just as important way the current version of the glove provides feedback is through small actuators that vibrate the fingers. This system allows the user to experience for example button clicks and the smoothness of certain surfaces. This design is meant to be an improvement over the vibration motors currently in the SenseGlove. The finger vibrotactile feedback motors will be placed on the intermediate phalanges of the fingers and the proximal phalanx of the thumb, marked in green in Fig. 2.1.

2.3.3. Palm Vibrotactile Feedback

SenseGlove wants to add another way of feedback in their products, and they want it to be the Lofelt actuator based in the palm. This is a sensitive area that can provide general purpose feedback. The Lofelt actuator will be placed in the palm of the hand, marked in red in Fig. 2.1.

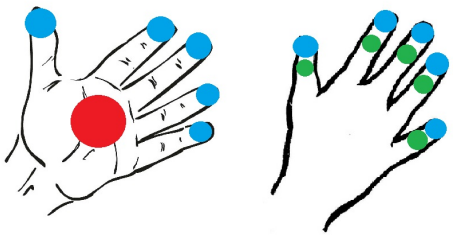

Figure 2.1: Overview of the placement of all subsystems on the hand of the user

2.4. Subsystem Requirements

As from Ch. 1 the subsystem that will be discussed in this thesis is the finger force feedback. This subsystem has some specific requirements beside the general requirements discussed in Sec. 2.2. In order to make the switching in force feedback feel fluent and realistic, the PWM signal to the actuators must have at least 100 different levels equally spread between 0 and 24. To make the SoftGlove as comfortable as possible, switching frequencies must be always outside the hearing spectrum. This means all switching frequencies must be above 25 kHz to avoid the components from making sound the user could hear. In order to minimize power consumption of the SoftGlove, requirement is set that the power conversions must have an efficiency of 90% or higher. The actuators are required to be able to deliver at least a torque of 0.045 Nm. To satisfy this requirement a voltage of 24 V is needed across the actuators, as can be seen in the data sheet in Appendix B.6. Summarized the specific requirements are listed below.

1. The boost converter must be able to deliver an output voltage of 24 V.
2. The PWM signal to the actuators must have at least 100 different levels.
3. The switching frequency of all switching components must be at least 25 kHz.
4. Converter efficiencies must be at least 90%.

3

General Design

Next to the designs of the separate subsystems described in Sec. 2.3, some general design choices have been made. These choices are applicable for all subsystems and are discussed in this chapter. The power supply consists of several parts that are split up between the subgroups. At first the battery charger circuit, which is done by the Palm Vibrotactile Feedback group, secondly the battery protection circuit, which is made by the Finger Vibrotactile feedback group, and thirdly the type of battery which is chosen by the Finger Force Feedback group. Besides the power supply, the microcontroller and programming language were chosen. The way in which the systems cooperate can be found in Fig. 3.2.

3.1. Power Supply

As described in the new assignment, which is shown in Sec. 2.1.2, the goal is to design a wireless glove. For the power supply this means a battery or multiple batteries have to be attached to the SoftGlove or to the human body. As can be seen in the program of requirements, which is shown in Sec. 2.2, the physical size is a major cost factor. Besides, a smaller system allows the gloves to be compatible for a wider audience, which is also a cost factor. Taking this into account, all considerations and final decisions for the battery type, charger and protection are outlined in this section.

3.1.1. Battery Type

Since the SoftGlove is designed for wireless application, a battery has been found that will not constrain the usage of the glove. From the general program of requirements, shown in Sec. 2.2, some requirements for the battery follow. The battery should be able to deliver a peak power of 20 W and the battery, as an extension of the glove to the wrist, should take up minimal space.

Types of Batteries

The requirements immediately shorten the list of usable batteries for the application. The used voltages in the system are 3.3 V, 5 V and 24 V, where the 24 V subsystem uses the most power. The highest efficiency will be achieved with a battery input voltage of between 5 V and 24 V. This efficiency is mainly based on the boost from the input voltage to the output voltage of 24 V. When boosting an input voltage lower than 5 V to an output of 24 V, the efficiency of one the boost converter often becomes lower than 75% which is too low to meet the power specifications as described in Sec. 2.4. This efficiency will be further discussed in the finger force feedback design, which is discussed in Ch. 4. The second option is to use two boost converters in cascade. However, this uses almost double the space, which is not available. Therefore the input voltage must be at least 5 V. Furthermore, for practicability and durability the battery needs to be rechargeable. Finally, the battery shape and weight influences comfort of the SoftGlove user. Taking all of this in account, five battery types were considered and discussed. Paper [23] was consulted, to further explain the differences between the different batteries. These battery types are shown and discussed below. The best battery type is used in the design of the SoftGlove.

- Lead-Acid
- Nickel Cadmium(Ni-Cd)
- Nickel-Metal Hydride(Ni-MH) item Lithium-ion(Li-ion)
- Lithium-ion Polymer (Li-Po)

Lead Acid Batteries Lead Acid Batteries are created as very reliable and low-cost power sources. As disadvantage they have a low energy-to-weight ratio. Because of their big size and high weight in comparison to other battery types, this is not an option for wearable application.

Nickel Cadmium Batteries have a couple of useful advantages. For example, they can handle many charge/discharge cycles in comparison to the other types of batteries. On the other hand, there are disadvantages which are so crucial that this type of battery is not chosen for the SoftGlove. Firstly, the presence of the so called 'memory effect': The batteries lose their maximum capacity when they are being recharged after not being fully discharged. Secondly, This type of battery also contains toxic metals and the energy density is not as high as some other battery types. Another disadvantage is that Nickel Cadmium batteries have a cylindrical shape, which is not ideal for efficient usage of the available space on the wrist.

Nickel-Metal Hydride Batteries have a higher energy density than Nickel Cadmium batteries but also have the cylindrical shape. The energy density is also not as high as with Lithium batteries. For the same capacity, a bigger and heavier battery is needed. Nickel-Metal Hydride batteries are not effected by the memory effect, which is an advantage. Despite this advantage, the self discharge rate is high and the maintenance to ensure a sufficient lifetime is very difficult. All the disadvantages makes the Nickel-Metal Hydride battery not suitable for usage by a wide and long term audience as for the SoftGlove.

Lithium-Ion Batteries are widely used for wearable applications. A disadvantage is that these batteries also have a cylindrical shape. This type of battery is comparable to Lithium-ion Polymer batteries [24], which have the advantage of a low profile and non-cylindrical shape. Their form factor makes it also easier to attach the batteries to the wrist. Li-Po batteries have a disadvantage of higher price comparing to Lithium-ion, however these costs are small compared to the advantages. Lithium-ion has a sufficient discharge current for the case of maximal dissipation of 5 A, where maximally 2.5 A can be drawn. Lithium-Polymer generally has even higher discharge rates. Looking at safety differences, Lithium-Polymer is more sensitive compared to Lithium-Ion regarding over voltage and over current while charging and discharging. However, when using reliable and good protection circuits this can be prevented. In Tab. 3.1 the batteries together with their advantages and disadvantages are summarized. Taking all advantages and disadvantages into consideration, Lithium-Polymer is chosen as the optimal battery type.

Table 3.1: Decision Matrix Battery Type

Battery type	Advantages	Disadvantages
Lead-Acid	- Non-cylindrical shape - Reliable - Low Cost	- Low energy density - Big size, high weight
Nickel Cadmium	- Many charge/discharge cycles	- Memory Effect - Toxic metals - Moderate energy density - Cycindrical shape - Self-discharge rate high
Nickel-Metal Hydride	Similar to Nickel Cadmium but: - Higher specific energy - No toxic Metals - No memory effect	Similar to Nickel Cadmium but: - Less charge/discharge cycles
Lithium-ion	- High energy density	- Cylindrical shape - Requires specific protection system
Lithium-ion Polymer	- High energy density - Non-cyclindral shape - Low profile - High discharge rate	- Higher price - Requires specific protection system

Integration in Design

Lithium-Polymer batteries have a nominal voltage of 3.7 V. As stated above, it is inefficient to directly convert from this voltage to the 24 V, which is needed for the finger force feedback subsystem. To achieve higher efficiency, two battery cells can be connected in series. This gives a nominal voltage of 7.4 V. The disadvantage of connecting multiple cells in series is the mandatory use of a balancing system between the multiple cells to ensure safety and durability of the cells. From 7.4 V highly efficient boost converters are available that can convert this input voltage to 24 V. Connecting more than two cells in series makes balancing even more difficult and increases size as well. This makes connecting two cells in series the optimal design choice.

Next to choosing the amount of cells, the cell capacity also has to be chosen. This is the amount of energy stored in the batteries. As already mentioned in Ch. 2 the glove should have equal or better specifications than the current model. The wireless kit, that is in development for the current SenseGlove, can last around 30 minutes on maximal power dissipation. To achieve this in the SoftGlove, the maximum power dissipation has to be estimated. Given the nominal battery voltage of 7.4 V, a maximum of 2.5 A can be drawn. At this power dissipation the battery must last 30 minutes or more, so a capacity of at least 1250 mAh is needed. A battery is chosen with 1500 mAh capacity, where a maximum continuous current of 4.5 A can be drawn. The size is 66x32x6.5 mm, such that the battery can fit comfortably within the width of most wrists. The weight of two cells is 60 g, not more than the weight of an average watch. These two cells are connected in series to achieve the required input voltage of 7.4 V.

3.1.2. Battery Charger

Since the system will be charged over USB the charger needs to accept an input voltage of 5 V. Unfortunately there is currently no IC available with support for boost mode charging, balancing and protection of a 2 cell (2S) lithium-polymer battery. Therefore a separate battery protection and charging IC is used. A single lithium-polymer cell is rated at a maximum of 4.2 V, two cells in series are rated at 8.4 V. Therefore the charger must be able to charge the lithium-polymer battery to 8.4 V. The IC used for charging the battery is the BQ25883 from Texas Instruments. This is a 2S boost mode Li-Ion and Li-Po battery charger. It can charge the battery with a maximum current of 2 A. When using the battery as stated in Sec. 3.1.1 the charging time will be 45 minutes. The final circuit and layout of the charger can be found in Appendix A.2 and A.3 respectively.

3.1.3. Battery Protection

As stated above lithium polymer batteries need some types of protections. The cells of a Li-Po battery get damaged when they are charged or discharged too far. In case of over discharge the battery will lose some of its capacity and its self-discharge rate will increase. In the case of over charge, the battery might catch fire or even explode. This poses a safety hazard that is not ethically permissible in a consumer product. Because of this, a solid protection circuit is needed. As stated in the section above there is no IC available that can charge, protect and balance a 2S battery. Therefore a separate protection IC is necessary. The battery protection IC that meets all these requirements is the BQ28Z610. While this IC is marketed as a gas gauge, a circuit meant to determine the state of charge of the battery, it also has many protections built in. The IC features over- and undervoltage protection, overcurrent protection, short circuit protection and overtemperature protection. Apart from these protections it also has the ability to balance a 2S battery. It therefore includes all the desired features that the battery charging circuit lacks. The final circuit and layout can be found in Appendix A.1.3.
Unfortunately the battery protection circuit is untested at time of writing. This is due tot the fact that the footprint of the IC was drawn incorrectly in the first PCB, both in terms of size and orientation. However, this has been rectified for the final prototype and the circuit has been checked multiple times to ensure there are no errors.

3.2. Microcontroller

The subsystems of the glove need to be controlled by a microcontroller. Since the desire was to make the system wireless a microcontroller with integrated wireless functionality is ideal. The ESP32 microcontroller was therefore chosen for the first design as it provides a sufficient amount processing power, storage, IO pins and has integrated Bluetooth and WiFi connectivity. For the final prototype the ESP32 Pico was selected. The Pico has all the same functionality as the bigger modules, but is a lot smaller with its 7*7mm QFN package and requires no external components like crystals since they are builtin to the package. Even though the Pico has Bluetooth and WiFi functionality, it does not have a built-in antenna. Therefore an external antenna has to be used. The Proant 440 was selected, because of it's simplicity, small size and good performance.

3.3. Programming Language

The chosen ESP32 supports the use of a multitude of programming languages, each with their respective advantages and disadvantages. The programming languages that were considered were Micropython, Arduino and ESP-IDF. The latter is the official development framework based on C provided by the manufacturer of the ESP32. Micropython has the advantage that it is easy to write and especially easy to debug since it is an interpreted programming language. This makes it possible to send commands and read out contents of variables over USB without needing to recompile and upload the code. There are however fairly major disadvantages to this approach. Micropython is slow when compared to Arduino and especially to using ESP-IDF and it provides little flexibility in regard to for example, assigning which pins the I^2C bus uses. Another disadvantage is that only a few people in the group have experience with Python and would therefore require some studying of the syntax and behaviour to write proper code. The Arduino programming language benefits from many built-in functions for controlling for example the I^2C or SPI bus and it supports the C and C++ languages. However, since it is designed to run on a multitude of microcontrollers it features the same flexibility disadvantage as Micropython and is still not as fast as C or C++ code written specifically for the used microcontroller. This is provided by the ESP-IDF, which stands for the Espressif IoT Development Framework. This is the most low level language that has a similar structure as C and C++ and thus provides only limited pre-made functionality, it does,however provide a lot of flexibility and speed. Since a main limiting factor in this project is latency, execution speed of the commands is critical. Furthermore since the whole group has experience in writing C and C++ code from Bachelor courses this would be relatively familiar. Therefore the ESP-IDF was chosen for developing the software that would run on the final prototype. For software development reasons the ESP-IDF code for all subsystems has to integrate with the current SenseGlove communication protocol that is described in [22].

3.4. Latency Budget

One of the most immersion breaking parts of virtual reality experiences is latency. It is therefore part of one of the major requirements, namely that the average latency may not be more than 40ms. In order to understand which parts of the design have the highest latency a latency budget was constructed. First of all an estimation was made regarding the various components of the design. After the design and assembly, the actual latencies of the components was measured to check if the estimations were correct. The wireless communication, processing on the microcontroller, the driving of the finger force feedback actuators, the per finger vibrotactile feedback and the Lofelt circuitry were considered in the estimation of the latency budget. The estimated latency budget can be seen in Tab. 3.2. The latencies of the different subsystems have been measured and can be found in Tab. 3.3. The latency of the finger force feedback stays the same because it is based on the known switching delay and rise time of the MOSFETs.
An important matter to consider about latencies is the exact definition of the latency. The latency can be taken as the purely electrical or processing latency but it can also include the mechanical latency of the (vibration) motors. In deliberation with SenseGlove, it was determined that latency would be defined as the time between the computer sending the data to the moment the system sends the signal to the actuators. So mechanical latency and latency within the PC software is not taken into account. Additionally, the latency of the microcontroller was not measured in the final design as it was already included in the latencies of the subsystems. The latency of the driver in the Palm vibrotactile Feedback department was hard to determine. This is due to the nature of the output, which is explained in the palm vibrotactile feedback report [2]. The latency of the palm vibrotactile feedback was estimated based on the data sheets.

Table 3.2: Estimated latency budget.

Component	Estimated latency
Wireless communication	10 ms
Microcontroller	1 ms
Per finger force feedback	0.1 ms
Per finger vibrotactile feedback	2.5 ms
Palm vibrotactile feedback	4 ms

Table 3.3: Measured latencies per subsystem.

Component	Measured latency
Wireless communication	7 ms
Per finger force feedback	0.1 ms
Per finger vibrotactile feedback	1.9 ms
Palm vibrotactile feedback	0.1 ms

3.5. Broad Design Choices

Some general design decisions were made during the design process. Firstly the type of component packages to use had to be chosen. Since everything had to be soldered by hand, BGA packages would be very difficult to solder properly. As can be seen in Fig. 3.1a the package has pins on the bottom which are very hard to reach during soldering. BGA is therefore avoided. The same goes for QFN packages, while they are easier to solder than BGA they still pose a challenge. However, the QFN package ended up being almost impossible to avoid in some cases. In Fig. 3.1b the QFN package is shown, it can be seen that the soldering pads are on the bottom but also reachable from the side. Another component choice was regarding the size for the passive components like resistors, capacitors, etc. Of course having smaller components would lead to an overall more comfortable design for the glove. This is due to a better fit on the wrist, because of the smaller PCB size. However, this would again make it hard to solder by hand. Therefore the imperial 0805 component size was chosen as a good compromise between size and ability to solder by hand. However, for the final prototype the space constraints were so tight that for the finger vibrotactile feedback subsystem, components with the size of 0603 were chosen. Another decision with a major impact on form factor was the amount of

layers of the PCB. With more layers less space is required to route all the wires as well as the fact that it improves power distribution and shielding due to the ability to add more power and ground planes. The downside of going from a 2 to a 4 layer PCB is monetary cost, with a 4 layer PCB being almost twice as expensive [20]. For the first PCB a 2 layer design was made and manufactured. Because of this experience and space constrains it is decided to use a 4 layer PCB for the final prototype.

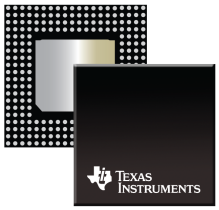

(a) BGA package [25].

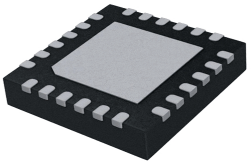

(b) QFN package [26].

Figure 3.1: BGA and QFN packages

3.6. General System Overview

In Sec. 2.3 all subsystems that are integrated in the SoftGlove are discussed. In Fig. 3.2 an overview of all connections between these subsystems is shown. The subsystems are abbreviated by FFF for per finger force feedback, FVF for per finger vibrotactile feedback and PVF for palm vibrotactile feedback. The blue lines represent the data lines between the modules, where the numbers show the amount of data lines. The red lines represent the power lines between the modules with the voltages shown on the lines. The USB block represents an USB micro input to charge the battery and connect to the microcontroller for programming. Furthermore, the power conversions block consists of a buck converter to create the required 5 V as well as a boost converter to generate the 24 V for the finger force feedback.

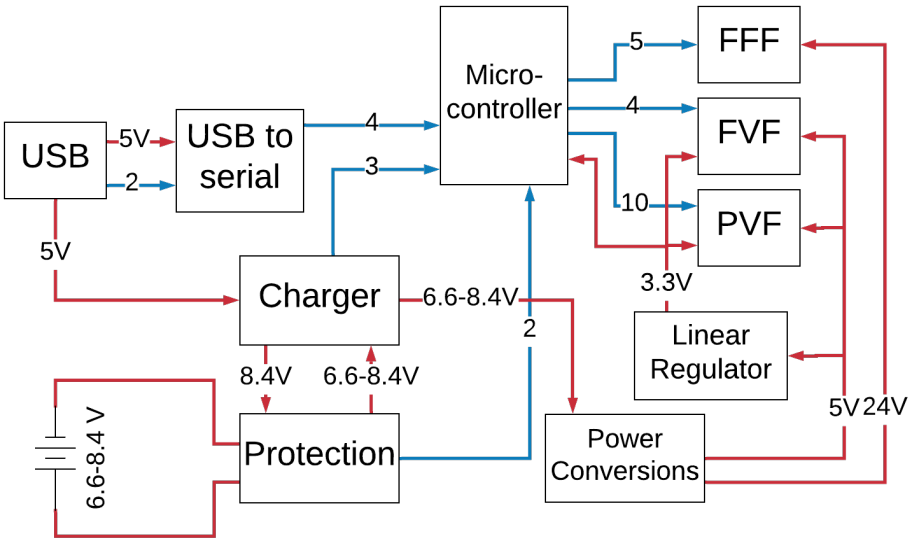

Figure 3.2: SoftGlove system overview. The subsystems on the top right are abbreviated as follows: Finger Force Feedback (FFF), Finger Vibrotactile Feedback (FVF) and Palm Vibrotactile Feedback (PVF).

All data lines are connected to the microcontroller. When determining all the data lines to the microcontroller, specifications had to be taken in account. First of all some pins output a PWM signal while the microcontroller is booting. Second, some pins are not allowed to be pulled up or down when the microcontroller is switching on. This is since these pins are responsible for selecting the boot mode. Third, some pins are specified to be just an input or just an output pin. The pin layout is therefore carefully designed and can be found in detail in Appendix A.7.

3.7. PCB Layout

The PCB stage consisted of two stages. A first PCB which is mainly focused on the functionality of the subsystems. The second PCB, which will be a revision of the first PCB, is mainly focused on the form factor and the placement of the subsystems. The second revisions will be the final prototype. The first PCB is 10.5 cm by 14.5 cm which is not the size that meets the requirement to fit on the wrist. The functionality of all subsystems is discussed and tested together with the revisions for the individual subsystem in the theses as described in Sec. 2.3. The layout of the second PCB, the final prototype, will be discussed in this section. As stated in Sec. 3.5, the first PCB is made with just 2 layers and the second PCB with 4 layers.

3.7.1. General Improvements for the Second PCB

After soldering and testing the first PCB, some general improvements had to be made when designing the second PCB. These improvements are listed below.

- A reset button for the microcontroller is needed.
- A power switch to turn the whole system on and of is needed.
- More test points need to be placed where possible.
- Pull-up resistors are required for both I^2C buses.
- Capacitors with a small capacitance need to be placed as close to the ICs as possible.

3.7.2. Final PCB Layout

All the improvements that are discussed in Sec. 3.7.1 together with the improved subsystems led to the final PCB layout that is shown in Fig. 3.3. The circuits schematics of the final PCB can be found in Appendix A.1. The final layout consists of two PCBs that both have a size of 40 mm by 70 mm, which is considerably smaller that the first PCB. The choice for two small PCBs gives the possibility to mount one PCB on the top of the wrist and the other one on the bottom of the wrist. Each PCB is mounted with one of the lithium-polymer cells, so a cell on the top and bottom of the wrist which can together deliver the 7.4 V. In Fig. 3.4 it is shown how this construction is set up. The PCB has all the components placed on one side to make sure nothing collides with the battery cells. The structure and design of all separate layers of the final complete PCB can be found in Appendix A.2.

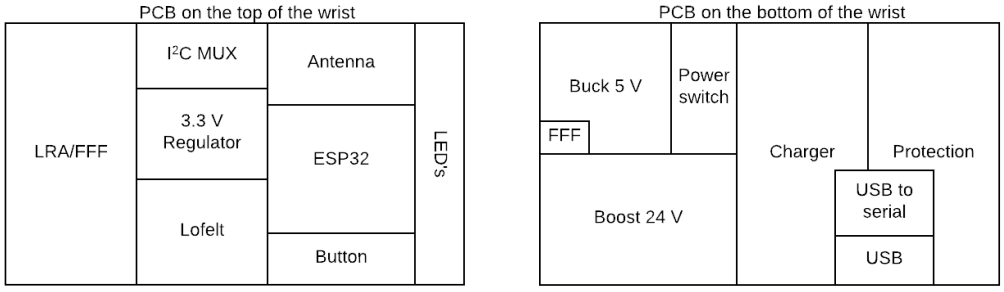

(a) Top PCB layout.

(b) Bottom PCB layout.

Figure 3.3: The layout of all subsystems on the final PCB

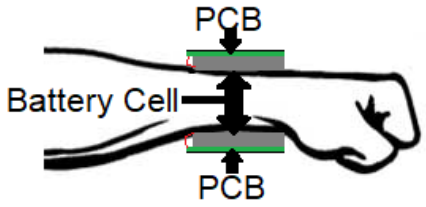

Figure 3.4: Mounting of the PCB and battery to the arm of the user.

4

Finger Force Feedback Design

In this chapter the design process of the finger force feedback subsystem is described and all design choices are justified. An overview of the finger force feedback and relevant subsystems is shown in Fig. 4.1. The designs of the parts colored in blue are part of the finger force feedback subsystem. At first the actuator characteristics were determined and the actuator control system was designed. Using the knowledge of the actuator characteristics and design, the power conversion designs were made, which includes both a boost and a buck conversion.

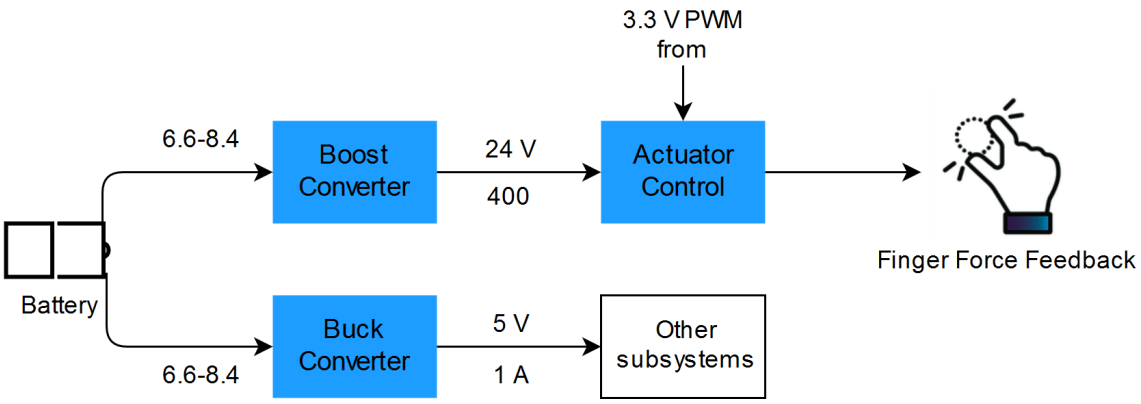

Figure 4.1: Black box of the entire finger force feedback system

4.1. Actuator Control Design

The actuators are the actual finger force feedback mechanism. The actuators are able the hold back the fingers when squeezing them. The actuators need to be controlled such the force they are performing on the fingers can be adapted depending on the needed feedback. The characteristics and control of the actuators are outlined and discussed.

4.1.1. Finger Force Feedback Actuator

The actuators used for the SoftGlove were already defined by SenseGlove, thus no design choice was to be made for the actuators. However, a lot of design choices for the subsystems connected to the actuators had to be made, to make sure that this subsystems are able to handle the characteristics of the actuator. Therefore determining the characteristics of the actuators in detail is of great value. The actuators are provided by the company SG Transmission. The original data sheet from SG Transmission can be found in Appendix B.6. Although provided in the data sheet, because of the importance of the actuator characteristics, the resistance with respect to time is verified by means of a test.

Internal Resistance With Respect To Time

The actuator becomes hot during intensive and long use. Keeping the temperature of the actuators low is not a requirement because the actuators fall outside the program of requirements. The hand of

the user is protected against the heat from the actuators. However, the change in resistance of the actuators due to intensive and long use is relevant for the design. Therefore a resistance test with respect to time was done. In this test the input of the actuator was connected to a programmable DC power supply. A voltage of 20 V, which is almost full power, was applied to the actuator for 10 minutes. The resistance of the actuator was measured every 30 seconds. The results of this test can be found in Fig. 4.2. It can be clearly seen that the resistance of the actuator increases when the time is passing. The resistance starts at 308 Ω and increases to almost 360 Ω after 10 minutes. However, the gradient of this graph decreases over time. This trend corresponds with the trend from the data sheet, which is shown in Appendix B.6. Therefore can be concluded that the internal resistance of the actuator will not drop below 300 Ω under normal operation conditions. This is an important actuator characteristic for designing the boost converters, since the heaviest load determines the current that the boost converter must be able to deliver.

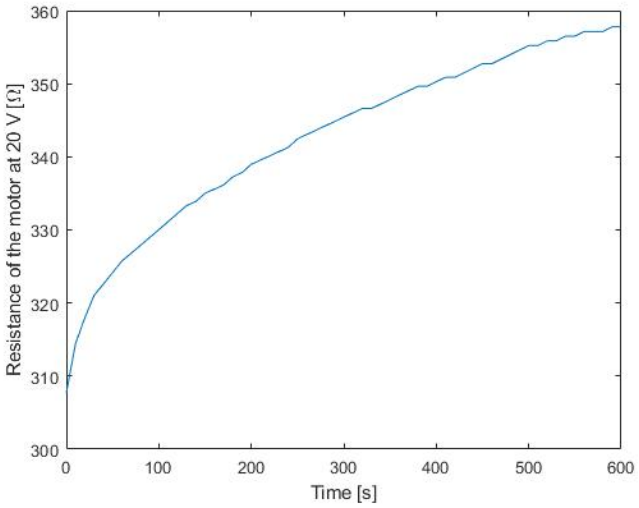

Figure 4.2: Actuator resistance with respect to time

4.1.2. Control Design

In order to change the force applied to a user depending on the needed level of feedback, the actuators need to be controlled. The actuator will not work on a fixed voltage, but at different voltages in the complete range between 0 V and 24 V. This 24 V is the maximum voltage, applied at the actuator, needed for the application. These different applied voltages determine the force feedback the actuators exert. This is valuable, because different objects in virtual reality require different strengths of feedback given to the fingers of the user. This gives the user the ability to squeeze a soft object like a ball, but not a hard object like a phone. In Sec. 4.2.1 is explained how 24 volt is made available from the input voltage. In the range from 0 to 24 V at least 100 different voltage levels are required, as shown in the program of requirements in Sec. 2.4. To create this range of voltages, Pulse Width Modulation(PWM) was used. PWM is used to reduce the average voltage, and therefore power, that is delivered to the load. This is done by switching the system on and off really fast. By changing the duty cycle of the switching, the power delivered to the load can be increased or decreased. When the duty cycle is 80%, the system will be switched on for 80% of the time and will be switched off for 20% of the time. This means, when applying a duty cycle of 80% the voltage over the actuator will be $0.8 * 24 = 19.2$ V. This PWM signal was created in the microcontroller and sent to the finger force feedback system. However, the PWM signal from the micrcontroller had an amplitude of 3.3 V which is obviously not sufficient to drive the actuators directly.

MOSFET

A MOSFET is used to control the actuator with the 3.3 V PWM signal from the microcontroller. The MOSFET is able to regulate the 24 V signal with the smaller 3.3 V PWM control signal. The MOSFET is able to switch with a frequency of 25 kHz. The switching frequency of the MOSFET was determined with the switching frequency of the 3.3 V control signal that is set at 25 kHz in the microcontroller. The

MOSFET was not placed on the 24 V line of the actuator, but on the ground line of the actuator. This is because the gate-source threshold voltage of a MOSFET is typically 1.5 V, which means that the gate voltage has to be at least 25.5 V when placed on the 24 V line. When the MOSFET is placed on the ground line of the actuator, the gate voltage has to be at least 1.5 V. In this case, the 3.3 V from the microcontroller is sufficient to control the gate of the MOSFET. The PWM signal that is connected to the gate of the MOSFET switches from 0 V to its amplitude of 3.3 V. To make sure the 0 V of the PWM signal is really 0 V, a pull down resistor was used. This resistor has a relative high resistance of $R = 100k\Omega$ and is connected between the ground and the gate of the MOSFET. This resistor ensures that the gate is not floating when the PWM signal is at 0 V. For the final design the N-channel BSS138L MOSFET was used. With a N-channel MOSFET, the current flows from the source to the drain. The MOSFET circuit which controls the actuator can be seen in Fig. 4.3a.

Flyback

The finger force feedback actuator can be represented as an inductor and a resistor in series. The resistor in series represents the small resistance of the inductor's wire windings. When the MOSFET is closed, the 24 V of the boost converter is applied to the finger force feedback actuator. Current will flow from the boost converter through the inductor and the resistor. The increase in current will cause a back EMF voltage across the inductor which opposes the change in current. The current through the inductor increases slowly because the change in current is limited at a constant value of V/L. Where V is the boost converter voltage of 24 V and L the inductor inductance of $L = 5.6\mu$H . When maximum energy is stored in the inductor's magnetic field, the 24 V will be completely dropped over the resistor. When the MOSFET is opened, the current drops rapidly. However, the current through an inductor can not suddenly change. The inductor will resist against current drop with a very large induced voltage that has a polarity opposed to the battery voltage. To prevent the MOSFET from these sudden voltage spikes, a diode was connected in parallel to the actuator. This diode is in reverse bias seen from the 24 V line, so it is not conducting current when the MOSFET is closed. The circuit design including the diode is shown Fig. 4.3b.

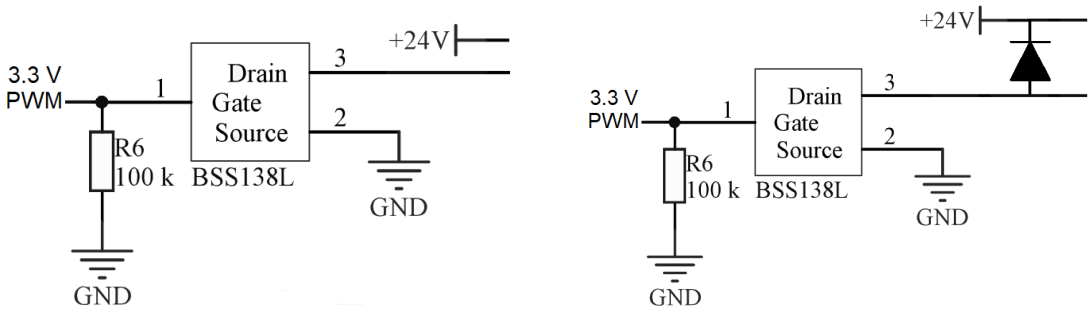

(a) MOSFET Circuit

(b) MOSFET circuit with diode

4.2. Power Converters Design

The power supply for the actuators used for the finger force feedback are two Lithium-Polymer cells, with a nominal voltage of 3.7 V each. These cells are connected in series, so the nominal voltage of the the available power supply is 7.4 V. The maximum voltage each battery can supply is 4.2 V. The minimum voltage is 3.3 V. This means the voltage that the batteries deliver, can differ between 6.6-8.4 V.

The actuators that must be able to deliver the force needed for the finger force feedback are provided by SenseGlove. Clearly the nominal battery voltage is not sufficient to drive the actuators at full power, so power conversion to 24 V was needed. The solution to this is a DC-DC boost converter. As shown in the data sheet in Appendix B.6, at full power each actuator draws around 80 mA, which means that all five actuators draw a current of 400 mA together. In the Program of Requirements in Ch. 2 is described that the total power must be 20 W or lower. The power needed for the force feedback actuators is already $P = U \cdot I = 24 \cdot 0.4 = 9.6W$ in case of 100% conversion efficiency. Since other subsystems also use power, it is important the efficiency should be as high as possible and at least 90% as described in Sec. 2.4.

Next to the actuators, there are also other subsystems that can not be driven with the battery voltage of 6.6-8.4 V. Subsystems finger vibrotactile feedback and palm vibrotactile feedback subsystems need a 5 V input and the microcontroller needs 3.3 V input. At maximum power these subsystems together draw a current up to 1 A. For these systems, DC-DC buck conversion is needed. The power usage will not be as high as the power usage by the actuators, but still a high efficiency is very important to keep the overall usage as low as possible.

4.2.1. Boost Converter

In order to choose the best boost converter, certain trade-off criteria had to be discussed. A black box from the conversion process is shown in Fig. 4.4. From the general program of requirements, shown in Ch. 2 can be seen, that the relevant topics are minimizing the space on the PCB and making all conversions as efficient as possible to keep the power dissipation of the overall system as low as possible, below 20 W. Next to this, there is a latency requirement of 40 ms, but since the converters and actuator control systems have delays in the order of nanoseconds, this requirement is less relevant. Two chips were found for this task, the LTC3872 by Lineair Technology and the TPS55340 by Texas Instruments. These were chosen because they can supply enough current and voltage to drive the actuators at full power with an efficiency of 90% or higher. The switching frequencies of the LTC3872 and TPS55340 are 550 kHz and 1.16 MHz and are outside the hearing spectrum as required in Sec. 2.4. Because both chips seemed suitable and both had their own advantages, more research was done into both chips before choosing the optimal converter.

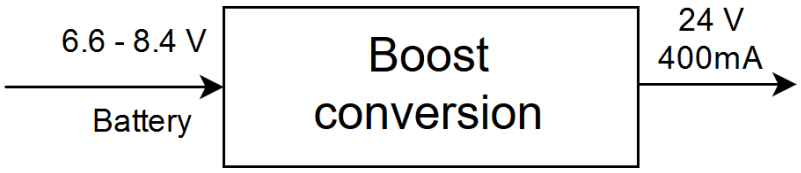

Figure 4.4: Black box of the boost conversion subsystem

Circuitry Design

The LTC3872 data sheet [27] shows an example circuit for 5-24 V conversion. Since the input voltage range is 2.75-9.8 V and the step-up to 24 V is smaller from 7.4 V, an even higher efficiency is expected with eventually some small component changes. The components are checked on their rated voltages and currents. According to these checks, the system should work as required in case a higher input voltage is used up to 8.4 V. Although all components are good enough in terms of functionality, one component is replaced: the inductor in the circuit. Since the original inductor has a relative big footprint, another smaller inductor with similar specifications was added. The footprint of this inductor was 2-3 times smaller. The circuit for this converter is shown in Fig. 4.5. As the converting efficiency is around 90% for a 5 V input according to the data sheet [27]. The converting efficiency, for the range of battery voltages, is expected to be higher than 90%.

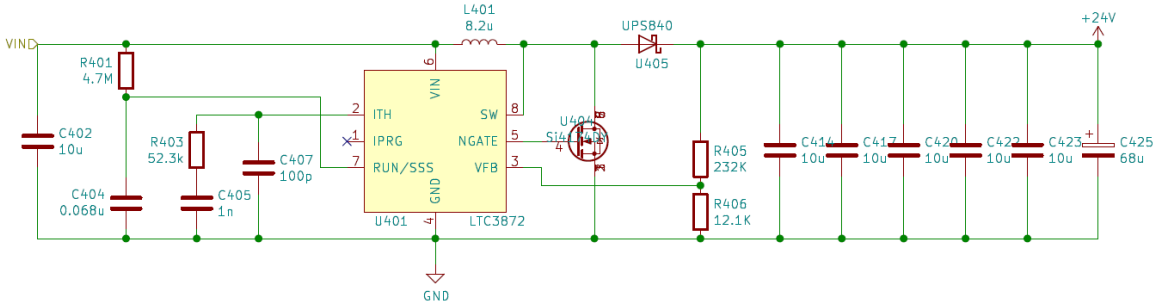

Figure 4.5: Boost converter circuit using the LTC3872 by Lineair Technology

The TPS55340 has both a data sheet [28] and online software provided by Texas Instruments available. The circuit needed for the chip to function properly was optimized for the input voltage range of

6.6-8.4 V and output voltage of 24 V by using the software from Texas Instruments. In this software, the costs, specifications and footprints of all components can be seen, as well as the efficiency of the total system when using those components. While using this software and choosing components, focus was on high efficiency while keeping the footprint minimal. The circuit, including all components, that was chosen is show in Fig. 4.6. As calculated by this software, the converting efficiency is between 95 and 95.6%, depending on the input battery voltage level. This is calculated when the optimal components as described by the software are used. However, the data sheet [28] shows only an efficiency between 92% and 95%, not taking into account all specific components.

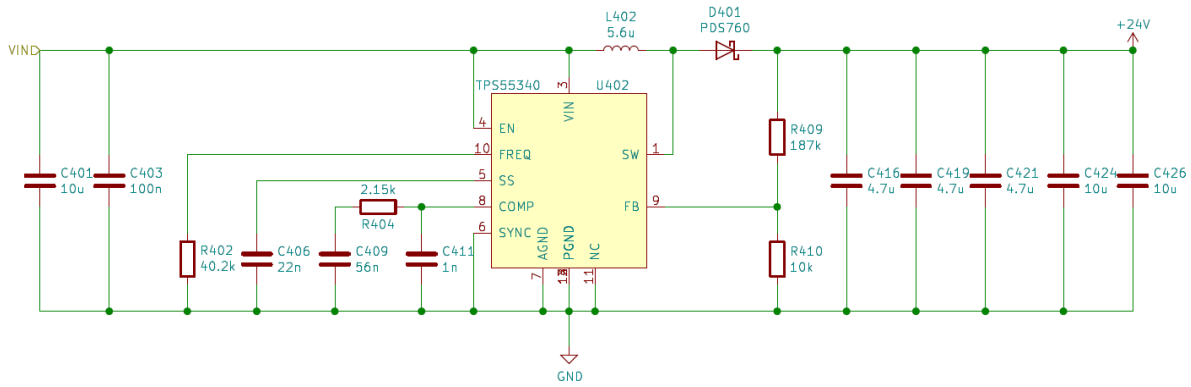

Figure 4.6: Boost converter circuit using the TPS55340 by Texas Instruments

Simulations

The LTC3872 chip was made available for simulation by Lineair Techonology in LTspice. This chip was simulated with a 5 V input, the voltage this circuitry is designed for. Beside this input voltage, the circuit is also with a 6.6-8.4 V input simulated. The circuit has to be optimized for 6.6-8.4 V for the SoftGlove. The loads used in this model were five resistors with a resistance of $R = 300\Omega$ connected in parallel, which represent the finger force feedback actuators. The circuits in LTspice are shown in Appendix B.1 and B.2. In this simulation the inductor model includes not only the inductance, but also the coil resistance. The simulations results are shown in Appendix B.5, B.6, B.7 and B.8 for 5 V, 6.6 V, 7.4 V and 8.4 V respectively as input voltage. As can be seen, the simulations met the requirements. According to these simulations the chip is able to convert from the battery input voltages to a stable 24 V needed for the finger force feedback actuators. The difference in conversion with various input voltages applied are minimal. The main different is start-up time. This varies between 1.7 and 2.1 ms, which is not causing any problems for the finger force feedback actuators.
From the simulation results can also be noted that the voltage does neither rise exponentially nor linear. Depending on the input voltage, there is a dip after approximately 0.2 ms, where the voltage drops around 1 V and then rises to 24 V after nearly 1 ms. Furthermore, when 24 V is reached, the voltage reaches first almost 25 V and then drops to a little lower than 24 V before supplying a steady 24 V output. This can be changed by replacing the output capacitors. When capacitors with high capacitor values are added, the first dip is smaller, but the converter reaches a steady 24 V later. Next to that, the little fluctuation around 24 V is bigger. When using smaller capacitor values, 24 V is reached quicker. However, the dip at the start gets bigger and for too small capacitors notable ripple on the output appears. The values given in the data sheet [27] seems to be the optimal values in the consideration between recovery time and output ripple.

The TPS55340 chip was available on online software from Texas Instruments itself. On this software, requirements can be filled in. The software then determines various circuitry options, where efficiency can be chosen with the different option within the component values. Real simulations are not possible while using this software, only guidance to circuitry design is provided. The circuit that was found optimal with the required efficiency is shown in Appendix B.3.

Testing

The LTC3872 was first soldered on a basic soldering board together with the whole circuitry around it, where attention was carefully paid to the PCB design guidelines in the data sheet, which can be seen in Appendix B.22. The setup of the soldering board containing the LTC3872 is showed in Appendix B.9 and B.10. First, tests were done with no load connected. Since the converter circuitry was optimized for an input of 5 V, conversion from 5 V was first tested. Conversion to 24 V went perfectly, as can be seen in Appendix B.13. Also from 7.4 V, conversion showed no problems.
Next, the circuit was tested using a load with a resistance of 75Ω, similar to the equivalent resistance of 5 actuators in parallel, which is 60Ω. In this case, the problem occurred that the converter was not able to convert to 24 V. At an input of 2.5 V, an output of 15 V was achieved. With an output of 15 V a current of 1.4 A was drawn. The output is shown in Appendix B.14 and the zoomed output is shown in Appendix B.15. At 2.9 V, the system clipped and only 0.18 A was drawn. The voltage dropped to 9.6 V. With an input of 5 V, an output of again 9.6 V was achieved, where 0.24 A was drawn, see Appendix B.16. When the load was attached, no flat constant output voltage of 24 V could be achieved. To eliminate the instability of the design, a decouple capacitor was soldered directly over the input of the LTC3872 chip. The optimal capacitor value was 1 ηF. Using this capacitor, the clipping did not start at 2.9 V, but at 3.8 V. This shows little improvement but not enough for the 6.6-8.4 V input voltage.
Because of sensitivity of the circuit, the circuit was tested on an existing PCB which is currently used in the exoskeleton of SenseGlove. This was possible, because SenseGlove uses the same boost converter in their current glove. This is a 2-layer PCB, where one layer is mostly used as ground. On this PCB attention was paid to the design rules such that ground loops were avoided. As expected, conversion from 5 V to 24 v worked properly with and without a load of 75 Ω. However, conversion from 7.4 V did not work. Again, instability caused problems. From 5.8 V the output voltage clipped again in the same way as for the previous instabilities.

The TPS55340 chip by Texas Instruments, was also tested on a basic soldering board and showed comparable results, instability showed up. A picture of the setup containing the TPS55340 is shown in Appendix B.11 and B.12. because of the instability, it was concluded that the instability could only be prevented by carefully designing according to the design guidelines. No deeper research to this boost converter was done to completely focus on the PCB design according to the guidelines. The design guidelines for the TPS55340 chip are shown in Appendix B.21.

4.2.2. Buck Converter

Similar trade-offs as for the boost converter are applicable and have been discussed. A black box of the required conversion is showed in Fig. 4.7. Minimizing footprint is very important, as optimizing efficiency. The TPS563231 chip by Texas Instruments is found that meets all requirements with a high efficiency up to nearly 96%. The chip can convert the battery input of 6.6-8.4 V to 5 V with a maximum output current of 3 A where only 1 A is needed. The switching frequency of the TPS563231 is 600 kHz which is outside the hearing spectrum as required in Sec. 2.4. Using the data sheet [29] and software provided by Texas Instruments, the optimal components needed in the circuitry around the boost converter chip were chosen. The circuit is shown in Fig. 4.8. The maximal power dissipation is at an output of 5 V where current of 1 A is drawn, which is equal to 5 W. According to the Texas Instruments software, the converting efficiency is between 95.1 and 95.8% at this maximal power dissipation, depending on the input battery voltage level.

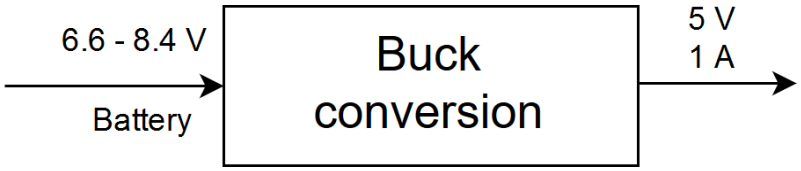

Figure 4.7: Black box of the buck conversion subsystem

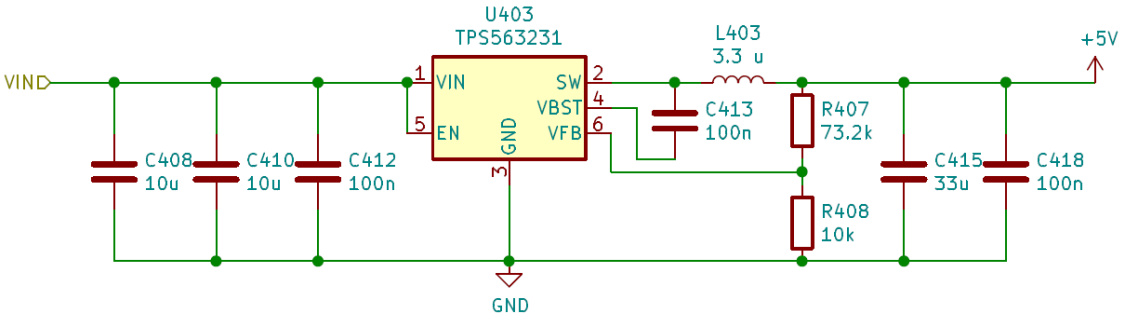

Figure 4.8: Boost converter circuit using the TPS563231 by Texas Instruments

Simulations

The TPS563231 chip is available for simulation on online software from Texas Instruments. In the same way as for the TPS55340 boost converter chip, requirements were filled in. The software then determined circuitry options. The circuit that was found optimal is shown in Appendix B.4. This circuitry was not tested on a soldering board, since instability due to high switching frequencies and no proper grounding was again to be expected. The buck converter should therefore be tested on a PCB which should be designed according to the design rules that are shown in Appendix B.23.

5 Prototype Implementation

In this chapter the implementation of the design discussed in Ch. 4 in a prototype PCB is discussed. First a PCB was designed which was made to test all functionality of the SoftGlove. After this, a second PCB was designed which is representative for the final prototype. Small improvements in functionality were done. As explained in Ch. 3, the form factor was also taken into account. This second PCB was designed more space efficient and contains components with smaller footprints in case necessary for integration in an actual SoftGlove.

5.1. PCB Design in Functionality Phase

After choosing the optimal components and designing the circuits, PCB design was done using KiCad. First the PCB design was done for the different subsystems separately. These subsystems were then connected to each other on one PCB. This first PCB was a test version, where the functionality was tested. The design was made such that as much as possible performance testing options were available. In this first design, the form factor and small footprint were not prioritized. As mentioned in Sec. 3.5, the PCB in the functionality phase has two layers.
Since high frequency switching paths in both the boost and buck converter circuits are used, PCB design is a very sensitive and therefore important step. When the layout is not designed carefully, instability and noise problems can appear. As described in Sec. 4.2.1, both boost conversion systems show clear instability on a soldering board. This proves the sensitivity and shows how crucial this step is for the power converters. After outlining the PCB design of the converters, the PCB layout of the actuator control system is discussed.

5.1.1. Boost Converter

To reduce instability in the PCB, attention was closely paid to the design guidelines of the used chips. For both circuits, the lower layer is mostly used as ground plane to reduce ground coupling. However, some signal traces had to be routed through the ground plane when no other option was possible. The Linear Technology chip already worked for the conversion of 5 V to 24 V, but not yet from 7.4 V to 24 V as mentioned in Sec. 4.2.1. The design guidelines, as shown in Appendix B.22, were strictly followed. The design was changed in comparison to the already existing design, to optimize performance such that the chip can also convert from 7.4 V to 24 V. The PCB layout design containing the LTC3872 chip is shown in Appendix B.24
For the Texas Instruments converter, the lower layer is fully used as ground plane. In the upper layer, components are placed as accurately as possible according to the design guidelines as shown in Appendix B.21. Components are also placed such that power planes could be made as big as possible to lower trace impedance and such that the switching trace is as short as possible. The PCB layout design containing the TPS55340 chip is shown in Appendix B.25.

5.1.2. Buck Converter

Next to the boost converter, also the buck converter switches at a high frequency and is therefore sensitive to instability and noise problems. The design guidelines for the buck converter can be found

in Appendix B.23. In the PCB layout design, the lower layer is used again mostly as a ground layer, except for some small signal traces. In the upper layer input, output and ground traces were made as wide as possible, partly using planes. The PCB layout design containing the TPS563231 chip is shown in Appendix B.26.

5.1.3. Actuator Control

Despite the switching from the MOSFET's in the actuator control design, the design is not sensitive for instability and noise. The design had no specific requirements regarding the placement of power or ground planes. However, some components had to be place on sufficient places to ensure the full functionality. The diode has to be placed as close to the actuator input as possible to reduce any impact of the voltage spikes. The pull down resistors had to be placed close to the MOSFET, to make sure the PWM signal at the gate of the MOSFET is at zero when is has to be zero. The design can be seen in Appendix B.27.

5.2. Performance in Functionality Phase

After designing the complete force feedback system, the PCB from the functionality phase is tested on performance. This performance check is needed before designing the prototype PCB. The theoretical performance that is described in Ch. 4 is verified. The procedure to validate this performance and the results of this performance from the force feedback design is discussed. Finally the design is concluded if all requirements as stated in Ch. 2 are met.

5.2.1. Boost Converters

To validate the performance of the boost converters, the conversion itself needs to be tested first. This circuit was tested using an input from a programmable power supply. The converter must be able to convert to a constant output voltage of 24 V, when an input voltage between 6.6 and 8.4 V is applied. This was first done without a load, secondly a load similar to the equivalent resistance of the finger force feedback actuators was applied. When a load is applied at the converter output it should be able to supply the required current. The converter has the highest change to instability when the maximum current is required.
If conversion shows no problems, validation of the expected conversion efficiency must be done. This was done by attaching a load similar to the finger force feedback actuators, and applying different input voltages between 6.6 and 8.4 V. Testing at minimal, nominal and maximal voltage is done to show the efficiency for all possible operating conditions. From these three tests a reasonable estimation of the average efficiency was concluded. The voltage and current at the input of the converter was compared with the voltage and current at the output. By calculating and comparing both the input and output power, the conversion efficiency was determined.
Next to this, the response to a load transient was determined in case no load is attached and suddenly a load is connected and when a load is connected and suddenly removed. The response of the converter says something about the performance. In the same way, the output response in case the power supply is turned off or turned on was determined.

LTC3872 Boost Converter

First, no load was attached to check whether the design was working correctly. Again it was first checked if it could convert from 5 to 24 V. Without load, a stable 24 V output was measured. Also from 7.4 V the converter was able to output a voltage of 24 V. Next, a load with an impedance of 58Ω was connected. At this point, instability as already shown in Sec. 4.2.1 showed up again. The output voltage dropped to 9 V. Converting from 7.4 V as input voltage did not change the instability at the output. The new design layout did not improve the functionality of the Linear Technology boost converter, but made it even worse. This boost converter is extremely sensitive for design mistakes, which makes the conversion of 7.4 V to 24 V very difficult. Therefore was decided to do further research on the Texas Instruments boost converter to improve this design.

TPS55340 Boost Converter

Similar to Linear Technology boost converter, this circuit was tested using a programmable power supply as power input. Since this system was optimized for a 6.6-8.4 V input, conversion from these inputs

was tested first without a load connected. The output of the converter showed a stable 24.2 V for all of these inputs. Following, a load of 58Ω was attached. This converter was able to output a voltage of 24.2 V when the maximal load was attached. This meant that strictly following the design guidelines of the Texas Instruments boost converter gives the ability to boost up to 24 V with the required current.

Efficiency Test To determine to what degree the converter meets the specifications, the efficiency was tested for various input voltages. Again the load of 58Ω was connected to represent the actuators. The results of the efficiency test are shown in Tab. 5.1. The efficiency is not as high as the theoretical efficiency. Still the average efficiency within the required voltage range is 91.78%, which meets the requirements.

Table 5.1: Efficiency test using a load equivalent to the actuators

V_{in}	6.62 V	7.40 V	8.40 V
I_{in}	1.605 A	1.423 A	1.246 A
P_{in}	10.63 W	10.53 W	10.47 W
V_{out}	24.21 V	24.20 V	24.19 V
I_{out}	0.400 A	0.400 A	0.399 A
P_{out}	9.68 W	9.68 W	9.66 W
Efficiency	91.14%	91.95%	92.26%

Start Up Output Response Even though the system normally functions in steady state and achieves a high efficiency as described in Sec. 5.2.1, there is more to know about the performance of the converter. To determine more characteristics on the behavior of the boost converter when the system is not in steady state, first a test was done to determine the start up response. Here the converter was connected to a programmable DC power supply and the output of the boost converter is measured using an oscilloscope. In Fig. 5.1 the response of the output from 0 V to 24 V can be seen. The first part of this measurement is the step in the beginning of the start up. This step up is to around 2 V which corresponds to the enable threshold voltage of the boost converter chip. The linear part after the step up is therefore the actual start up of the chip. The rest of the start up to 24 V does not correspond to inductor or capacitor voltage typical charge/discharge trends and is therefore likely to be the start up of the complete boost converter system including the compensation circuits.

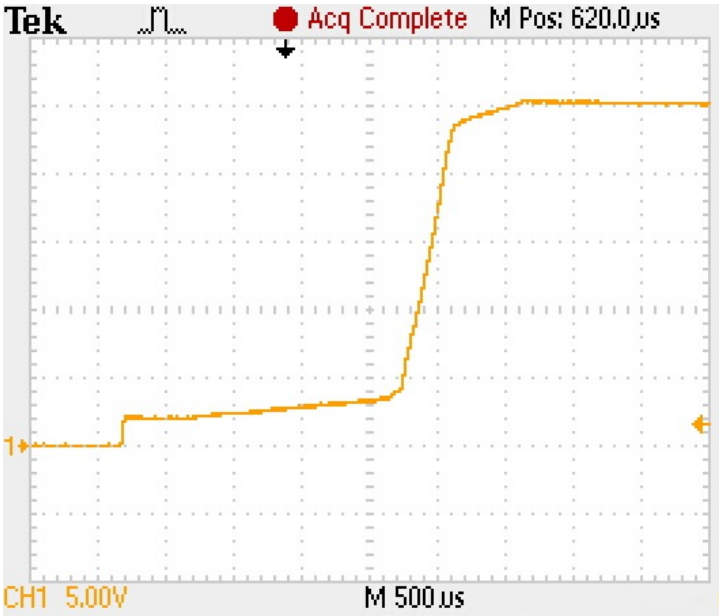

Figure 5.1: Turn on response without load

Turn Off Output Response Next to a start up response, also the turn off response of the system was determined. In Fig. 5.2 the result is shown from this test. In this test no load is attached to the output. In steady state the capacitors are fully charged. From this graph the RC time can be determined using Eq. 5.1 as shown in Eq. 5.2, where V_c is the voltage over the capacitors, V_s the nominal output voltage and t the discharging time. Values used in this equation were taken from the results.

$$V_c = V_s = \cdot \exp \frac{t}{RC} \tag{5.1}$$

$$RC = \frac{t_c}{\ln \frac{V_c}{V_s}} = 430ms \tag{5.2}$$

When looking at the circuit, theoretically the capacitors can only discharge over the feedback resistors and the chip, since they can not be discharged over the diode, which is in reverse bias seen from the output capacitors. In this case, a theoretical RC time was calculated by using the feedback resistors and the output capacitors, as shown in Eq. 5.3. The resistance of the chip is not taken into account. Since the 'R' is mostly determined by the $187k\Omega$ resistor, the chip in parallel to the $10k\Omega$ does not have a big influence. The theoretical value using only the feedback resistors does not come down to the same RC time as determined in Eq. 5.2.

$$RC = 34.1\mu F \cdot 197k\Omega = 6.7s \tag{5.3}$$

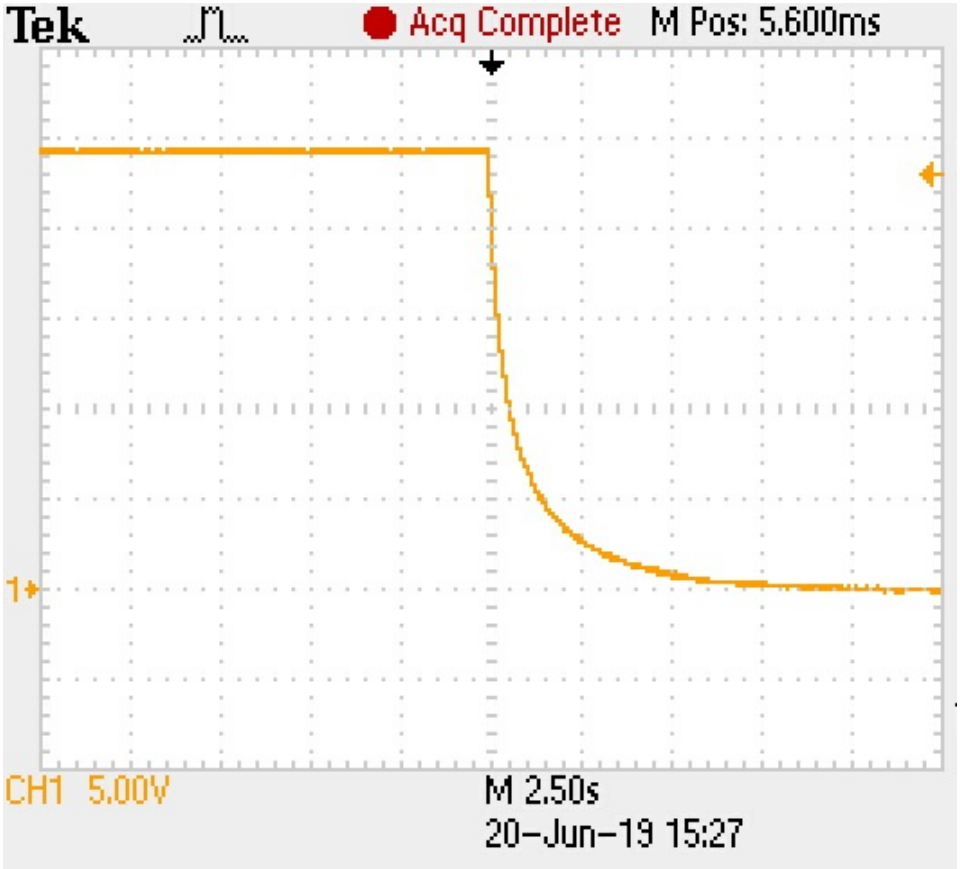

Figure 5.2: Turn off response without load

Detach Load Output Response Aside from the input transient tests, a test was done on the behavior when detaching a load. A load similar to the equivalent resistance of the actuators together was chosen. The boost converter was still connected in the same way, instead now there was first a load attached, such that steady state was achieved. At some point the load got detached. The output looked like shown in Fig. 5.3a. All results seen from the oscilloscope are shown in Appendix B.4.2. This result can

be explained again by the output capacitors but also the inductor in the circuit plays a role. First the output voltage increases because the inductor tries to maintain the current going through it, but there is no load which can draw that current. When the inductor is discharged, the output voltage does not drop immediately because the capacitors have to discharge. Since the output is an open circuit they have to be discharged by the rest over the circuit. Theoretically, the output capacitors would discharge in the same way as explained in Sec. 5.2.1. In Fig. 5.3b a zoomed in graph is seen from that input turn off response test. These curves have the same gradient, which shows the capacitors discharge in the same way in both cases.

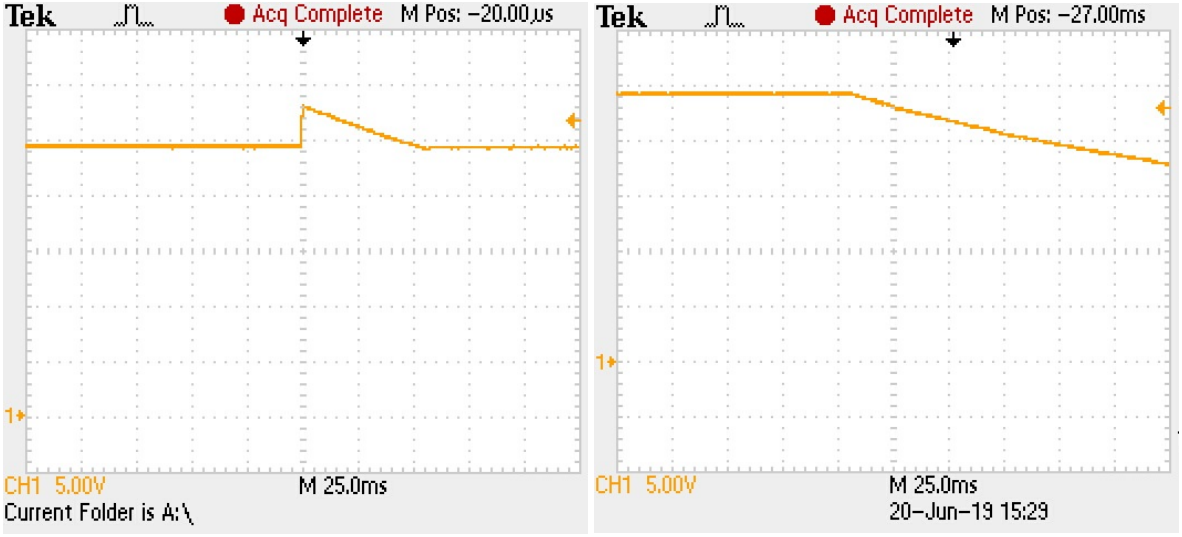

(a) Load Transient response for detaching the load (b) Input Transient without load attached zoomed in

Figure 5.3: Output response when detaching the load compared to the output response when the input is turned off

Attaching Load Output Response To determine the behavior of the converter when a load gets connected, a test was done. The output looked like shown in Fig. 5.4. The results of all tests are shown in Appendix B.4.1. In this graph first no load is attached. At the moment a load got attached, as can be seen there is a voltage drop to around 20.5 V after which it takes some time to go back to 24 V. This can be explained by looking at the output capacitors. At the time of this first drop, all the capacitors are charged fully. Then in the middle of the graph, the load is attached, which forces the capacitors to discharge to compensate for the chip which can not deliver this power to start up all at once. After around $50\mu s$ the capacitors are charged up again. From this charging up until full, the RC time can be determined. At the point the capacitor switch from discharging to charging, the capacitor voltage is $V_c = 20.5V$. The time it takes to back to $V_s = 24V$ is on average $t_c = 350\mu s$. For a RC charging circuit, the voltage across the capacitor, as a function of time is defined as can be seen in Eq. 5.4.

$$V_c = V_s \cdot (1 - \exp{(\frac{t}{RC})} \tag{5.4}$$

Using this formula, a value of the RC time can be estimated, which can be compared to the theoretical value of RC. In Eq. 5.5 is shown how the value of RC is determined.

$$RC = \frac{t_c}{\ln \frac{V_c}{V_s}} = 2.10ms \tag{5.5}$$

Since the value of the output capacitance and load resistance are known, the theoretical value of the RC time can easily be calculated as is shown in Eq. 5.6

$$RC_{theoretical} = R \cdot C = 58\Omega \cdot 34.1\mu F = 2.0ms \tag{5.6}$$

The estimated RC time is very close to the value of the theoretically calculated RC time, which proves that the voltage drop is caused by the output capacitors.

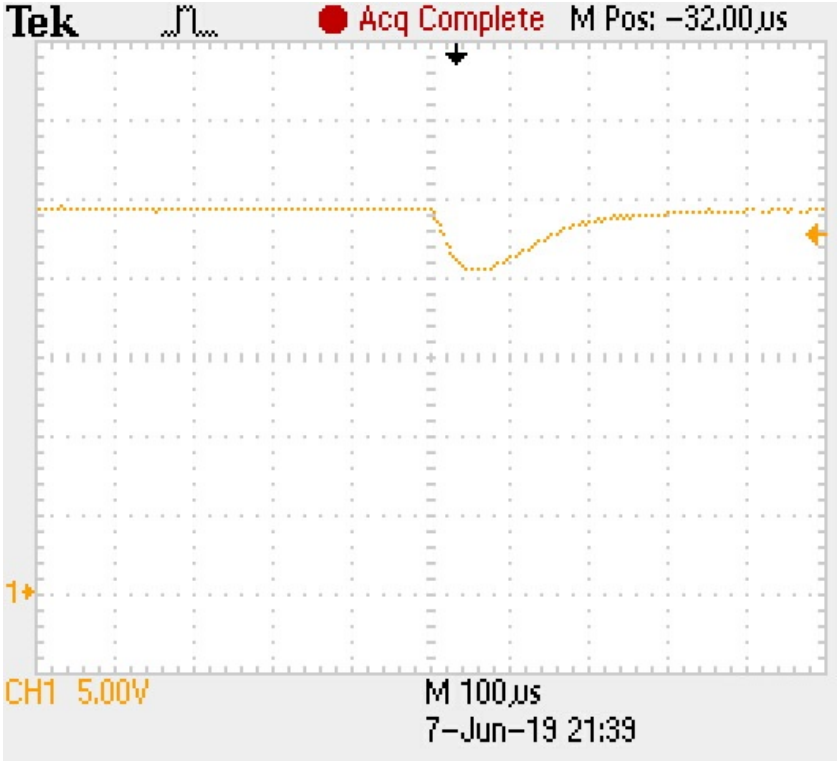

Figure 5.4: Attaching load Output Reponse

5.2.2. Buck Converter

Performance specifications regarding efficiency are difficult to validate for the buck converter. This is because the test point to measure the current directly after the buck converter was not taken into account in the PCB design. Validating conversion is possible by directly testing the other subsystems which use the voltage supplied by the buck converter. The subsystems connected to the buck converter are also the relevant load. When connecting all the subsystems, the buck converter was able to deliver a steady 5 V output to all this subsystems. This means the buck converter is able to convert the input voltage between 6.6-8.4 V to the required voltage of 5 V.

5.2.3. Actuator Control

To validate the performance of the actuator control system, the actuators can be connected to the 24 V output of the boost converter. A 3.3 V PWM signal can be programmed to the microcontroller, which is connected to the gate of the MOSFET. The validation of the actuator control was done for each control system separately. Because the MOSFET is connected to the ground it is not possible to directly measure a 24 V PWM signal. For validation two measurement points with respect tot the ground were used. The first one was connected to the positive pole of the actuator, which always has a voltage of 24 V. The second one was connected to the negative pole of the actuator, which switches between ground and being an open circuit. An open circuit means in this case a 24 V output. So the negative pole will switch between 0 V and 24 V. When subtracting the negative pole from the positive pole, the PWM signal over the actuator will be the result. The mean voltage of this PWM signal will be the actual voltage over the actuator. In Fig. 5.5 the 0% and 80% duty cycle are shown. The yellow signal shows the positive pole of the actuator and the blue signal shows the negative pole of the actuator. The red signal shows the actual PWM signal over the actuator. The measurements of 20%, 40%, 60% and 100% can be found in Appendix B.40a, B.40b, B.41a and B.41b respectively. All the measured voltages and current at different duty cycles can be found in Tab. 5.2. When the MOSFET starts switching the measured voltage is different from the expected voltage. This can be explained as the losses in the MOSFET regarding the rise and fall times. When adding up the voltage over the MOSFET and measured voltage the sum is around 24.0 V. This means the voltage drop over the MOSFET is around 0.4 V when it is switching.

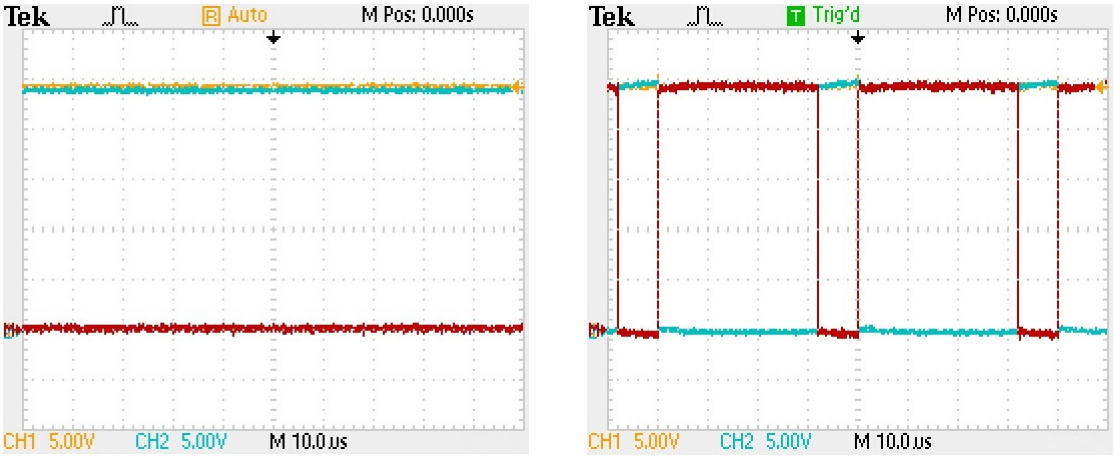

(a) Actuator test with a duty cycle of 0%

(b) Actuator test with a duty cycle of 80%

Figure 5.5: Actuator test with different duty cycles applied to the MOSFET gate

Table 5.2: Actuator control tests

Duty Cycle	Expected Voltage [V]	Measured Voltage [V]	Voltage over MOSFET [V]	Measured Current [mA]	Calculated Power [W]
100%	24.00	24.02	0	74.6	1.79
80%	19.20	18.88	5.18	60.6	1.14
60%	14.40	14.02	10.00	44.2	0.62
40%	9.60	9.15	14.93	29.4	0.27
20%	4.80	4.33	19.67	14.0	0.61

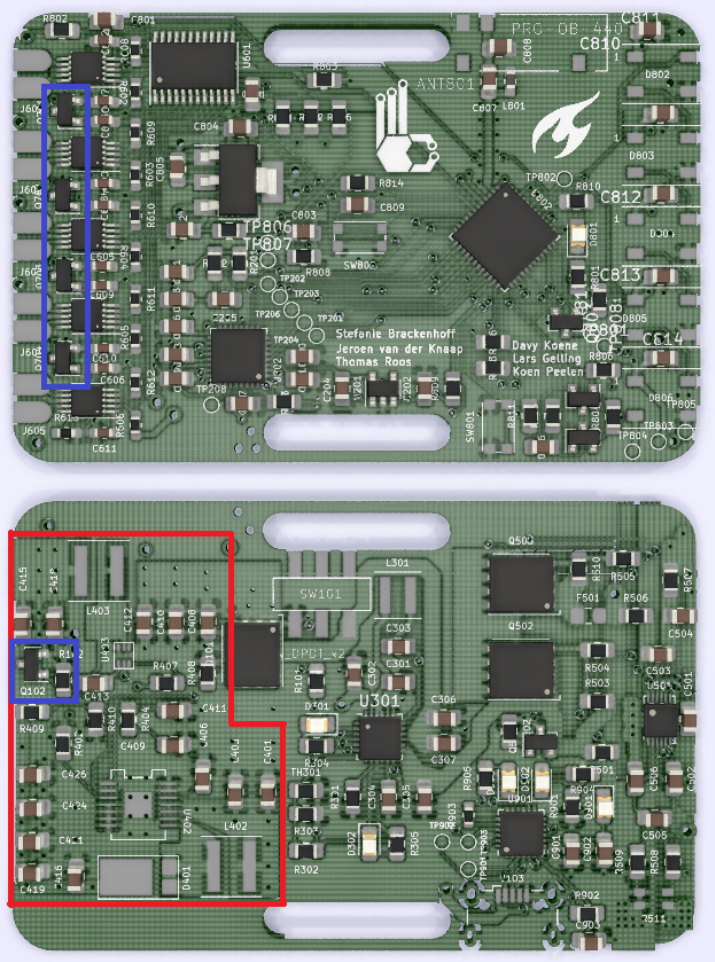

Figure 5.6: Final PCB design for the SoftGlove

5.3. PCB Design in Prototype Phase

After testing the first PCB design, a final PCB is designed. The results of the tests shown in Sec. 5.2 and more priority for PCB form factor and small footprint determined the layout of the final PCB layout. For this second PCB four layers are used, to minimize footprint and optimize tracing.
This prototype is representative for a final design, because both functionality and form factor needed for mass usage is included in this design. The final PCB design for the SoftGlove is shown Fig. 5.6. A full page image is shown in Appendix B.31. In this figure, the power conversion part is colored in red. The actuator control part is colored in blue. The schematics the power conversions of the final prototype PCB is shown in Appendix B.19.

5.3.1. Boost Converter

The circuit containing the Texas Instruments chip is used in the prototype PCB, because the TPS55340 performed better on the first PCB than the LTC3872 and its respective footprint is smaller. Possibly some component changes could have been done to minimize footprint, such as the input and output capacitors. Fewer capacitors with a higher capacitance values could be used instead of the current capacitors. However, to be sure of a working prototype, this has not been done.
The PCB layout was designed again to minimize the footprint, also using four layers instead of only two layers. The power conversion PCB design is shown in Fig. 5.7. Here the boost converter is colored in red. The PCB layout design for only the boost converter is shown in Appendix B.29. Following the PCB layout design rules, components were placed at a closer distance to each other to minimize the size on the PCB. Because the system does not use many small signals, not all four layers are needed for efficient routing. Because the middle two layers are thicker than the outer layers, the middle

layers generally are used for power (upper middle layer) and ground (lower middle layer). In the boost converter the upper layer is used for signal traces, a short wide plane for the high frequency switching path, the input power plane, the output 24 V line and ground planes. The second layer is used to make an input power plane and a big output 24 V power plane. The third layer is used as ground plane, shielding the entire circuit. The fourth layer is used to make an extra 24 V output plane below the boost converter. Because the power planes are placed in the upper layers and the ground plane in the third layer with dielectric in between, a capacitor is formed which filters out high frequencies. The big ground plane keeps the currents short and helps avoiding ground coupling. The big planes also minimize trace impedance, which is mostly important for the high current paths to minimize losses. Beside the minimization of trace impedance, heat dissipation is optimized when planes are used.

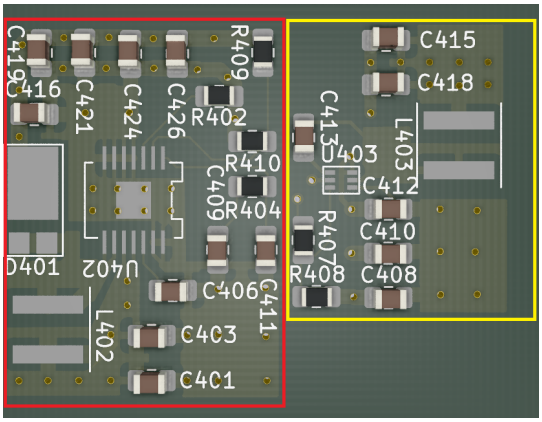

Figure 5.7: Final PCB design for the entire power conversion subsystem

5.3.2. Buck Converter

The buck converter functioned properly on the first PCB. To make sure the circuit works again on the revised PCB, no components changes have been done. Similarly as for the boost converter, less input and output capacitors with higher capacitance values are possible. But it was decided not to make changes to increase the chance of proper functioning.
To make the footprint on the revised PCB minimal, the layout of the buck converter was designed again. In a similar way as for the boost converter, the components were places closer to each other while still following the design rules. The design together with the buck converter is shown in Fig. 5.7. Here the buck converter is colored in yellow. The PCB layout design for only the buck converter is shown in Appendix B.29. The upper layer is used for signal tracing, the high frequency switching path, the input power plane and the 5 V output plane. The second layer is mostly used for the input power plane and the 5 V input plane. Also a 5 V trace for the enable is added in this layer. The third layer is fully used as a ground plane. The third layer is fully used as ground layer. The third layer is mostly used a ground layer, except for a corner where a trace from another subsystem needs to cross.

5.3.3. Actuator control

The actuator control PCB layout is quite straightforward. A minimal change is done, the flyback diodes were removed because they must be attached closer to the actuators outside the PCB. When the flyback diode is too far from the actuator a magnetic field between the actuator wires occurs. This magnetic field is created by the voltage spike that is explained in Sec. 4.1.2. This resulted in the MOSFET and pull down resistor as the actuator control components on the PCB. The final circuit of the actuator control can be found in Appendix B.20. It can be seen that only four actuator controllers are designed in this circuit. The fifth actuator controller is from the thumb and can be seen in the layout of the entire system in Fig. 5.6, where all actuator controllers are outlined in blue. This controller was routed on the bottom plate as shown in 3.3b. The finger vibrotactile feedback and actuators from the finger force feedback are both connected close to the fingers of the users. Therefore in the final prototype, the finger vibrotactile feedback and actuator control design of the four remaining fingers were merged together as shown in 3.3a for space optimization. Beside this merge, the footprints of the pull down resistors were downsized to 0603 instead of 0805.

6 Discussion

In this chapter the results from Ch. 5 are discussed together with the expected results of the final PCB. This final PCB design is representative for a final design, but yet some aspects are to be discussed. The validation of performance for the boost converters as described in Sec. 5.2.1 showed different results than expected.

The Linear Technology converter does not function as expected. Even on a previously designed PCB by SenseGlove, the circuit did not function properly for an input voltage of 6.6-8.4 V. For the design, focus was on optimizing the PCB layout, but clearly some important design rules were not followed close enough. When comparing the guidelines to the current SenseGlove design, it seemed that only one guidelines can have caused the problem. The others guidelines were followed actually closer than on the SenseGlove PCB. In the newly designed layout, the distance from the switching point to to the SW pin from the LTC3872 chip, is longer than in the SenseGlove design. According do the design guidelines this distance should be kept as short as possible.

The Texas Instruments boost converter functions properly as described in Sec. 5.2, but showed a lower efficiency than expected by 3-4% as shown in in Ch. 4. There are several possible reasons which have caused this difference in efficiency. Firstly, the software by Texas Instruments might not be very accurate. It calculates the optimal efficiency after filling in only the needed input voltage and the output current and voltage. This software might be based on an optimal model, which does not use all environmental factors and does not know the PCB layout. In addition, the data sheet shows lower efficiency values than the software does. Secondly there are losses in the boost converter by non-optimal components that can have deviations from their indicated value. Also a non-optimal PCB layout could have been responsible for a part of the losses.
The start up output response was also completely explained, as described in Sec. 5.2.1. A reasonable explanation was found which could cause this type of graph. However, it was hard to find out how this response could be changed by varying components. Because the behavior of the chip is not easily modeled and not shown in data sheets, this is hard to check.
The turn off output response, which is discussed in Sec. 5.2.1, was also not completely explained. The curve looks like an RC circuit discharging, which makes sense because the output capacitors and feedback resistors. When estimating the RC time from this graph, this did not match with the theoretical value of the RC time. The difference was so big that this could not be explained by tolerances of the resistors and capacitors.
The attach load output response, which is described in Sec. 5.2.1, does also not completely match the theoretically determined value. However, this can be explained by the tolerance on the capacitance and resistance values, which is up to 10%.
The Texas Instruments converter proved to work correctly and has a smaller footprint than the Linear Technology converter. The Texas Instruments chip was therefore the best boost converter, so the Linear Technology converter was used anymore.

For the Buck Converter the efficiency was not determined, As discussed in Section 5.2.2. Because no test point at the converter output was available, it was impossible to determine this efficiency without having to cut traces. Cutting the traces on the first PCB was not done because not yet is proved the final design functions properly. Since the buck converter circuit and its expected efficiency are similar to the boost converter circuit and efficiency, probably the buck converter efficiency is above 90%, but this could not be proven.

The Actuator Control meets all the required specifications. An additional improvement can be made with a change in MOSFET's to reduce the voltage drop over the MOSFET's. To improve space within the actuator control it is possible to reduce the size of the pull down resistors even more. This is not done in the final PCB design because the PCB is soldered by hand. When taking component sizes smaller than 0603, hand soldering becomes to difficult.

7 Conclusion

The finger force feedback subsystem is an important part for a future soft version of the current exoskeleton that is now used by the company SenseGlove. With finger force feedback the user of the glove is actively hold back when he or she tries to squeeze the fingers. For this SoftGlove the old electric design including the finger force feedback subsystem had to be redesigned. The new electric design had more components but must still be able to fit in a comfortable design for the user. The form factor was therefore extremely important with minimal space for all subsystems. A program of requirements is set up for the complete SoftGlove system and specific for the finger force feedback subsystem. All of requirements for the finger force feedback subsystem are met.

1. The boost converter is able to deliver a voltage of 24 V.
2. The SoftGlove has per finger force feedback.
3. The PWM signal to the actuators can have 256 levels.
4. The switching frequency of all switching components is above 25 kHz.
5. Converter efficiency of the boost conversion is above 91%.

A system is designed which can be implemented in the SoftGlove, which will not limit the capability and scale of implementation anymore. In the future, this SoftGlove may play a big role in the revolution of virtual reality related products.

7.1. Recommendations and Future Work

To minimize the footprint even more, certain output and input capacitors can be removed. Some of capacitors were added for testing purposes to have the ability to remove or add capacitance to the output or input of the power converters. These capacitors can be removed and the remaining capacitors can be increased to match with the desired value. A second improvement for minimization of the footprint is reducing the size of all capacitors and resistors from 0805 to 0603, or if possible even smaller.
Further improvements can be made regarding the finger force feedback actuators. These actuators were predefined by SenseGlove and could not be changed. When optimizing the actuator torque, voltage characteristics, the maximum voltage applied to the actuator can be decreased. The boost converter footprint can be made smaller and the efficiency can be increased, when the maximum output voltage is decreased.

A Appendix General

A.1. Schematic

A.1.1. Module overview

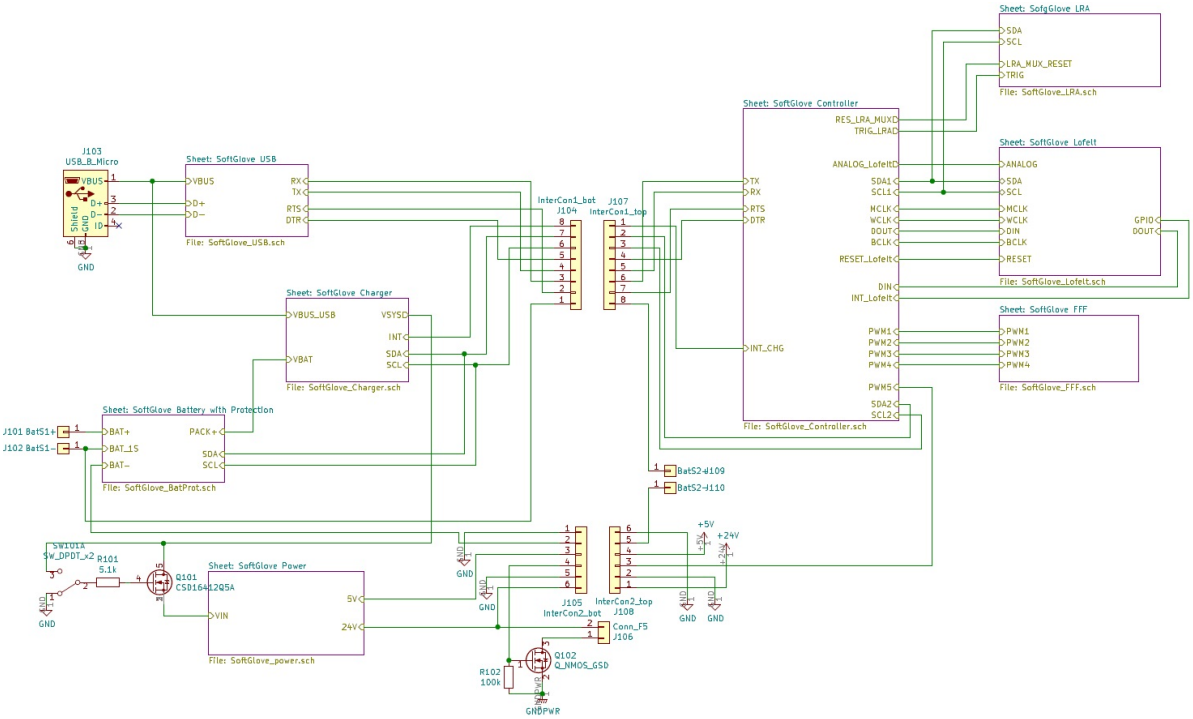

Figure A.1: Schematics of the complete system.

A.1.2. Battery charger

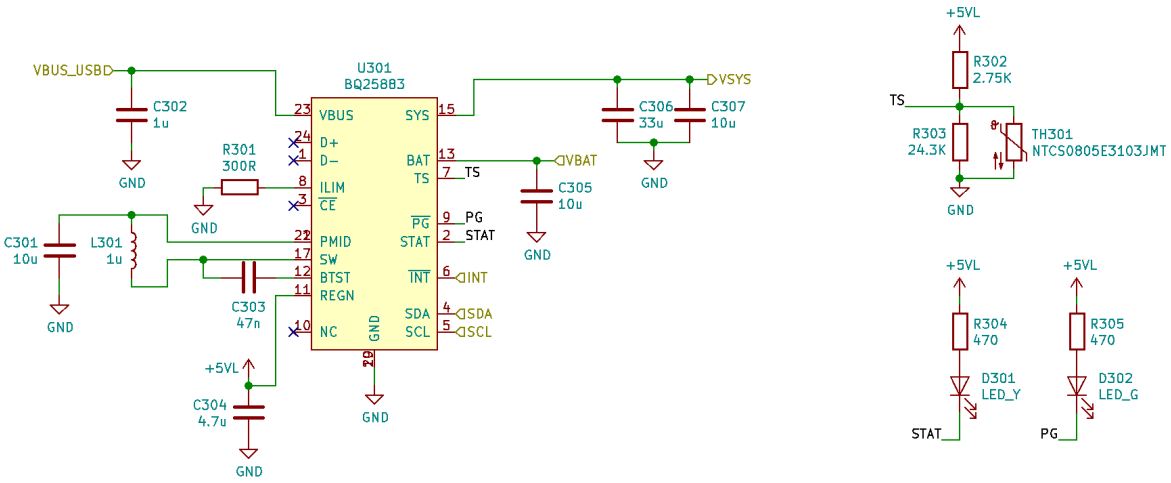

Figure A.2: Schematics of the battery charger.

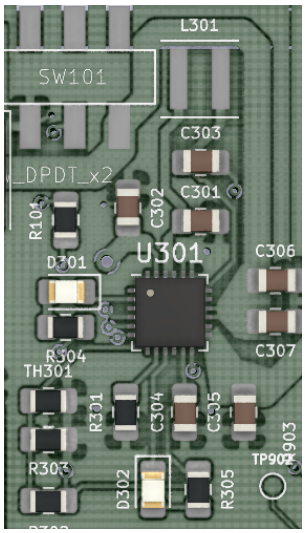

Figure A.3: PCB design of the battery charger.

A.1.3. Battery protection and USB

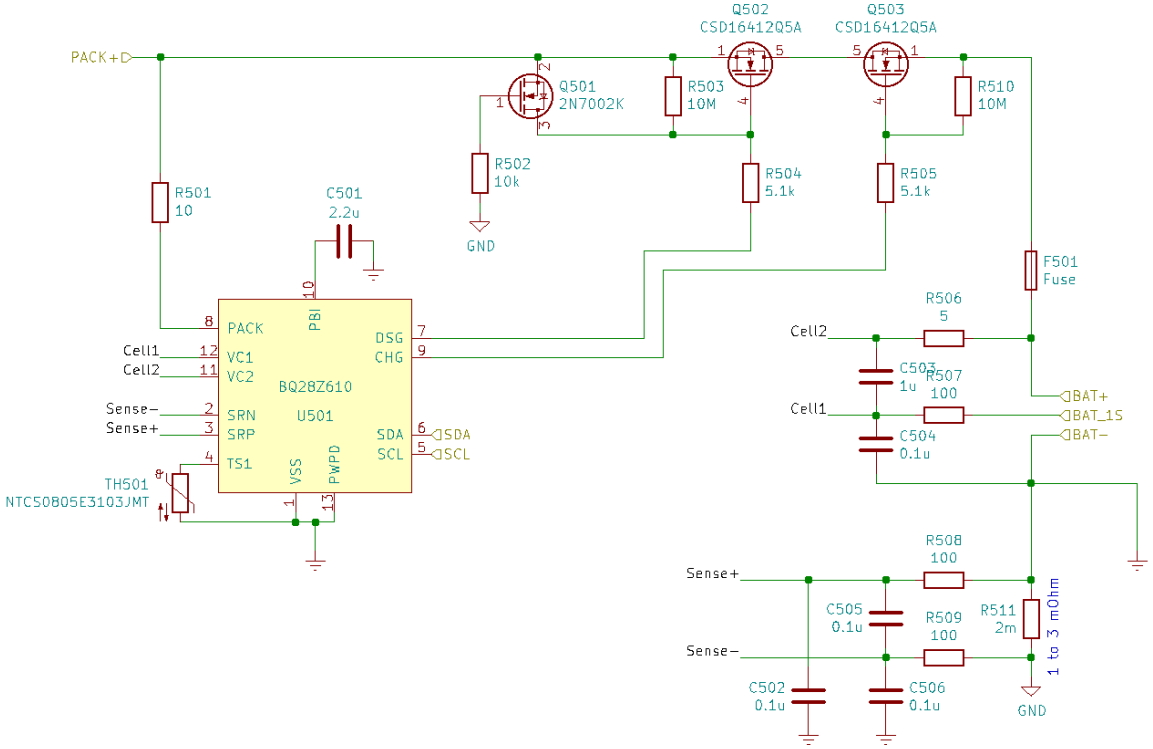

Figure A.4: Schematics of the battery protection.

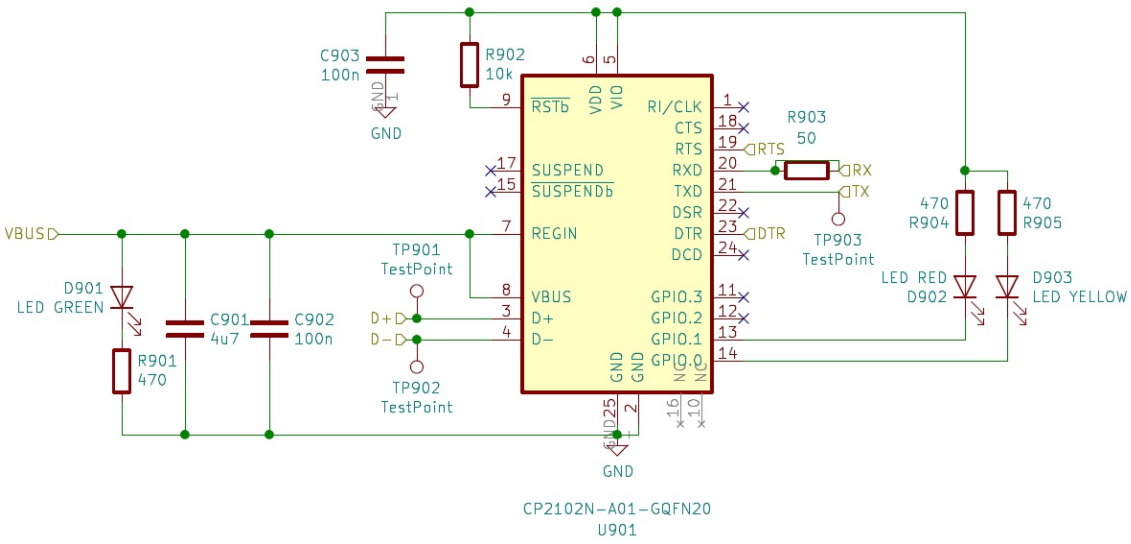

Figure A.5: Schematics of the USB to serial.

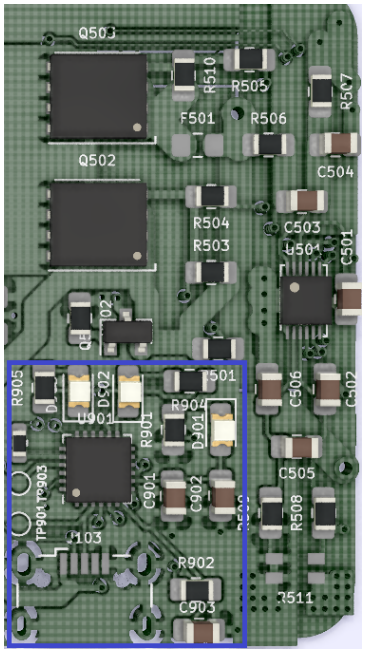

Figure A.6: PCB design of the battery protection and USB to serial design in the blue box.

A.1.4. ESP Layout

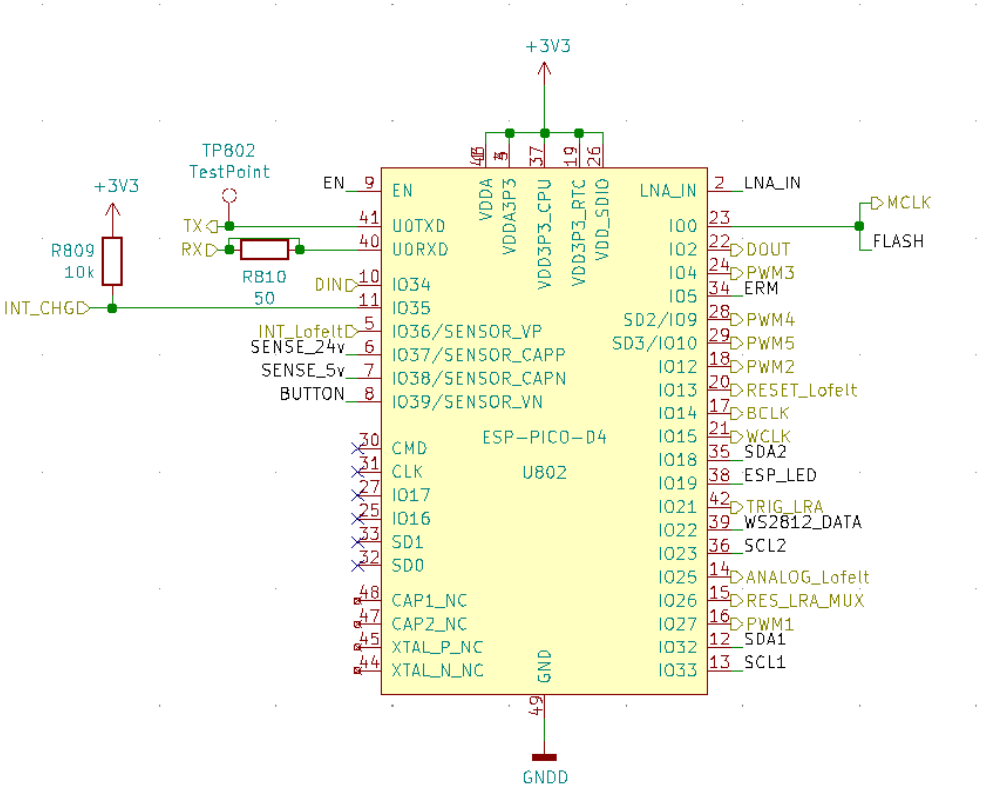

Figure A.7: The layout of the ESP with all pin connections.

A.1.5. ESP Schematics

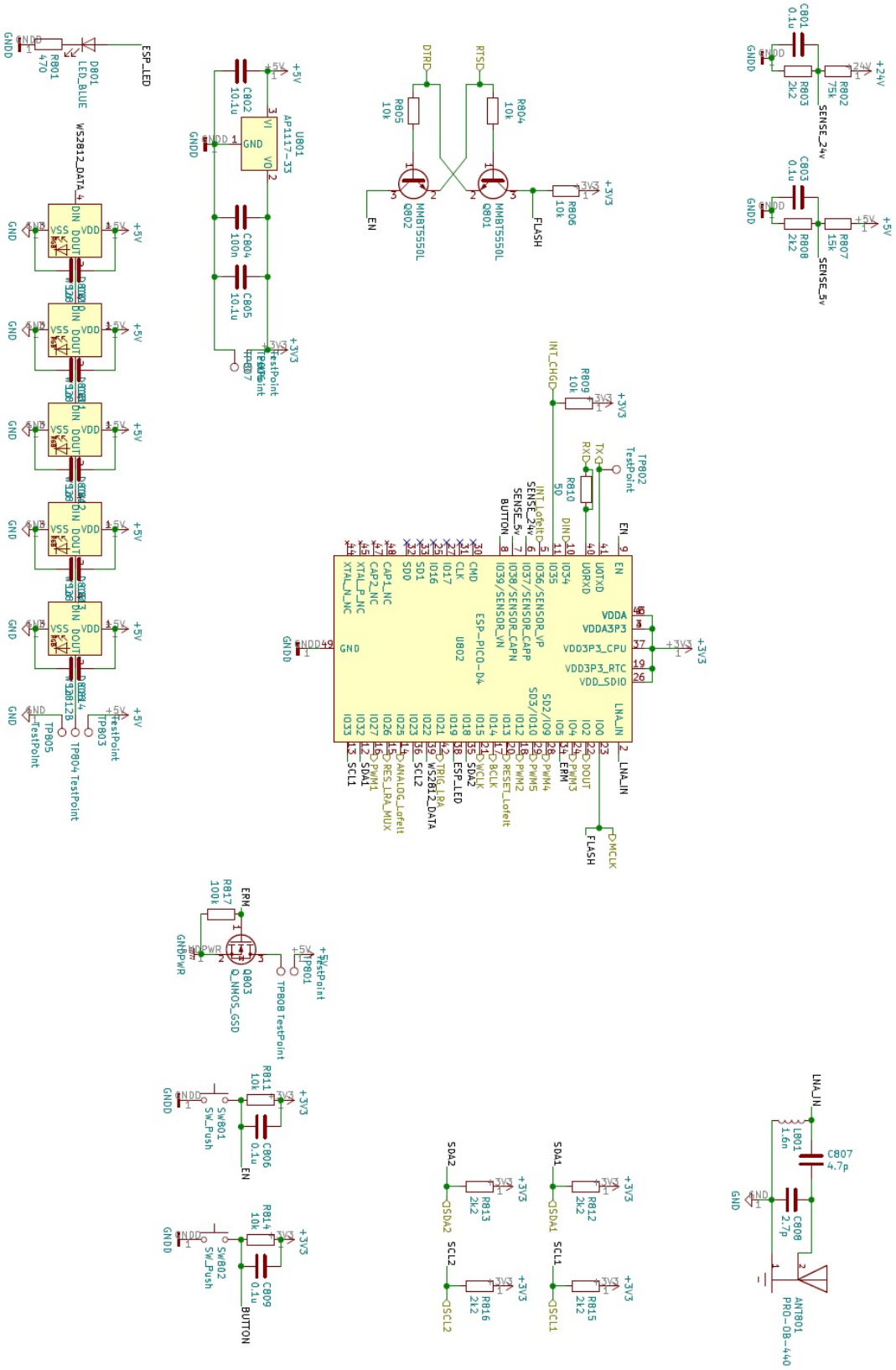

Figure A.8: Schematics of ESP.

A.2. PCB Structure of all layers

A.2.1. Copper layer 1

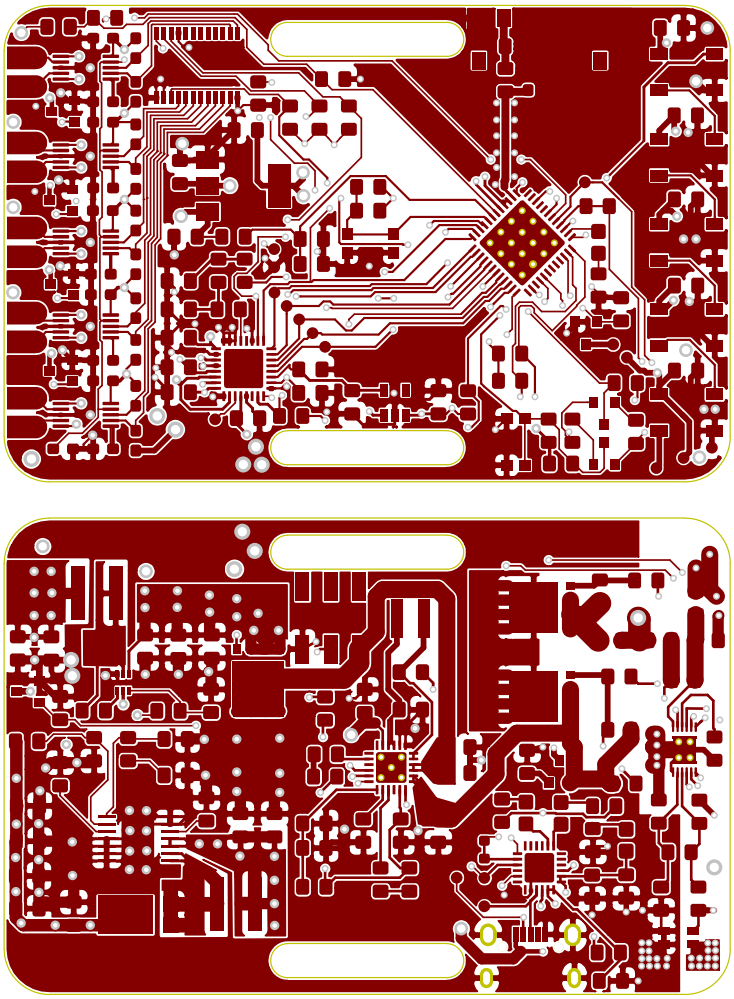

A.2.2. Copper layer 2

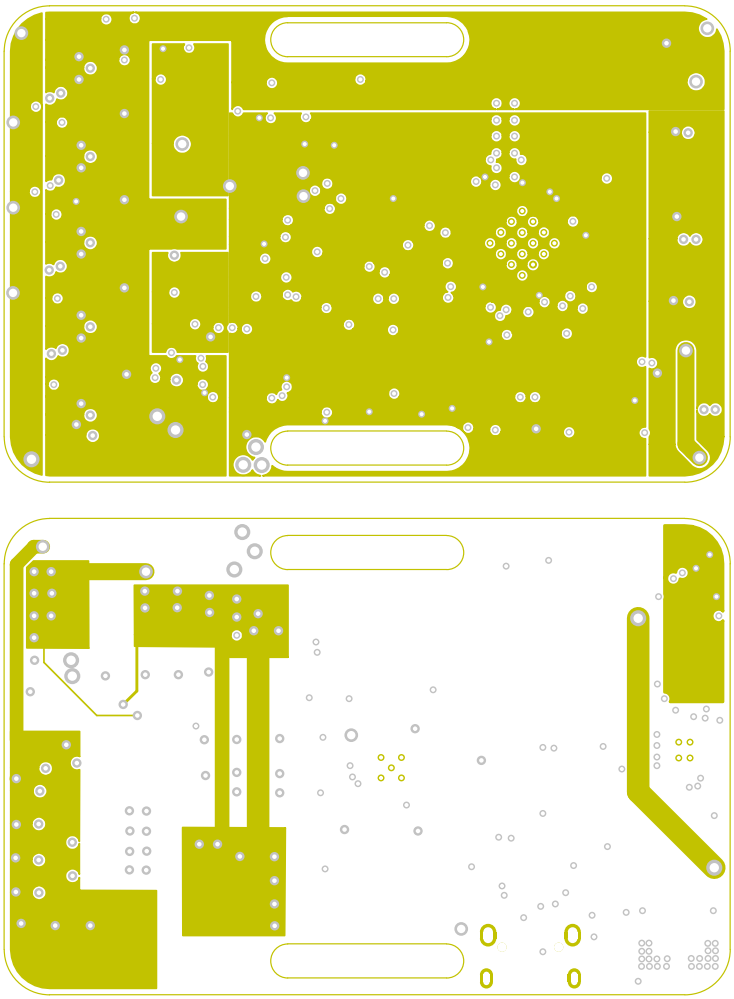

A.2.3. Copper layer 3

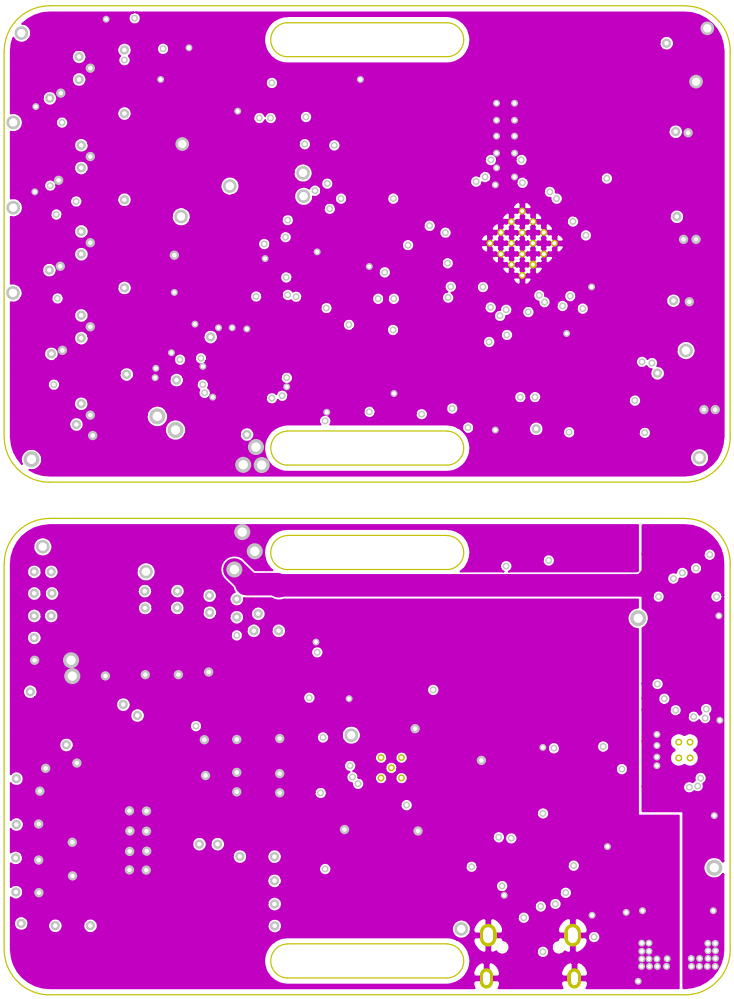

A.2.4. Copper layer 4

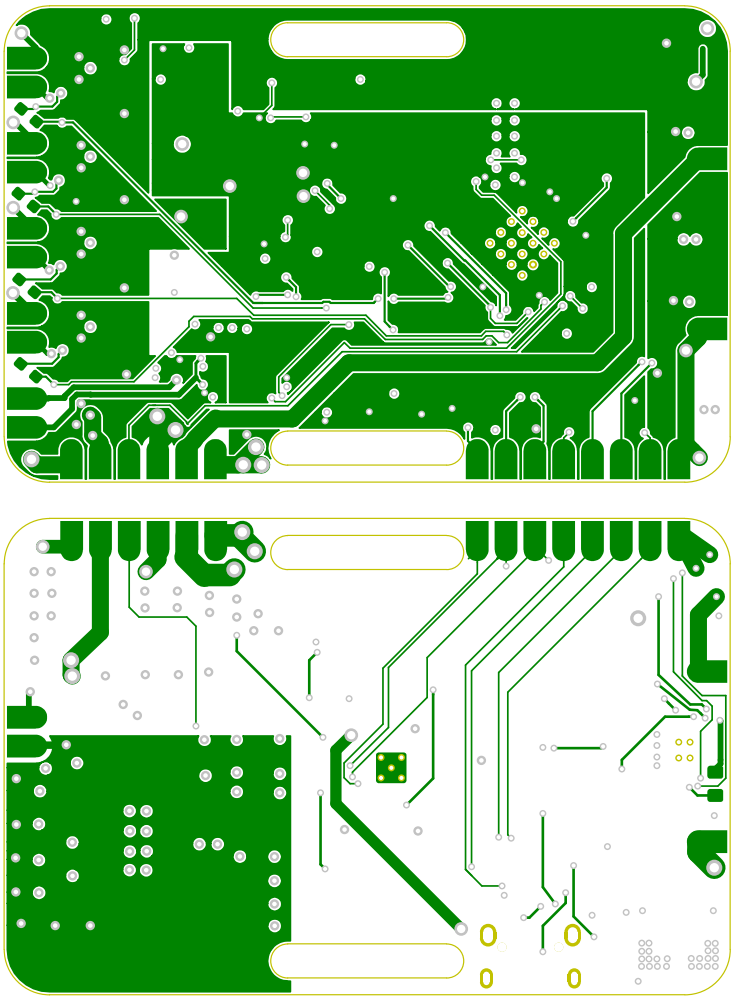

A.2.5. Silkscreen top

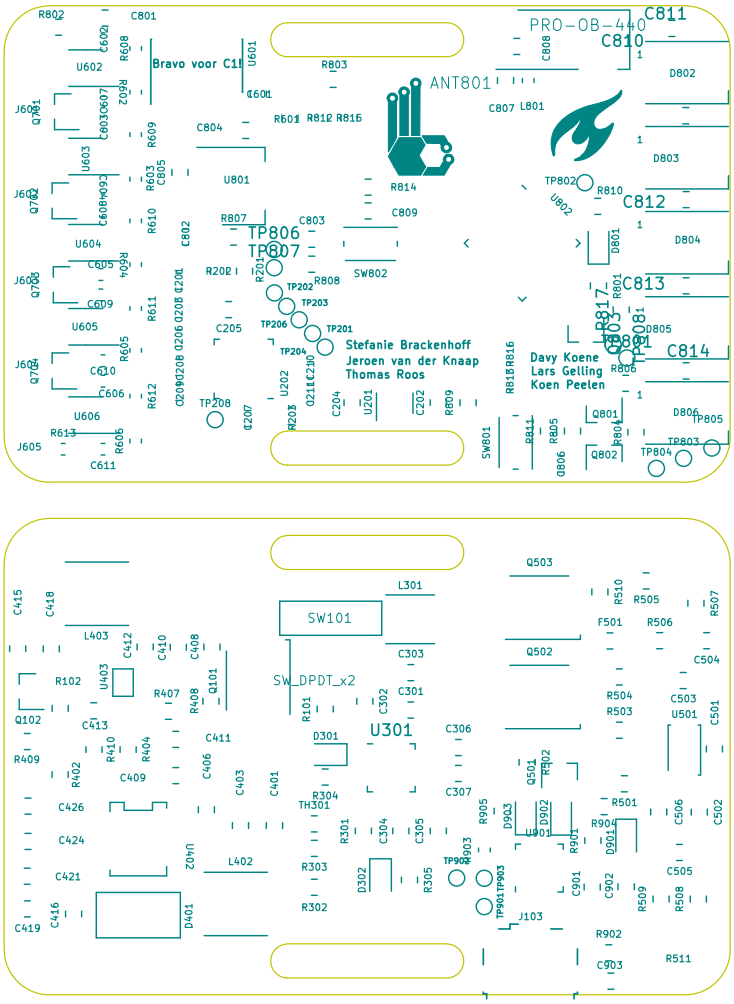

A.2.6. Silkscreen bottom

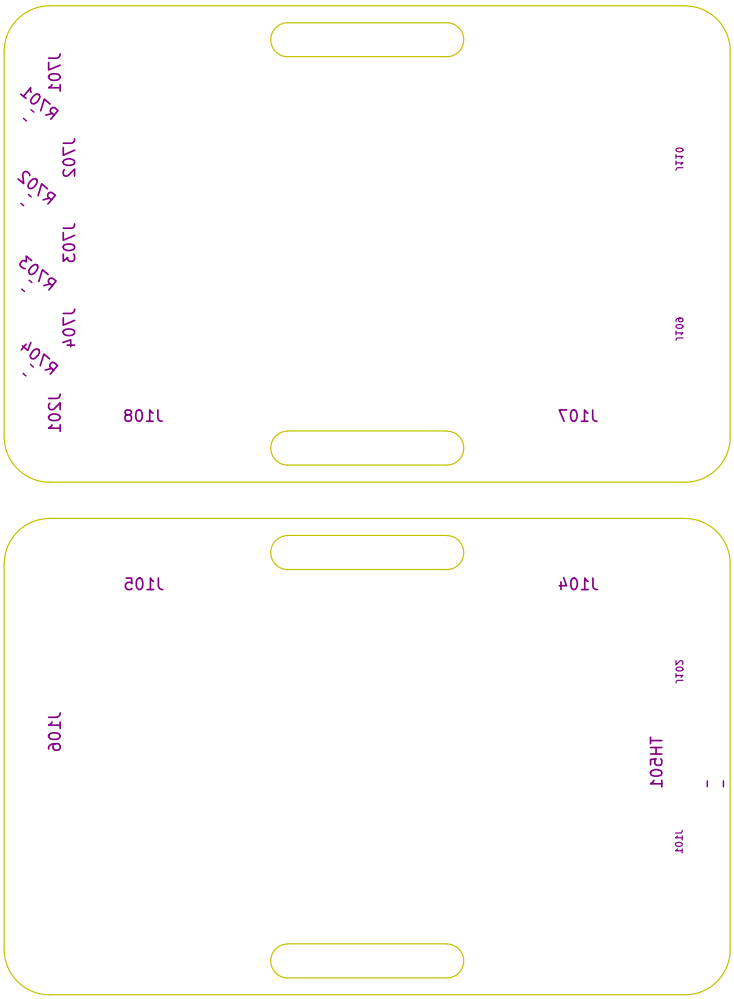

A.2.7. Edges and routing

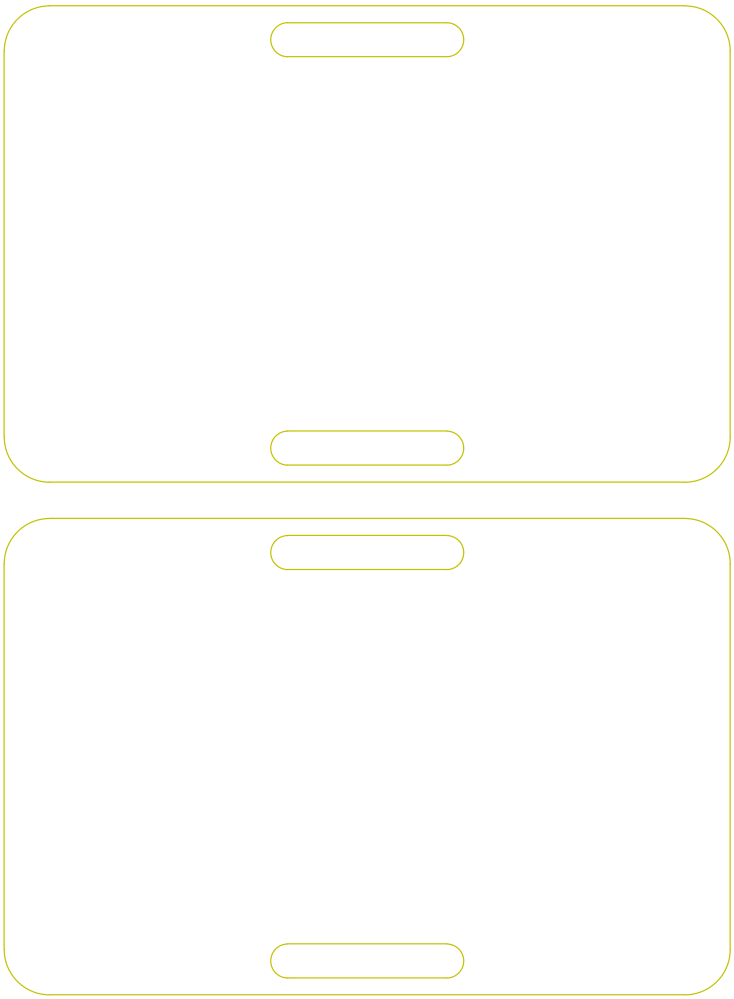

A.2.8. Component placement top

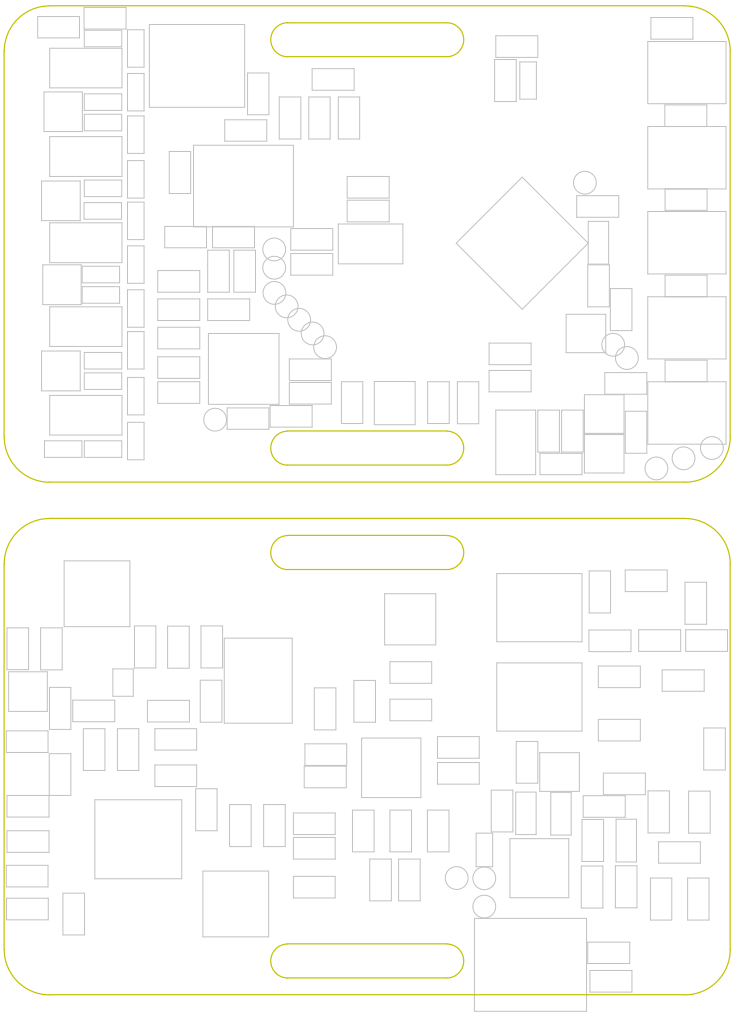

A.2.9. Component placement bottom

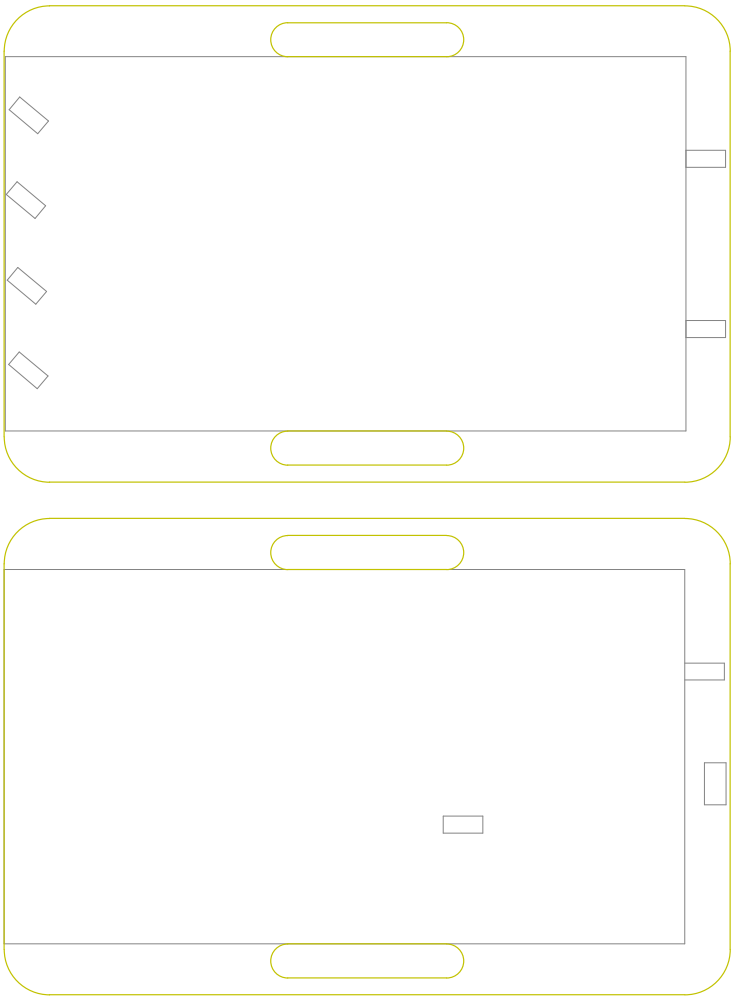

A.3. Assignments

A.3.1. Old assignment

Sense Glove: Soft Glove Prototyping

Bachelor Final Project

Company:
At Sense Glove we develop a VR glove that translates the hands of a user to the virtual world: the Senseglove. The capabilities of the Senseglove allow a user to handle virtual objects the same as real objects. Capabilities such as per finger force- and vibrotactile feedback in addition to accurate self-contained hand tracking. The Senseglove is used in training simulators for car mechanics in a digital factory, VR CAD, proxy robotics and many more. Currently, Sense Glove has produced and sold their initial development kit. In addition to selling the Senseglove, Sense Glove helps companies to integrate interactable physics into existing VR environments. With the current development kits targeting the business-to-business market; a consumer version will be designed.

Problem:
The current Sense Glove uses an exoskeleton to track the position of the fingers and provide the force- and vibrotactile feedback. For Augmented Reality applications, an exoskeleton design is limiting the usability and its scale of implementation. Therefore, a "softglove" is required. The softglove needs to have similar capabilities as the SenseGlove exoskeleton, however the finger tracking will be excluded. With the launch of the Hololens 2, the finger tracking will be done with optical sensors from the head mounted displays.

Assignment

1. Design and realize a semi-flex PCB for the softglove, which integrates
    a. Per finger force feedback
    b. Linear Resonant Actuators in the fingertips
    c. Integration of LoFelt haptic drivers on the palm of the hand
2. Write firmware for the PCB, which can communicate to a PC through USB.
3. (Optional) Make it wireless through Bluetooth.

Sense Glove MAKING VIRTUAL REALITY REAL

A.3.2. New assignment

Sense Glove: Soft Glove Prototyping
Bachelor Final Project

Company

At Sense Glove we develop a VR glove that translates the hands of a user to the virtual world: the Senseglove. The capabilities of the Senseglove allow a user to handle virtual objects the same as real objects. Capabilities such as per finger force- and vibrotactile feedback in addition to accurate self-contained hand tracking. The Senseglove is used in training simulators for car mechanics in a digital factory, VR CAD, proxy robotics and many more. Currently, Sense Glove has produced and sold their initial development kit. In addition to selling the Senseglove, Sense Glove helps companies to integrate interactable physics into existing VR environments. With the current development kits targeting the business-to-business market; a consumer version will be designed.

Problem

The current Sense Glove uses an exoskeleton to track the position of the fingers and provide the force- and vibrotactile feedback. For Augmented Reality applications, an exoskeleton design is limiting the usability and its scale of implementation. Therefore, a "softglove" is required. The softglove needs to have similar capabilities as the SenseGlove exoskeleton, however the finger tracking will be excluded. With the launch of the Hololens 2, the finger tracking will be done with optical sensors from the head mounted displays.

Assignment

Design and realize a PCB:

- With a formfactor that does not interfere with the movement of the hand.
- Which integrates the following feedback methods:
  - Per finger force.
  - Linear Resonant. Actuators on the fingers
  - Integration of LoFelt actuator on the palm of the hand.
- (Wish) Write firmware for the glove which integrates with SenseGlove's systems.
- No immersion-breaking latency.
- (Optional) Make a wireless datalink.
- (Optional) Powered by a battery.

A.4. Planning

A.4.1. New assignment

Softglove - Work packages

ID	Subject	Start date	Finish date
48	Start project	23-04-2019	23-04-2019
43	Literature study	24-04-2019	01-05-2019
70	Reading up on HW	01-05-2019	04-05-2019
65	Proof of concept	01-05-2019	12-05-2019
46	Literatuur studie	02-05-2019	02-05-2019
69	Tests w/o micro or only Arduino	05-05-2019	12-05-2019
47	GreenLight Planning	10-05-2019	10-05-2019
55	Proto version	13-05-2019	07-06-2019
59	Draw schematic and PCB of proto version	13-05-2019	22-05-2019
53	Topic proposal Ethics	16-05-2019	16-05-2019
67	Code proto software	22-05-2019	01-06-2019
54	Proto PCB being manufactured and parts shipped	22-05-2019	29-05-2019
68	Order proto PCB	22-05-2019	22-05-2019
71	Greenlight deadline	27-05-2019	27-05-2019
64	Assemble proto version	29-05-2019	01-06-2019
63	Test and check prototype	01-06-2019	07-06-2019
49	First Full Draft Ethics	06-06-2019	06-06-2019
52	Final version	07-06-2019	01-07-2019
58	Redraw schematic and PCB	07-06-2019	14-06-2019
45	Final PCB being manufactured and parts shipped	14-06-2019	21-06-2019
72	Writing report	14-06-2019	20-06-2019
42	Report: final deadline	21-06-2019	21-06-2019
62	Assembling final version	21-06-2019	25-06-2019
61	Coding final demo code	24-06-2019	01-07-2019
50	Ethics: final deadline	27-06-2019	27-06-2019
60	Creating presentation	02-07-2019	04-07-2019

B

Appendix Finger Force Feedback

B.1. Simulations

B.1.1. Simulation circuits

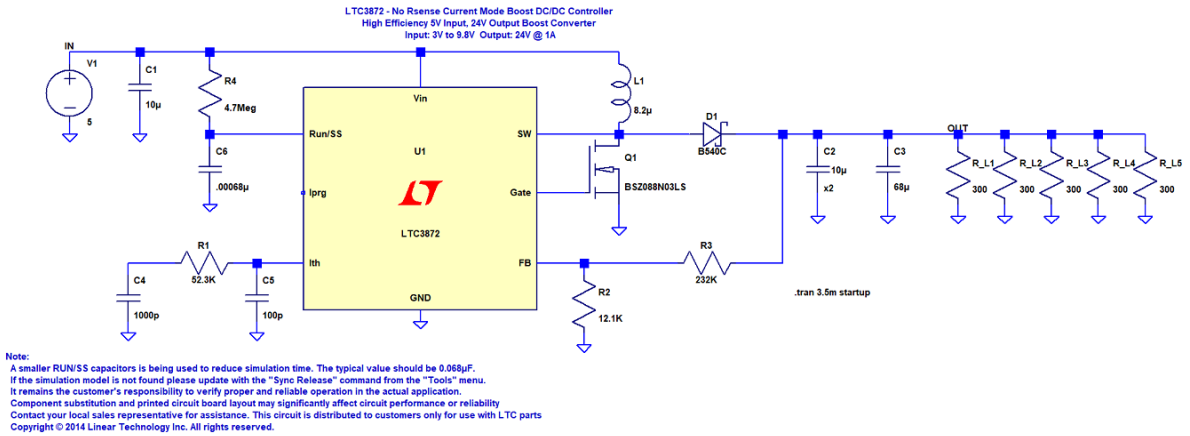

Figure B.1: Schematics of LTC3872 converter with 5 V input

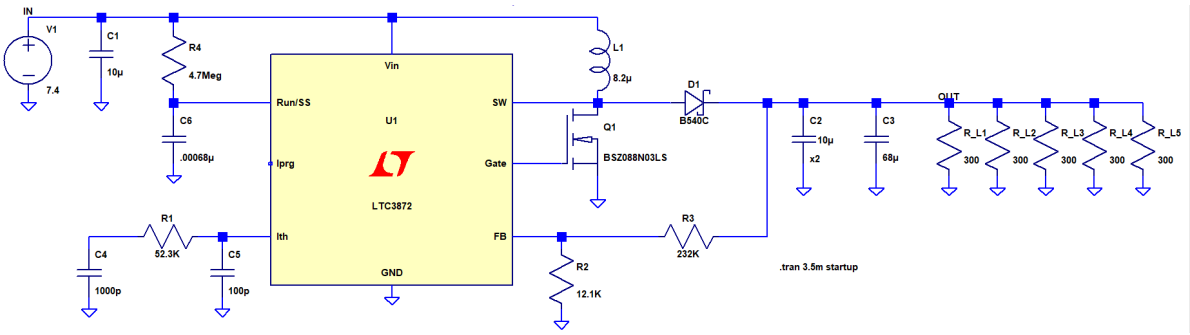

Figure B.2: Schematics of LTC3872 converter with 7.4 V nominal battery input

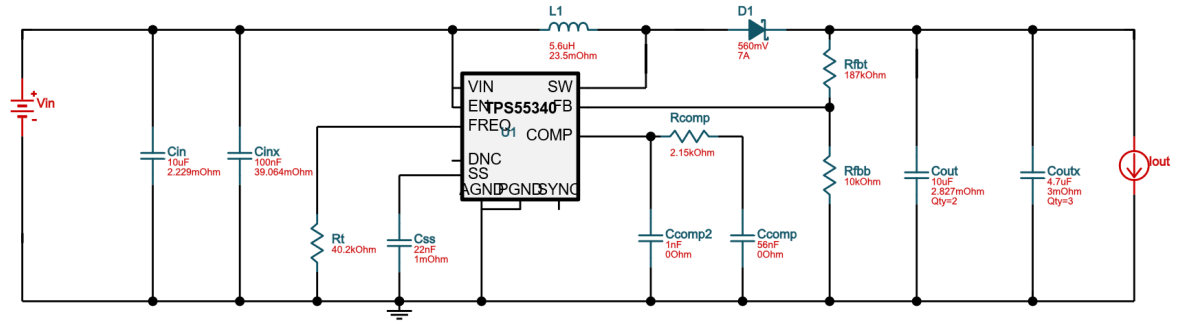

Figure B.3: Schematic TPS55340 converter

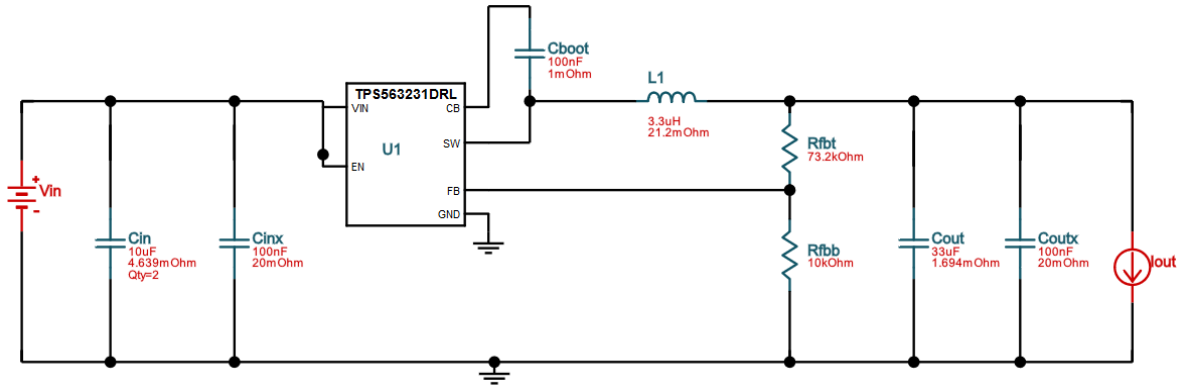

Figure B.4: Schematic TPS563231 converter

B.1.2. Simulation results

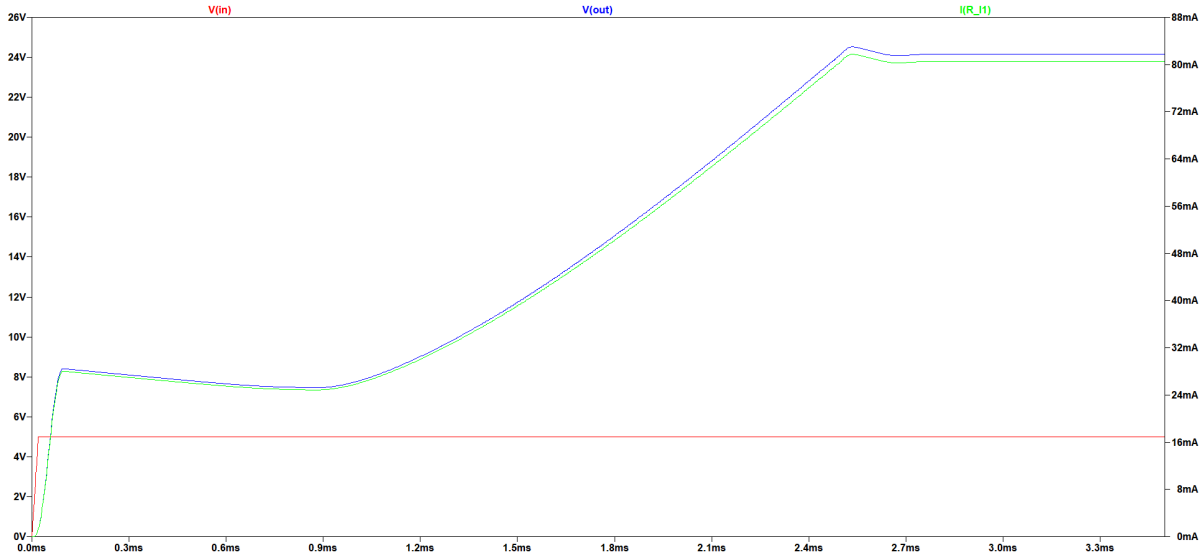

Figure B.5: Boost conversion simulation results from 5-24 V

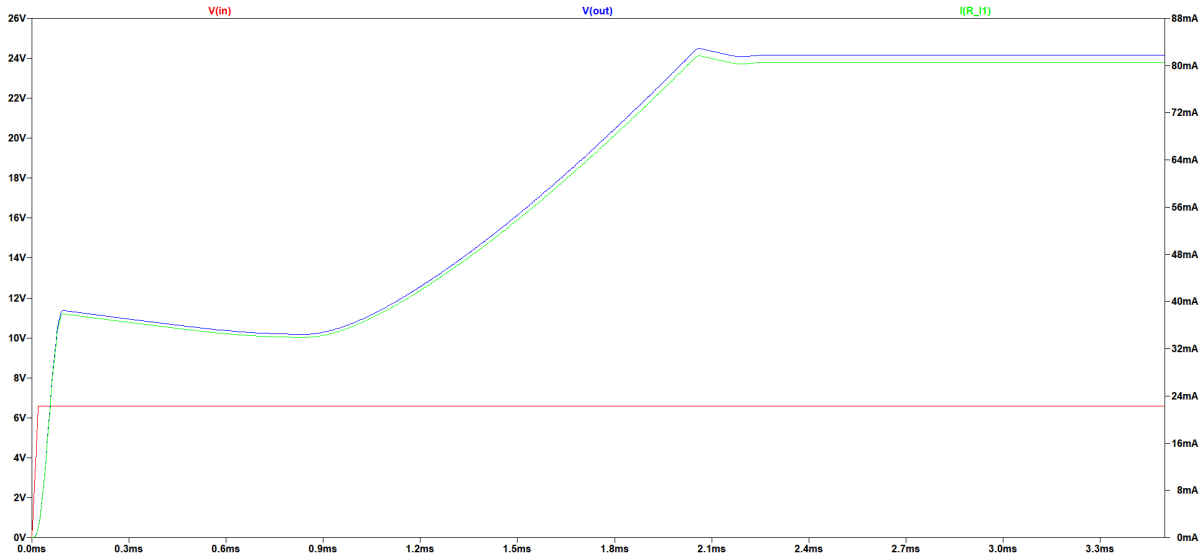

Figure B.6: Boost conversion simulation results from 6.6-24 V

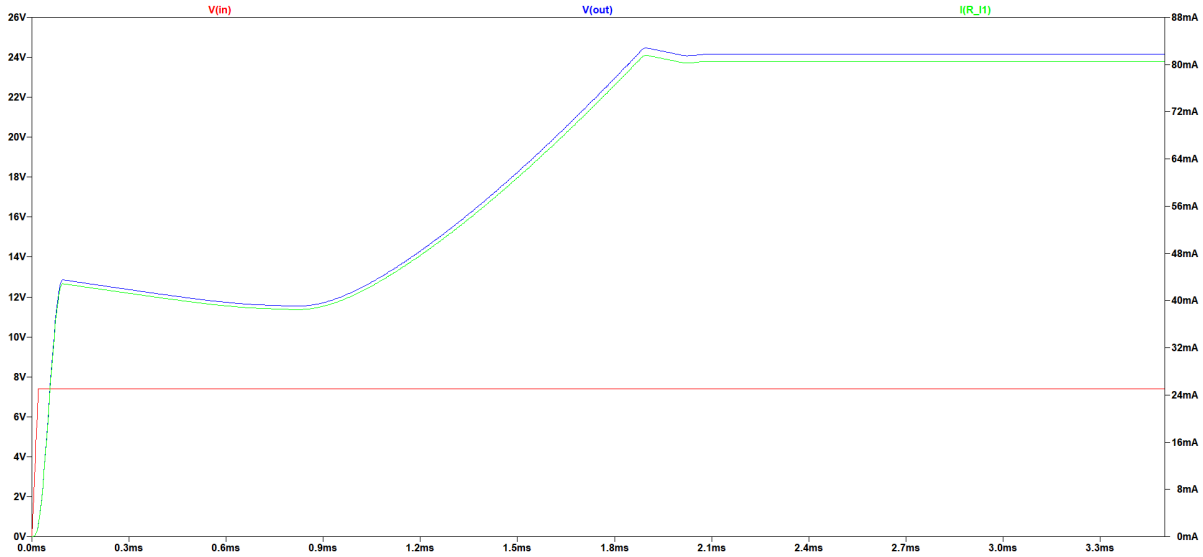

Figure B.7: Boost conversion simulation results from 7.4-24 V

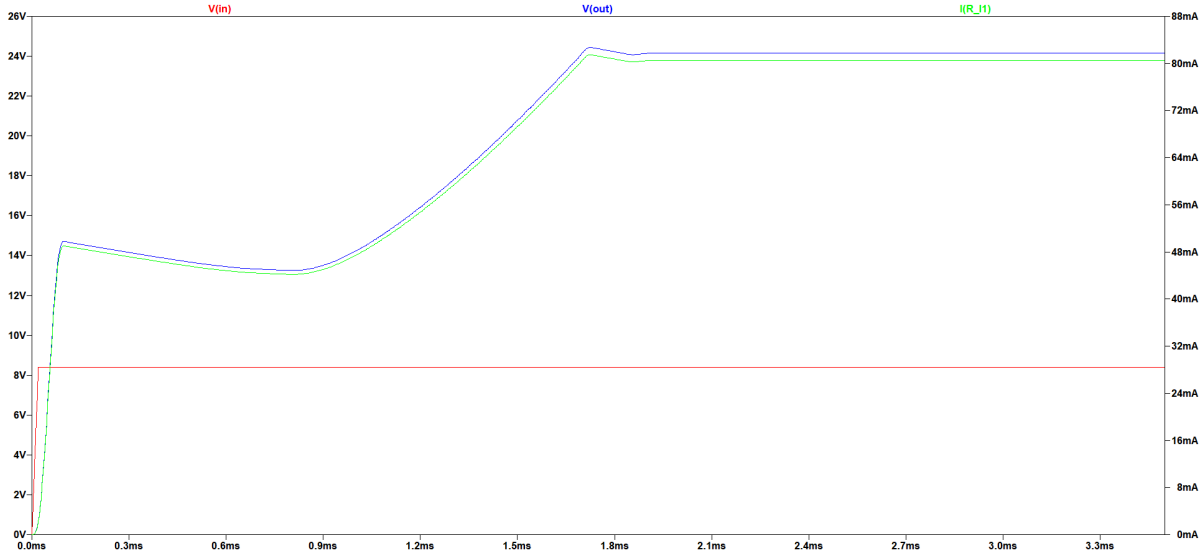

Figure B.8: Boost conversion simulation results from 8.4-24 V

B.2. Testing Boost Converters on Soldering Boards

B.2.1. Test circuit

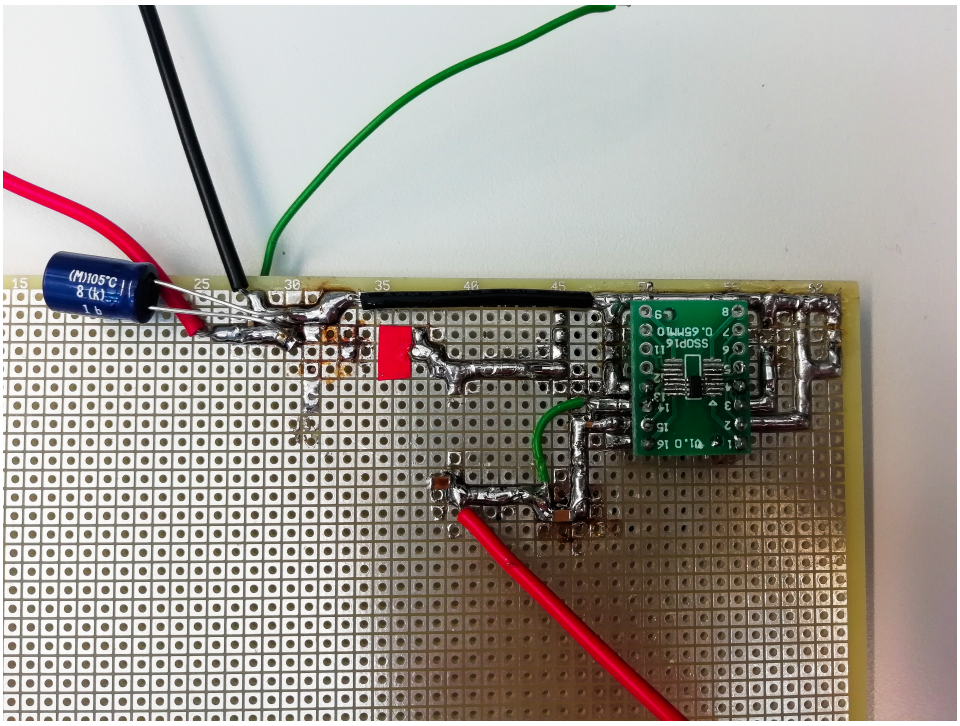

Figure B.9: Soldering board containing the LTC3872 (front)

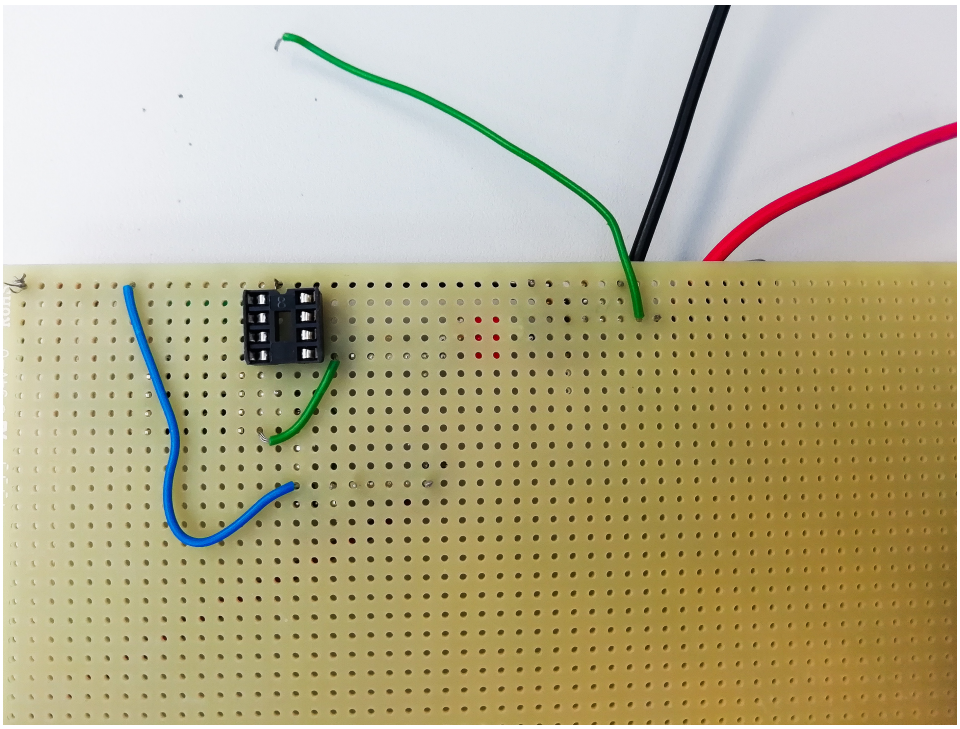

Figure B.10: Soldering board containing the LTC3872 (back)

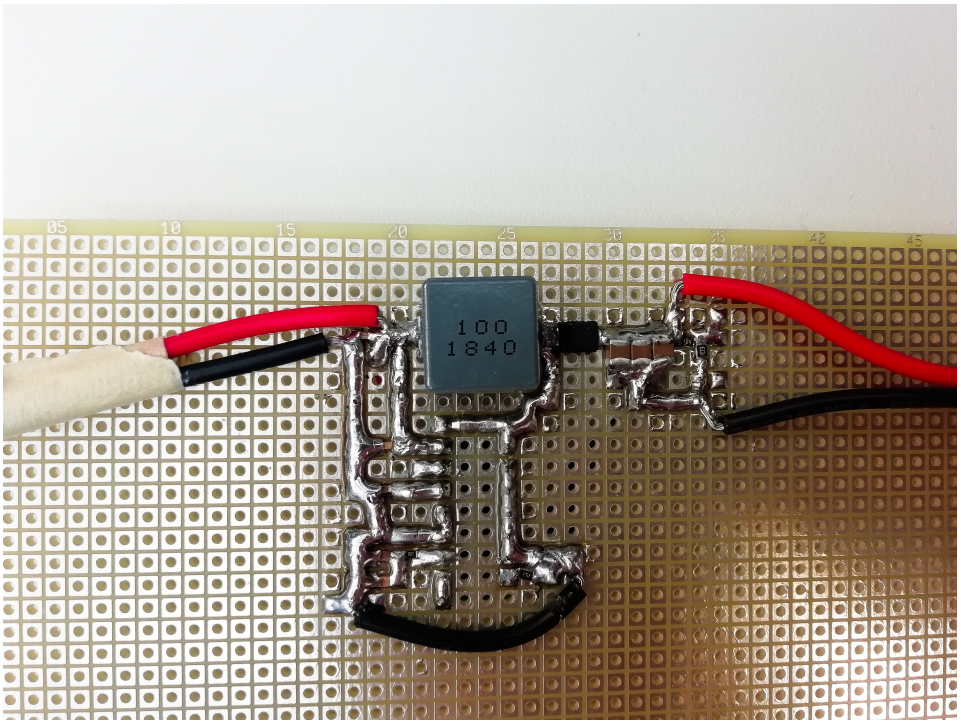

Figure B.11: Soldering board containing the TPS55340 (front)

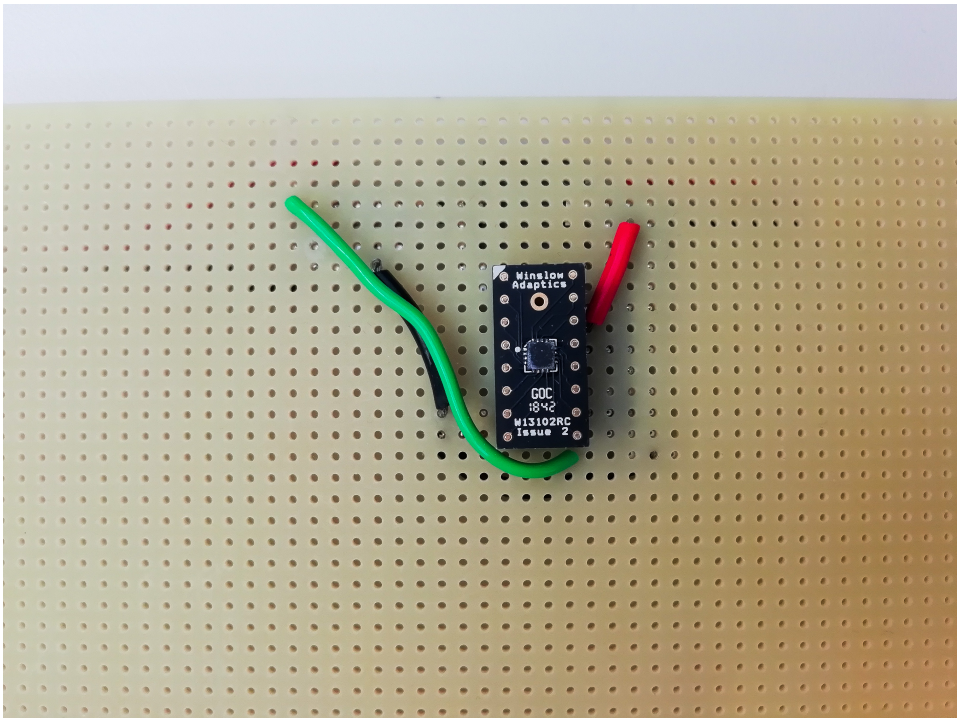

Figure B.12: Soldering board containing the TPS55340 (back)

B.2.2. Test Results

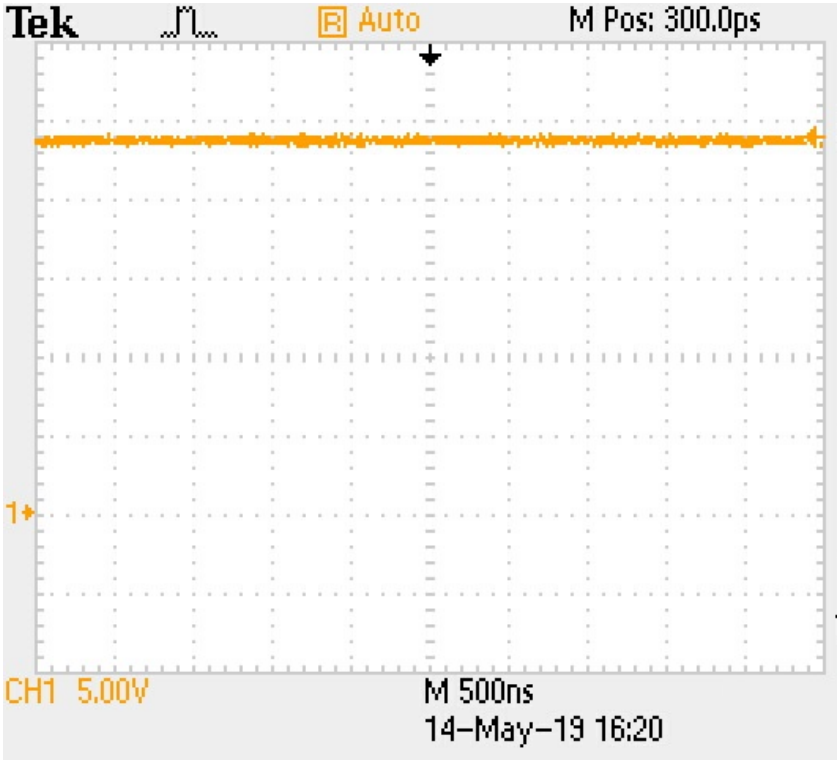

Figure B.13: Test of the boost converter with no load attached and a 5 V input

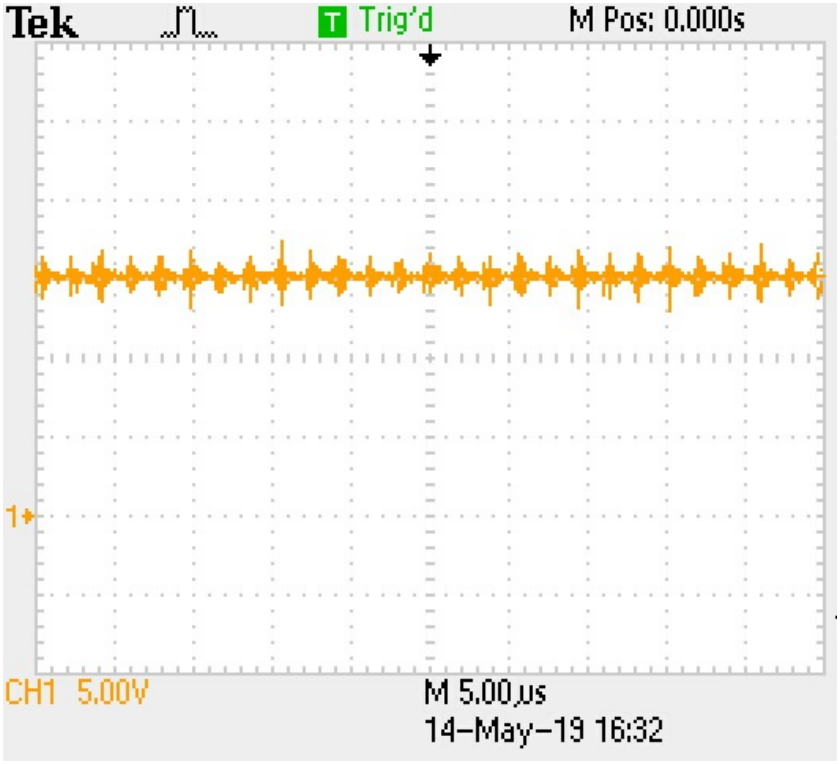

Figure B.14: Test of the boost converter with a 75Ω load attached and a 2.5 V input

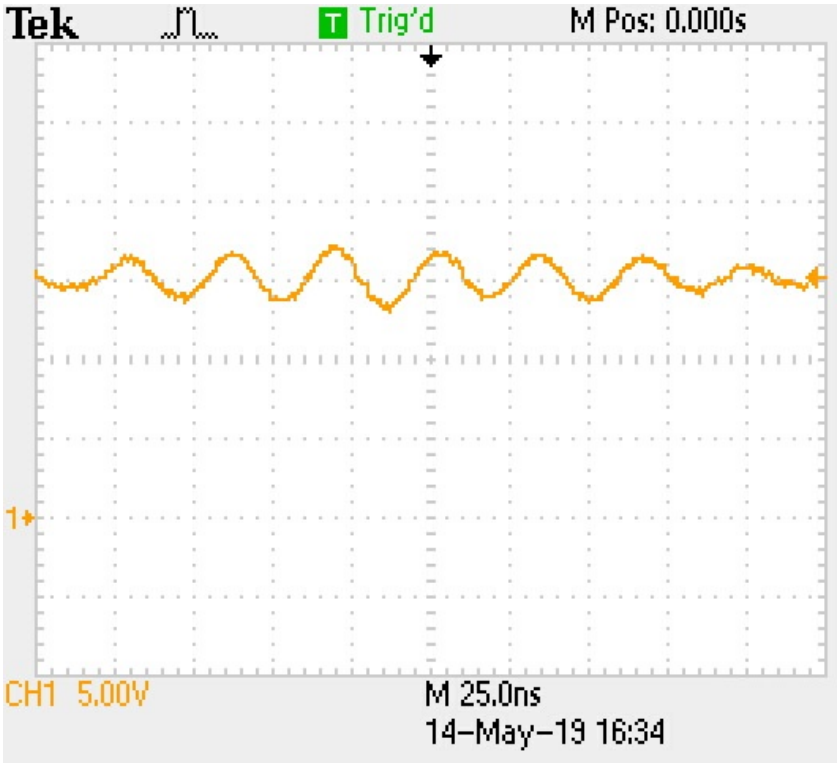

Figure B.15: Zoomed in test of the boost converter with a 75Ω load attached and a 2.5 V input

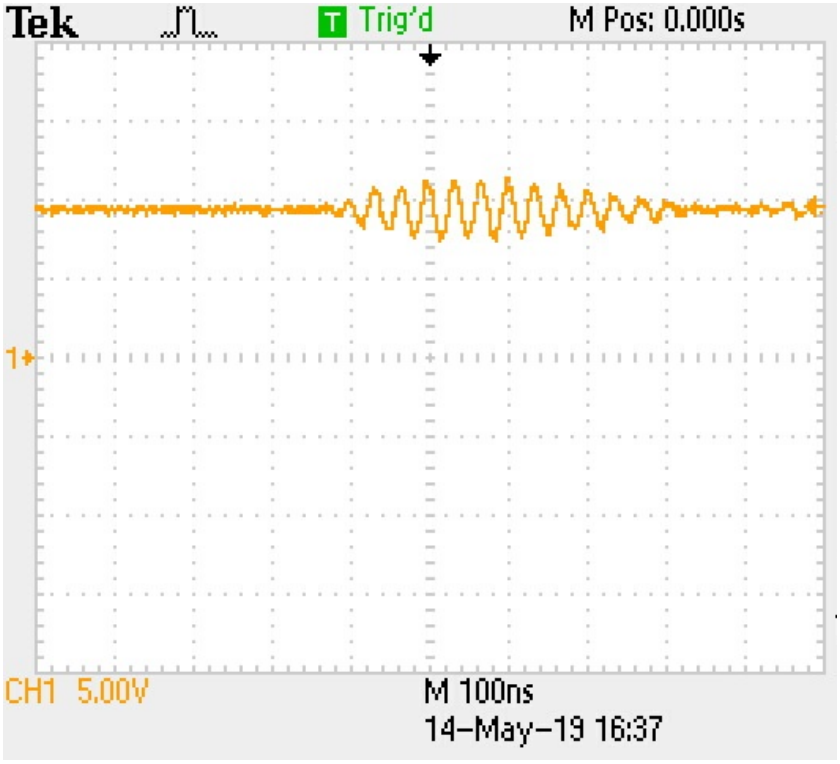

Figure B.16: Test of the boost converter with a 75Ω load attached and a 5 V input

B.3. PCB Layout Design

B.3.1. Schematics

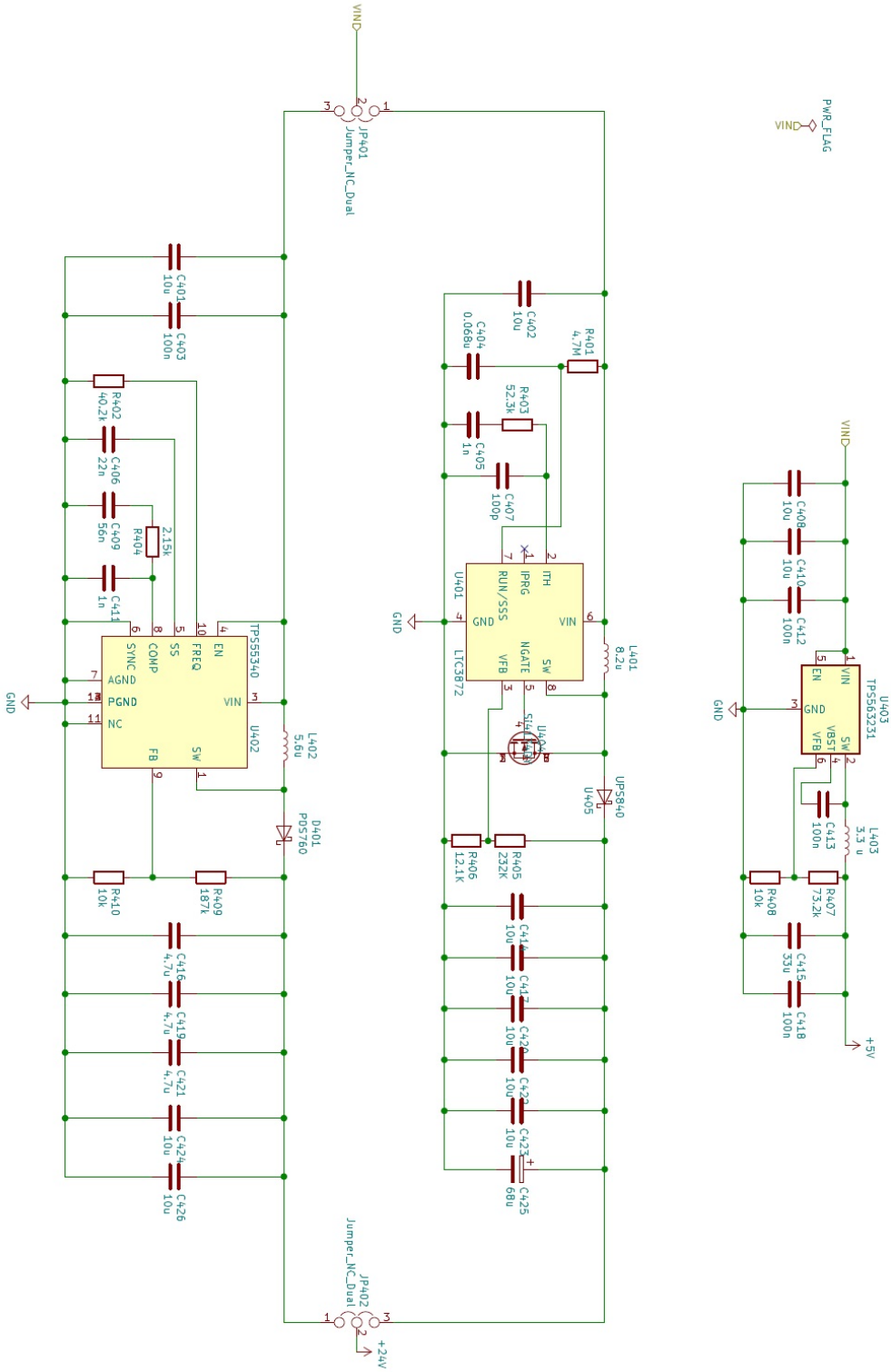

Figure B.17: Schematics of power circuits on the first PCB

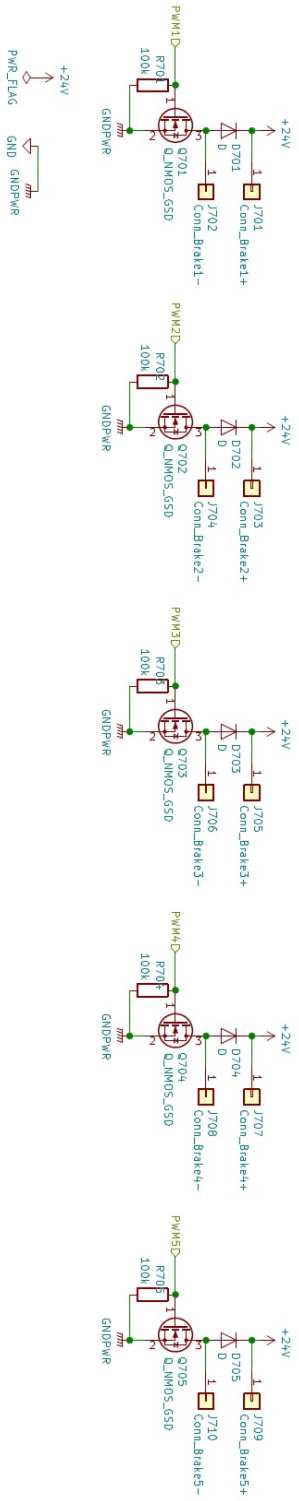

Figure B.18: Schematics of actuator control circuits on the first PCB

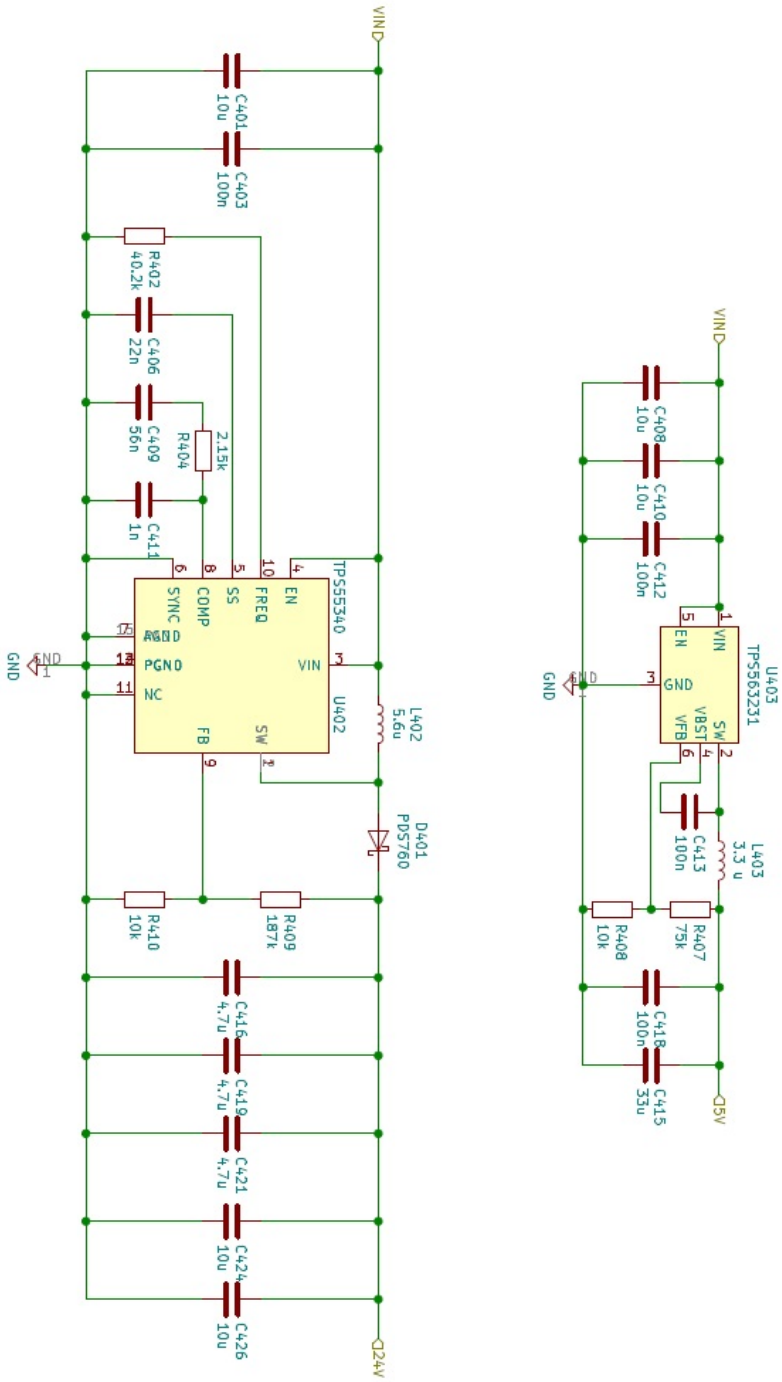

Figure B.19: Schematics of power circuits on the revised PCB

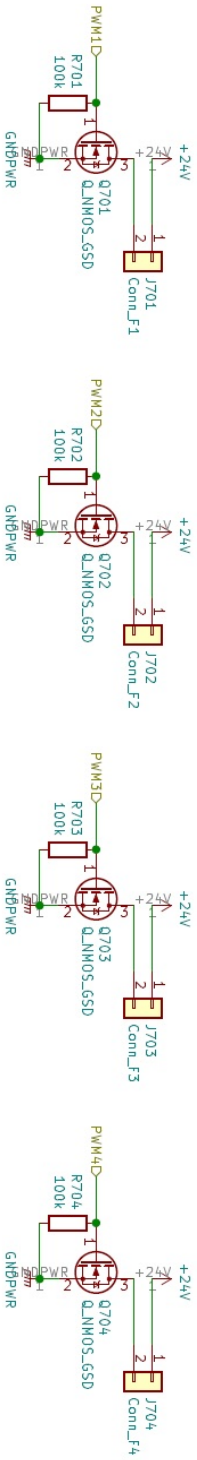

Figure B.20: Schematics of actuator control circuits on the revised PCB

B.3.2. PCB guidelines

10 Layout

10.1 Layout Guidelines

As for all switching power supplies, especially those with high frequency and high switch current, printed-circuit board (PCB) layout is an important design step. If the layout is not carefully designed, the regulator can suffer from instability as well as noise problems. The following guidelines are recommended for good PCB layout.

- To prevent radiation of high-frequency resonance problems, use proper layout of the high-frequency switching path.
- Minimize the length and area of all traces connected to the SW pin and always use a ground plane under the switching regulator to minimize inter-plane coupling.
- The high current path, including the internal MOSFET switch, Schottky diode, and output capacitor, contains nanosecond rise times and fall times. Keep these rise times and fall times as short as possible.
- Place the VIN bypass capacitor as close to the VIN pin and the AGND pin as possible to reduce the IC supply ripple.
- Connect the AGND and PGND pins to thermal pad directly on the same layer.

10.2 Layout Example

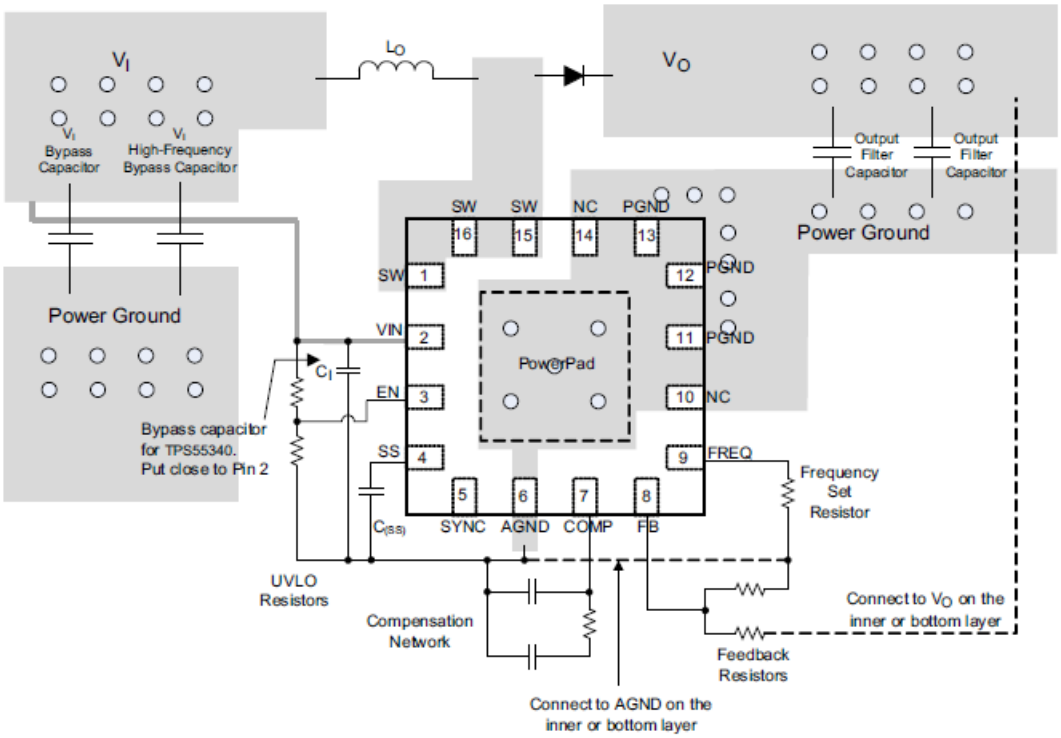

Figure 32. TPS55340 Layout Example

Figure B.21: PCB design guidelines for the TPS55340 boost converter circuit

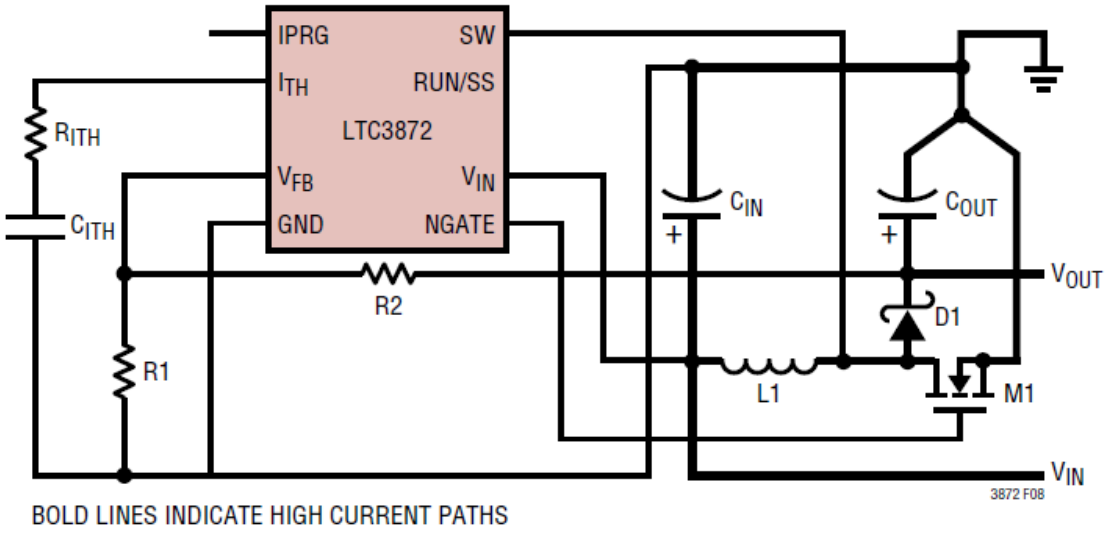

Figure 8. LTC3872 Layout Diagram (See PC Board Layout Checklist)

PC Board Layout Checklist

When laying out the printed circuit board, the following checklist should be used to ensure proper operation of the LTC3872. These items are illustrated graphically in the layout diagram in Figure 8. Check the following in your layout:

1. The Schottky diode should be closely connected between the output capacitor and the drain of the external MOSFET.

2. The input decoupling capacitor (0.1µF) should be connected closely between V_{IN} and GND.

3. The trace from SW to the switch point should be kept short.

4. Keep the switching node NGATE away from sensitive small signal nodes.

5. The V_{FB} pin should connect directly to the feedback resistors. The resistive divider R1 and R2 must be connected between the (+) plate of C_{OUT} and signal ground.

Figure B.22: PCB design guidelines for the LTC3872 boost converter circuit

10 Layout

10.1 Layout Guidelines

1. VIN and GND traces should be as wide as possible to reduce trace impedance. The wide areas are also of advantage from the view point of heat dissipation.
2. The input capacitor and output capacitor should be placed as close to the device as possible to minimize trace impedance.
3. Provide sufficient vias for the input capacitor and output capacitor.
4. Keep the SW trace as physically short and wide as practical to minimize radiated emissions.
5. Do not allow switching current to flow under the device.
6. A separate VOUT path should be connected to the upper feedback resistor.
7. Make a Kelvin connection to the GND pin for the feedback path.
8. Voltage feedback loop should be placed away from the high-voltage switching trace, and preferably has ground shield.
9. The trace of the VFB node should be as small as possible to avoid noise coupling.
10. The GND trace between the output capacitor and the GND pin should be as wide as possible to minimize its trace impedance.

10.2 Layout Example

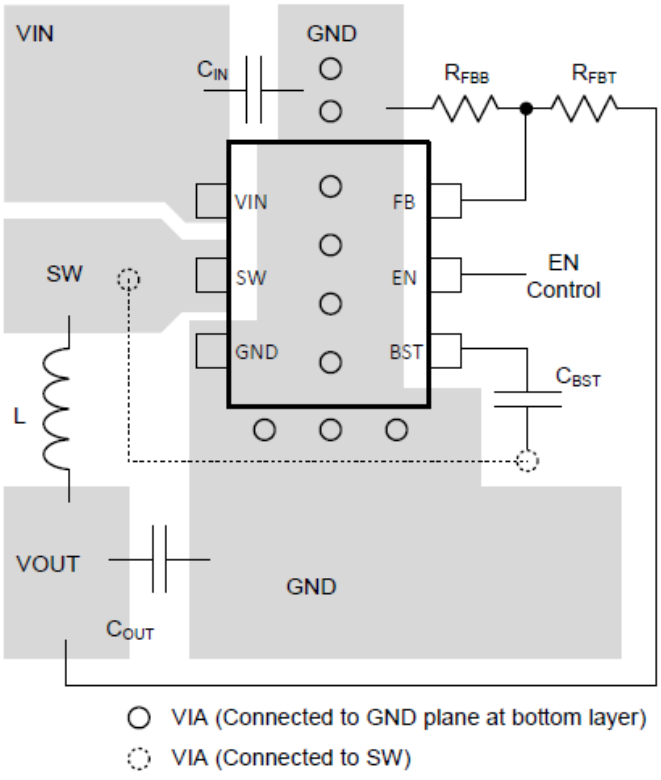

Figure 22. TPS563231 Layout

Figure B.23: PCB design guidelines for the TPS563231 buck converter circuit

B.3.3. PCB Layout

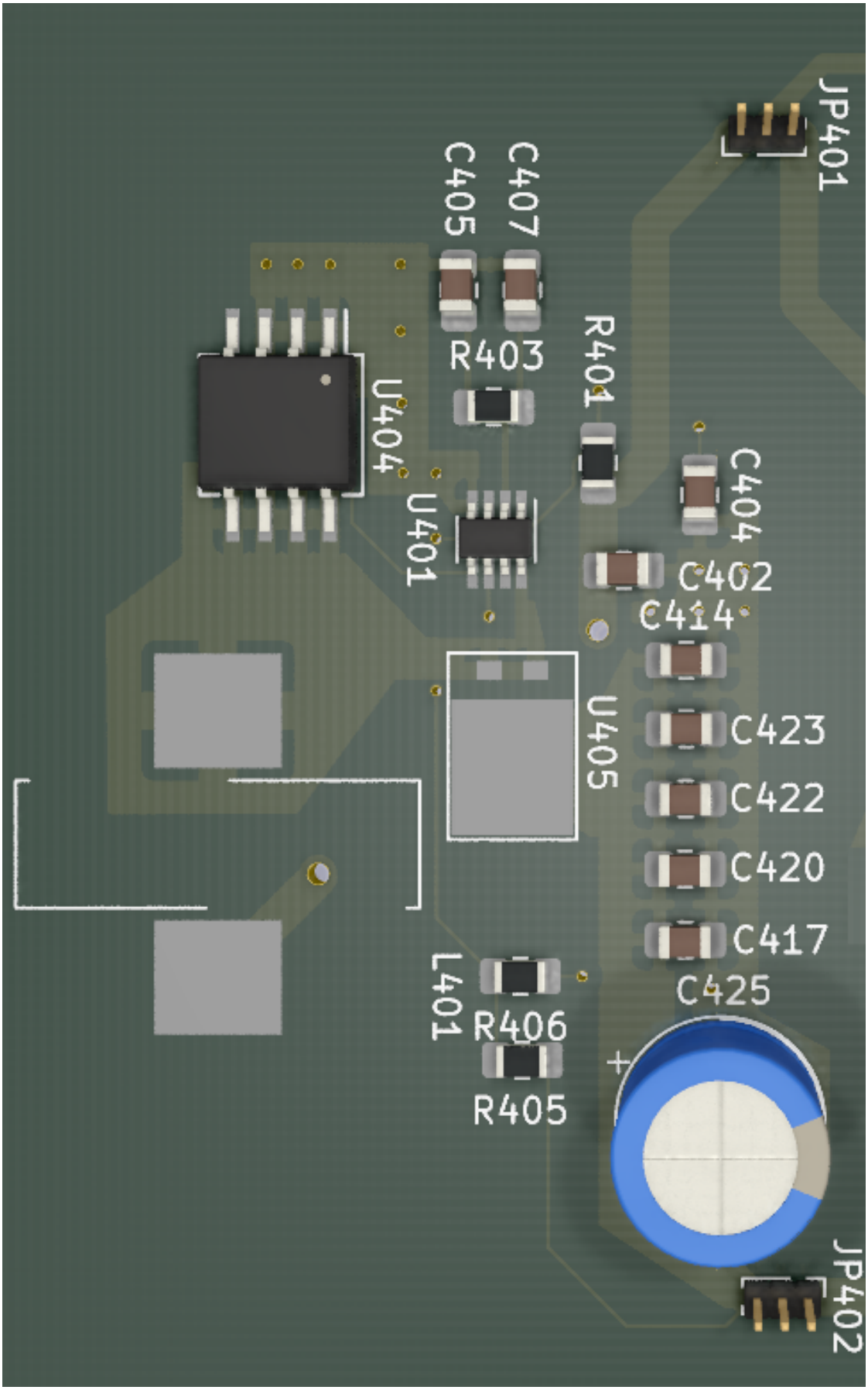

Figure B.24: PCB design for the LTC3872 converter circuit on the first PCB

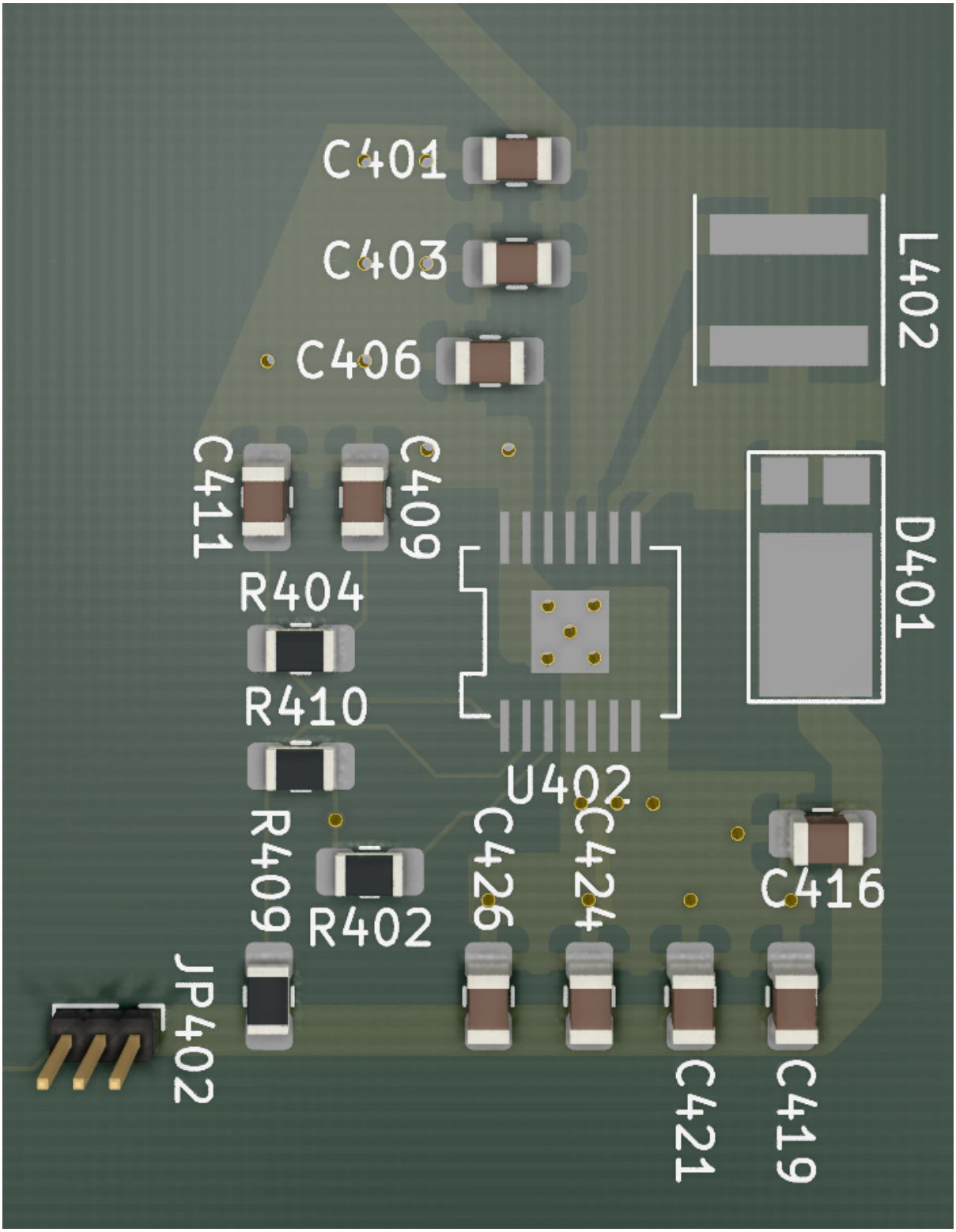

Figure B.25: PCB design for the TPS55340 converter circuit on the first PCB

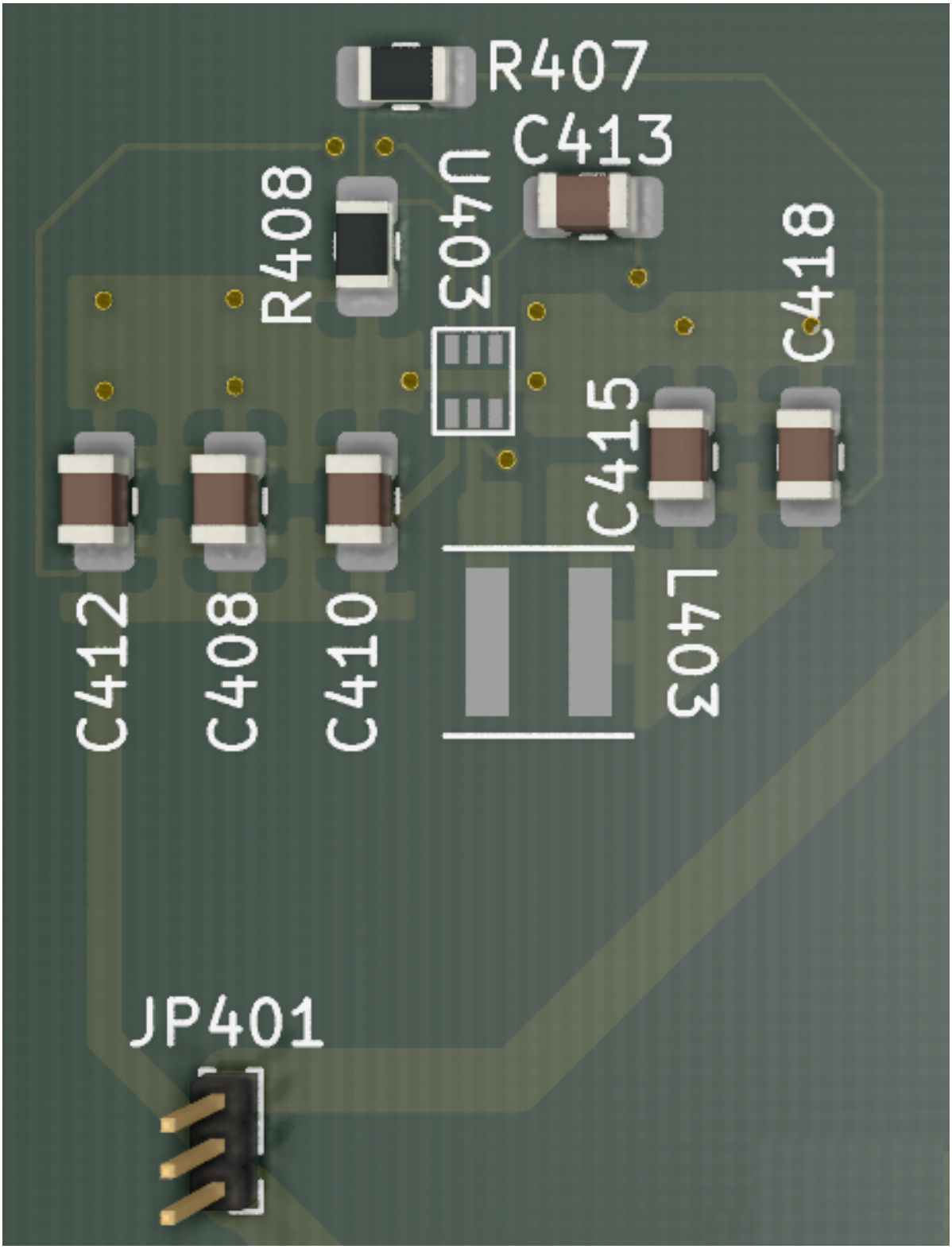

Figure B.26: PCB design for the TPS563231 converter circuit on the first PCB

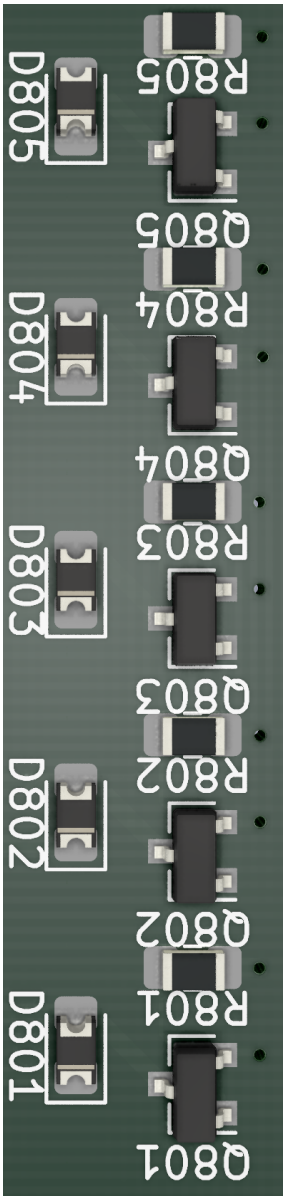

Figure B.27: PCB design for the Actuator Control on the first PCB

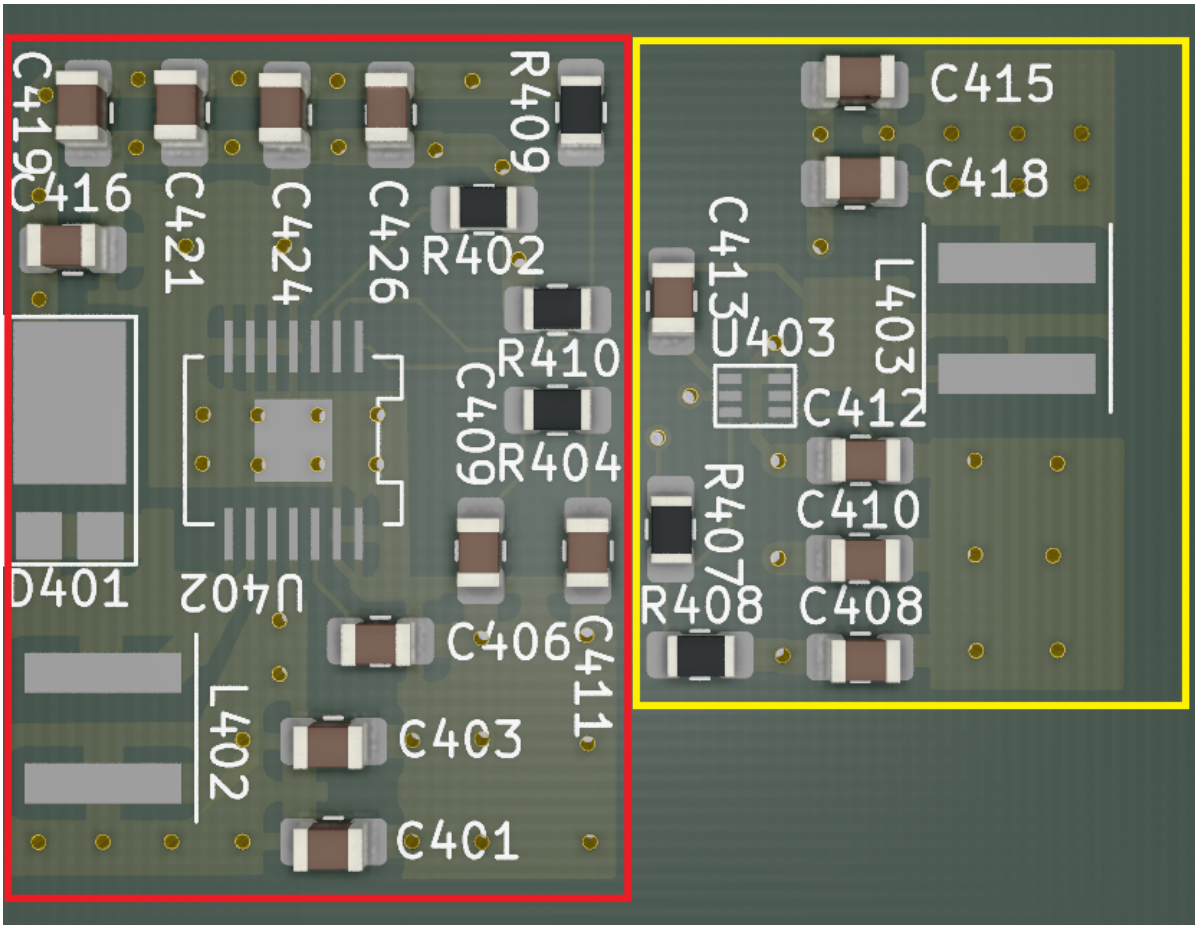

Figure B.28: Final PCB design for the entire power conversion subsystem on the revised PCB

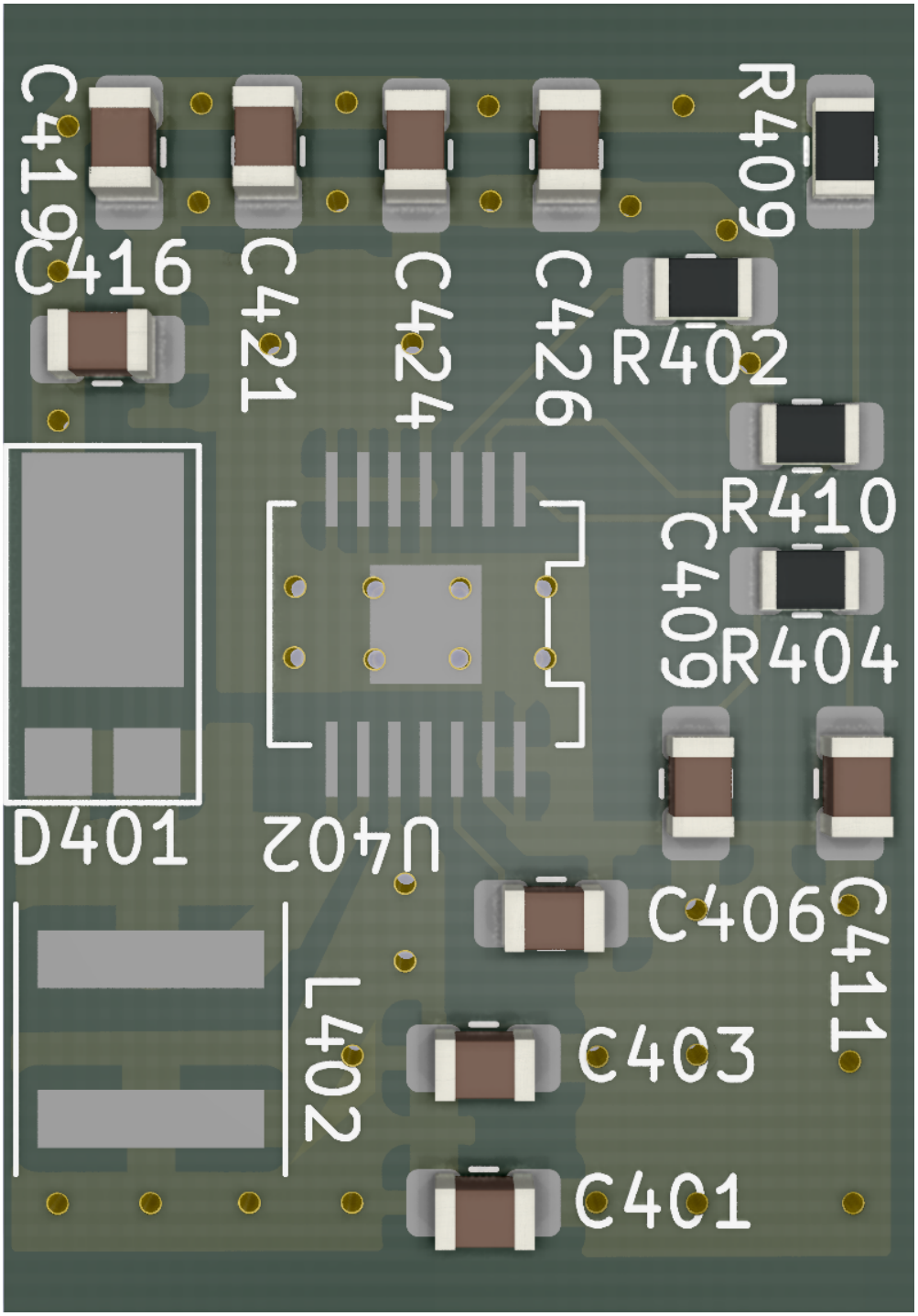

Figure B.29: PCB design for the TPS55340 converter circuit on the revised PCB

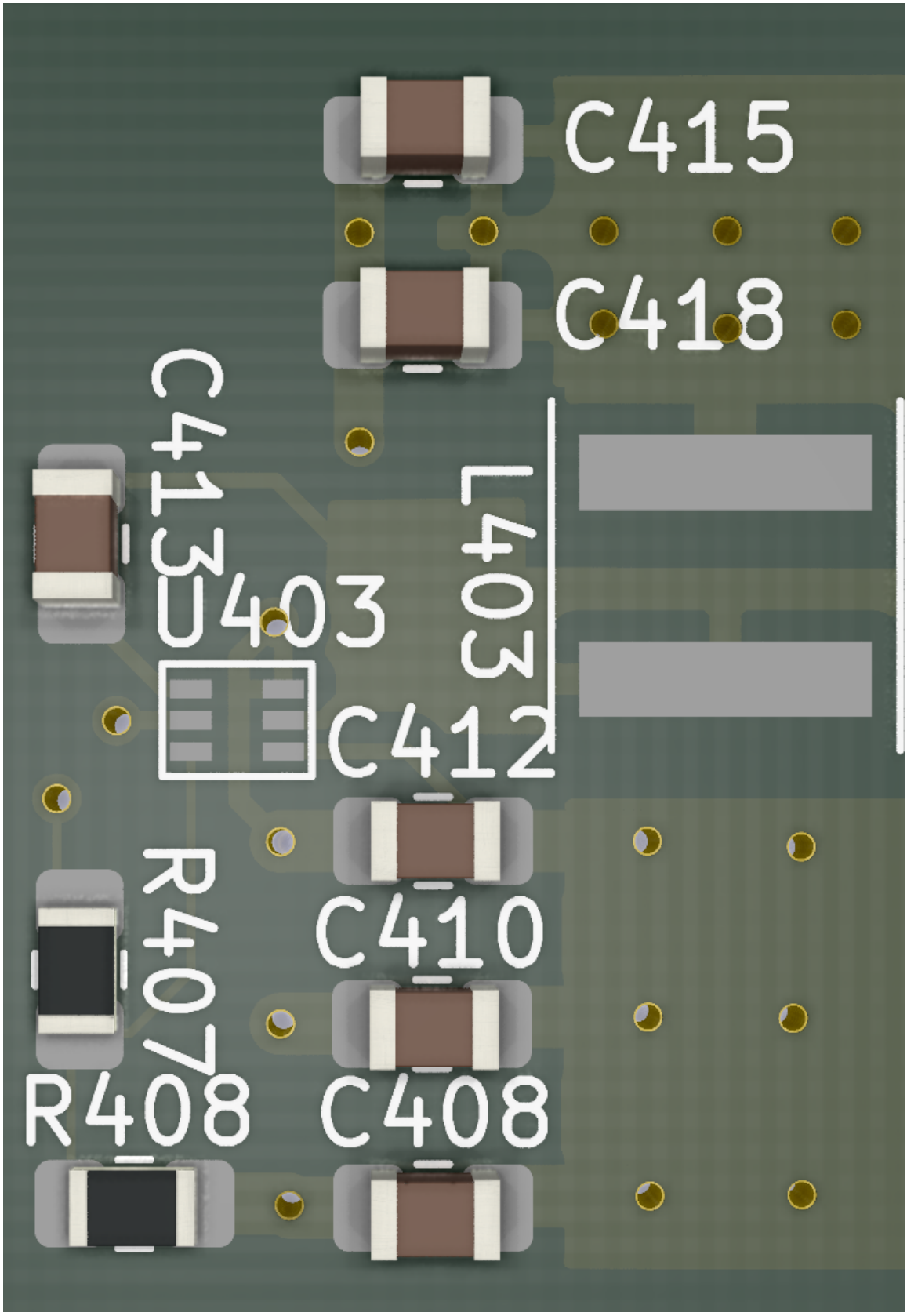

Figure B.30: PCB design for the TPS563231 converter circuit on the revised PCB

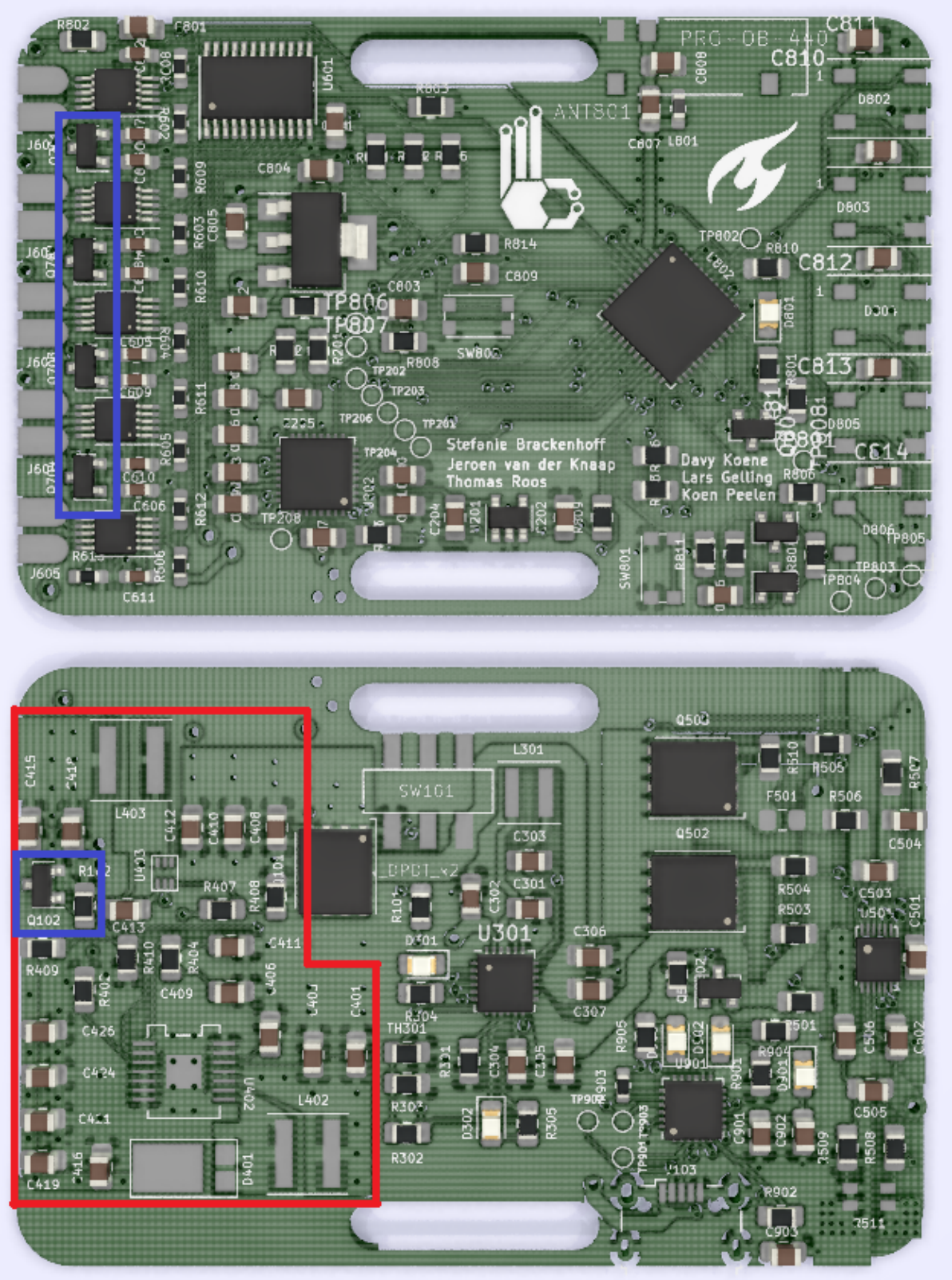

Figure B.31: PCB design for the SoftGlove revised PCB

B.4. Tests PCB Boost converter

B.4.1. Attaching the load

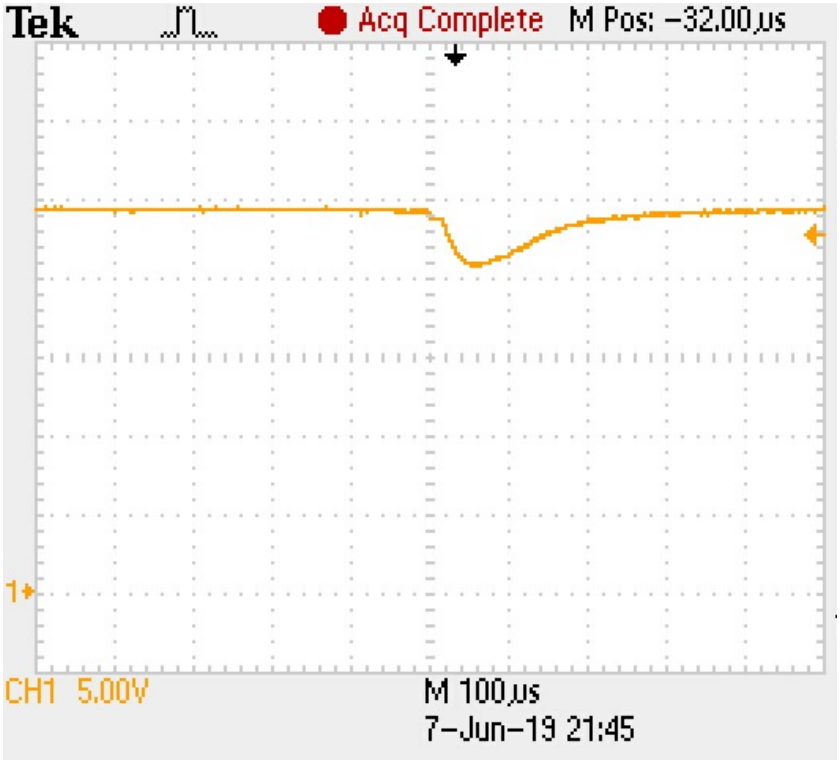

Figure B.32: Load Transient response for attaching the load 2

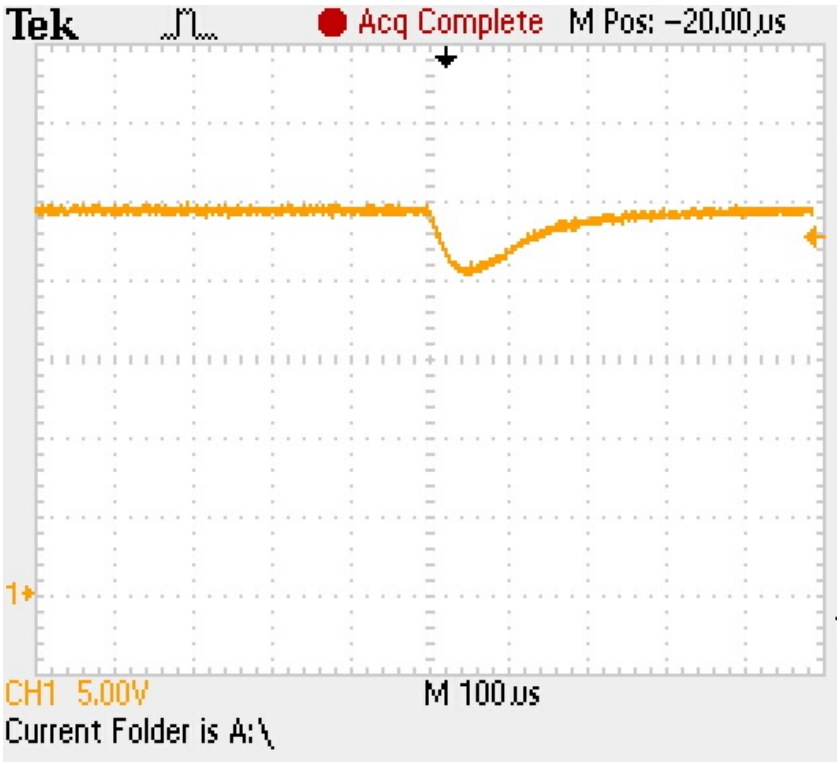

Figure B.33: Load Transient response for attaching the load 3

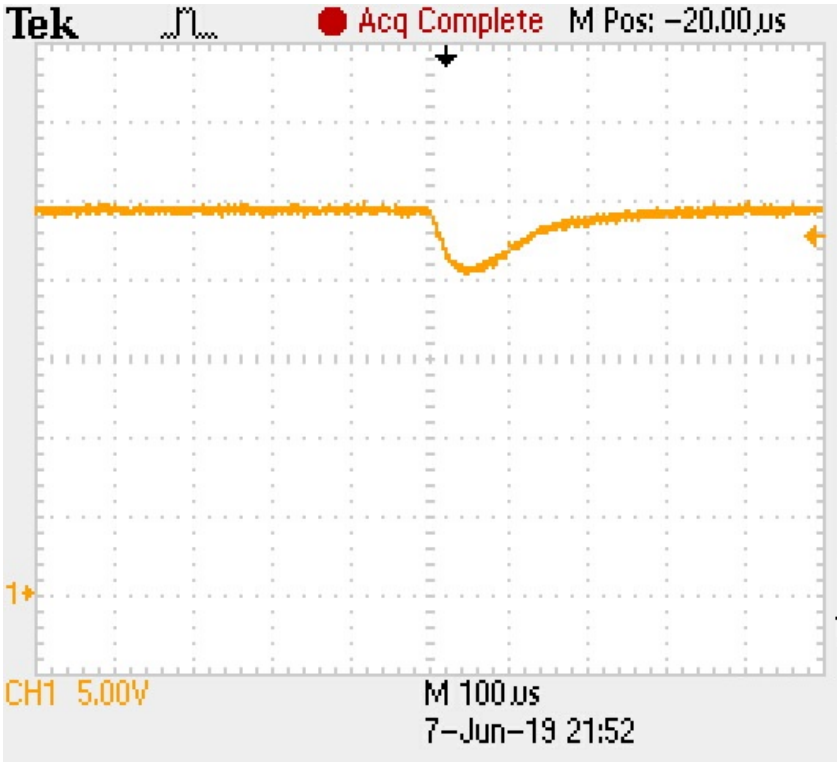

Figure B.34: Load Transient response for attaching the load 4

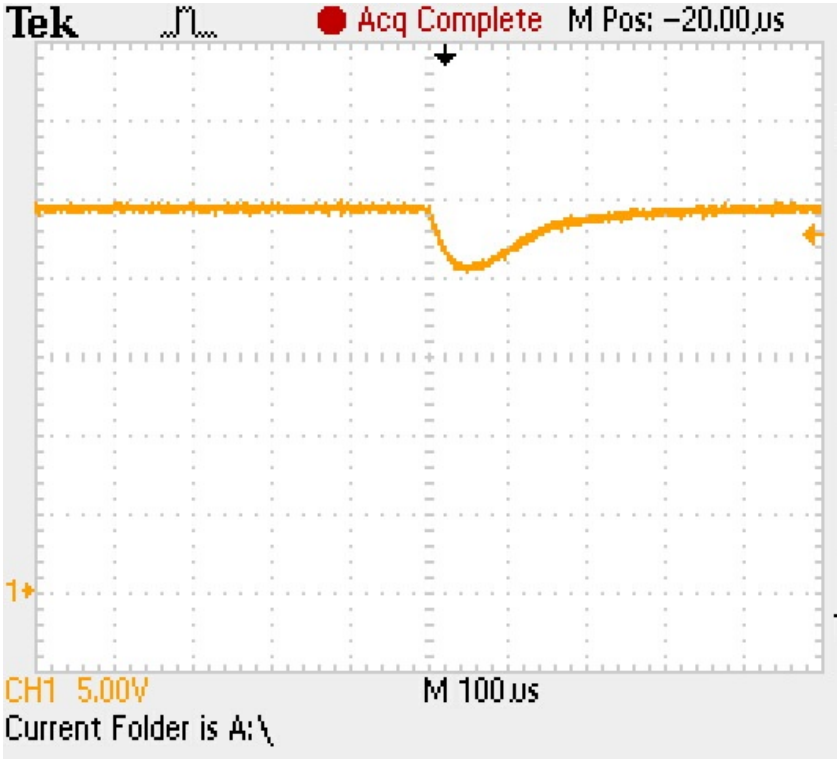

Figure B.35: Load Transient response for attaching the load 5

B.4.2. Detaching the load

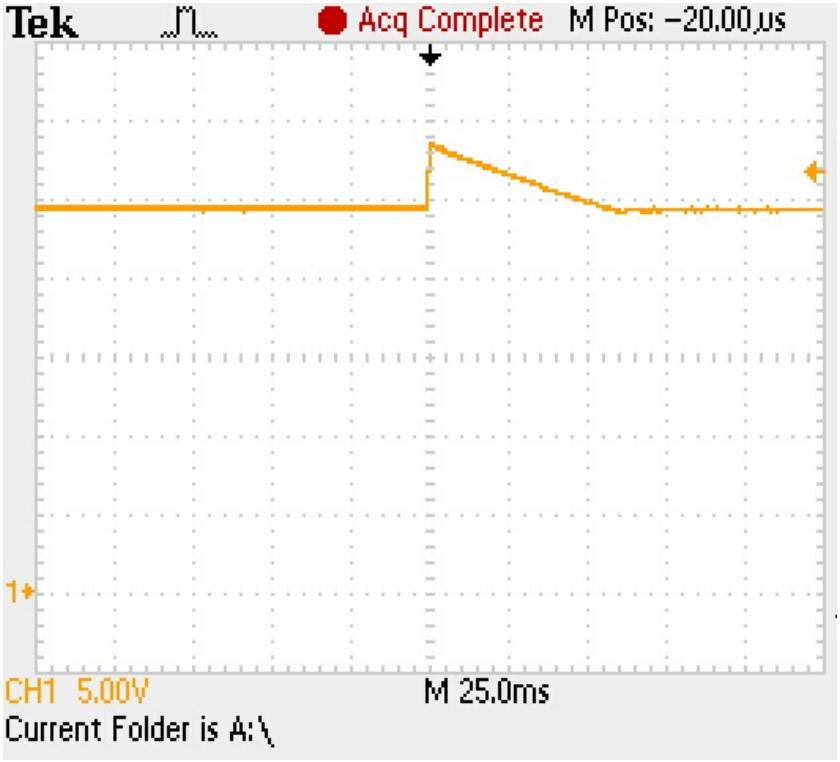

Figure B.36: Load Transient response for detaching the load 1

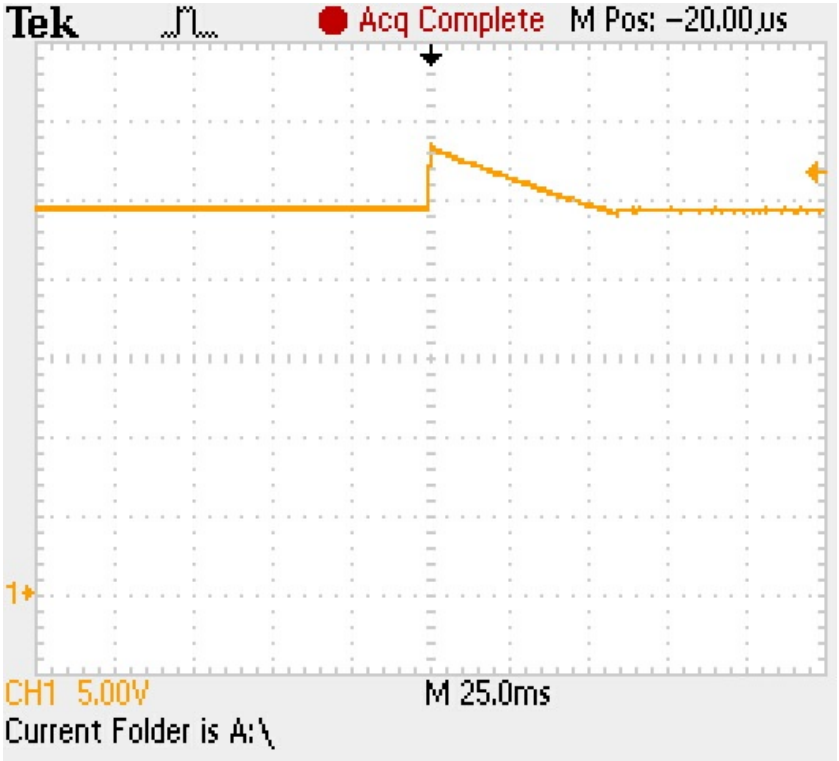

Figure B.37: Load Transient response for detaching the load 2

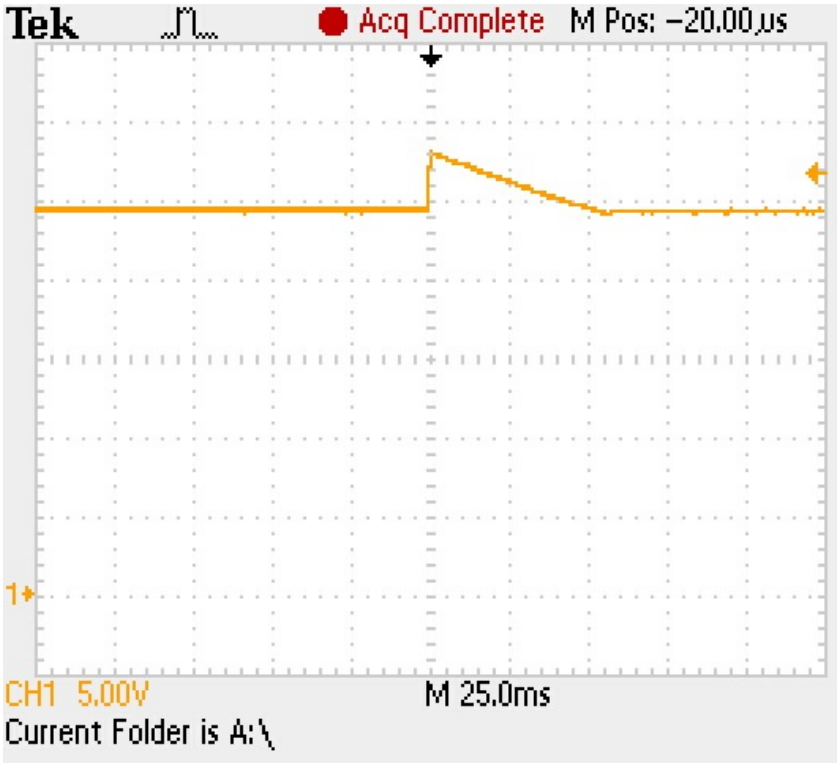

Figure B.38: Load Transient response for detaching the load 3

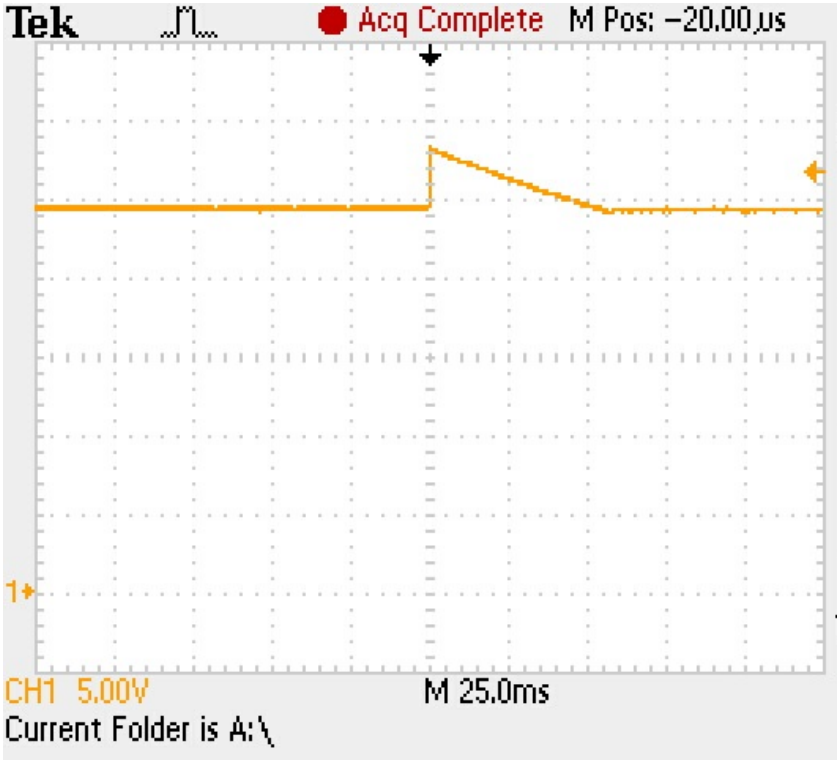

Figure B.39: Load Transient response for detaching the load 4

B.5. Tests Actuator Control

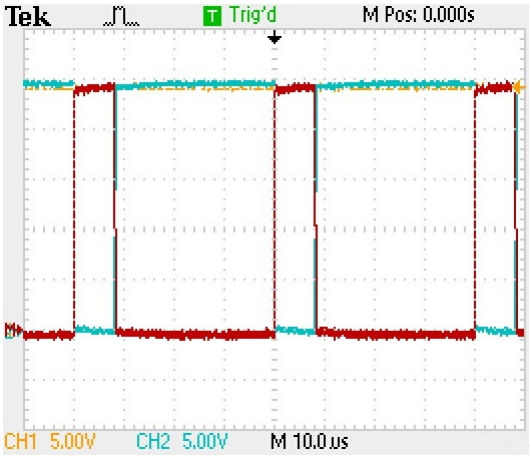

(a) Motor test with a duty cycle of 20%

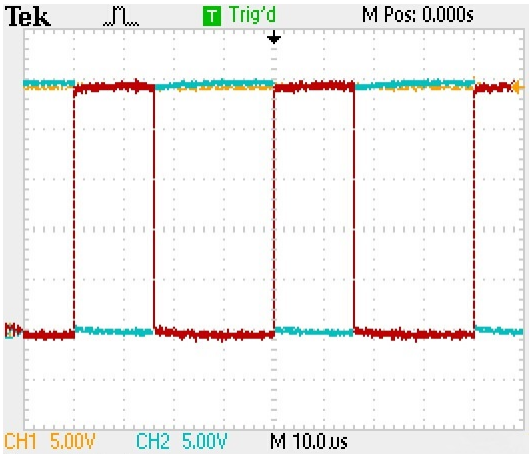

(b) Motor test with a duty cycle of 40%

Figure B.40: Motor test with different duty cycles applied to the MOSFET gate

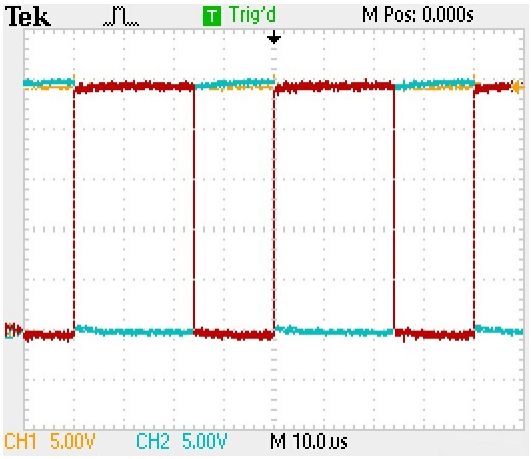

(a) Motor test with a duty cycle of 60%

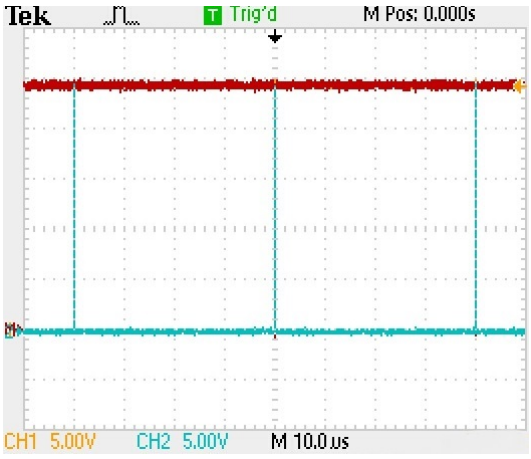

(b) Motor test with a duty cycle of 100%

Figure B.41: Motor test with different duty cycles applied to the MOSFET gate

B.6. Datasheets

Datasheets are confidential and belong to SenseGlove.

Bibliography

[1] S. B. D.A.M. Koene, "Softglove: Per finger vibrotactile feedback," Bachelor thesis, Delft University of Technology, 2019.

[2] T. R. K. Peelen, "Softglove: Palm vibrotactile feedback," Bachelor thesis, Delft University of Technology, 2019.

[3] A. El Saddik, "The potential of haptics technologies," *IEEE Instrumentation & Measurement Magazine*, vol. 10, no. 1, pp. 10–17, 2007.

[4] W. M. B. Tiest and A. M. Kappers, "Haptic perception of force," *Scholarpedia*, vol. 10, no. 2, p. 32732, 2015, revision #151740.

[5] B. Alexander and K. Viktor, "Proportions of hand segments," *Int. J. Morphol*, vol. 28, no. 3, pp. 755–758, 2010.

[6] M. W. Uddin, X. Zhang, and D. Wang, "A pneumatic-driven haptic glove with force and tactile feedback," in *2016 International Conference on Virtual Reality and Visualization (ICVRV)*. IEEE, 2016, pp. 304–311.

[7] M. Hosseini, A. Sengül, Y. Pane, J. De Schutter, and H. Bruyninck, "Exoten-glove: A force-f eedback haptic glove based on twisted string actuation system," in *2018 27th IEEE International Symposium on Robot and Human Interactive Communication (RO-MAN)*. IEEE, 2018, pp. 320–327.

[8] M. G. V. Bautista, W.-R. Liou, and M.-L. Yeh, "Dimmable multi-channel rgb led driver," in *2013 IEEE ECCE Asia Downunder*. IEEE, 2013, pp. 1259–1262.

[9] S. Balaji and M. Venkatesan, "Bldc motor control based on duty cycle," in *2017 IEEE International Conference on Computational Intelligence and Computing Research (ICCIC)*. IEEE, 2017, pp. 1–4.

[10] V. G. Popescu, G. C. Burdea, M. Bouzit, and V. R. Hentz, "A virtual-reality-based telerehabilitation system with force feedback," *IEEE transactions on Information Technology in Biomedicine*, vol. 4, no. 1, pp. 45–51, 2000.

[11] C. Wusheng, W. Tianmiao, and H. Lei, "Design of data glove and arm type haptic interface," in *11th Symposium on Haptic Interfaces for Virtual Environment and Teleoperator Systems, 2003. HAPTICS 2003. Proceedings.* IEEE, 2003, pp. 422–427.

[12] S. Das, Y. Kishishita, T. Tsuji, C. Lowell, K. Ogawa, and Y. Kurita, "Forcehand glove: a wearable force-feedback glove with pneumatic artificial muscles (pams)," *IEEE Robotics and Automation Letters*, vol. 3, no. 3, pp. 2416–2423, 2018.

[13] J. Ha, D. Kim, and S. Jo, "Use of deep learning for position estimation and control of soft glove," in *2018 18th International Conference on Control, Automation and Systems (ICCAS)*. IEEE, 2018, pp. 570–574.

[14] S. Jadhav, V. Kannanda, B. Kang, M. T. Tolley, and J. P. Schulze, "Soft robotic glove for kinesthetic haptic feedback in virtual reality environments," *Electronic Imaging*, vol. 2017, no. 3, pp. 19–24, 2017.

[15] B. Hasaneen and A. A. E. Mohammed, "Design and simulation of dc/dc boost converter," in *2008 12th International Middle-East Power System Conference*. IEEE, 2008, pp. 335–340.

[16] Q. Zhao and F. C. Lee, "High-efficiency, high step-up dc-dc converters," *IEEE Transactions on Power Electronics*, vol. 18, no. 1, pp. 65–73, 2003.

[17] N. Boujelben, F. Masmoudi, M. Djemel, and N. Derbel, "Design and comparison of quadratic boost and double cascade boost converters with boost converter," in *2017 14th International Multi-Conference on Systems, Signals & Devices (SSD)*. IEEE, 2017, pp. 245–252.

[18] C. Lam, "Sense glove: Dissertation rev. a," Master's thesis, The Hague University of Applied Sciences, The Netherlands, 2018.

[19] M. Corten, "Sense glove haptics research 2018: Human machine interface optimization," 2018.

[20] EuroCircuits, 2019. [Online]. Available: https://www.eurocircuits.com/

[21] J. Fjelstad, *Flexible Circuit Technology, Third Edition*. Br Publishing, Incorporated, 2007.

[22] C. Lam, "Senseglove communication protocol," 2018.

[23] P. V. den Bossche, F. Vergels, J. V. Mierlo, J. Matheys, and W. V. Autenboer, "Subat: An assessment of sustainable battery technology," *Journal of Power Sources*, vol. 162, no. 2, pp. 913 – 919, 2006, special issue including selected papers from the International Power Sources Symposium 2005 together with regular papers. [Online]. Available: http://www.sciencedirect.com/science/article/pii/S0378775305008761

[24] G. E. Blomgren, "Current status of lithium ion and lithium polymer secondary batteries," in *Fifteenth Annual Battery Conference on Applications and Advances (Cat. No. 00TH8490)*. IEEE, 2000, pp. 97–100.

[25] T. Instruments, 2019. [Online]. Available: https://www.ti.com/packaging/docs/searchtipackages.tsp?packageName=BGA

[26] Distrelec, 2019. [Online]. Available: https://www.distrelec.nl/nl/converter-ic-qfn-24-ic-haus-ic-tw4-qfn24/p/17350861

[27] "Ltc3872 datasheet." [Online]. Available: https://www.analog.com/media/en/technical-documentation/data-sheets/3872fc.pdf

[28] "Tps55340 datasheet." [Online]. Available: http://www.ti.com/lit/ds/symlink/tps55340.pdf

[29] "Tps563231 datasheet." [Online]. Available: http://www.ti.com/lit/ds/symlink/tps563231.pdf